

Aus dem Zentrum für Medizinische Forschung

der Medizinischen Fakultät Mannheim
Direktor: Prof. Dr. med. Norbert Gretz

Therapeutic potential of human ABCB5+ cells and different conditioned media
in a cisplatin-induced nephrotoxicity model

Inauguraldissertation
zur Erlangung des akademischen Grades
Doctor scientiarum humanarum (Dr. sc. hum.)
der
Medizinischen Fakultät Mannheim
der Ruprecht-Karls-Universität
zu
Heidelberg

vorgelegt von
Cristina Daniele

aus
Chiaravalle Centrale, Italy
2019

Dekan: Prof. Dr. med. Sergij Goerd
Referent: Prof. Dr. med. Norbert Gretz

Table of Contents

1. Introduction	1
2. Aims of the study	9
3. Animals, material and methods	11
4. Results	20
5. Discussion	68
6. Summary	83
7. References	85
8. Curriculum vitae.....	96
9. Acknowledgment	99
Abbreviations	100

1. Introduction

1.1. Renal diseases

Renal diseases represent a global public health problem that affects every year a large number of patients worldwide. Indeed, due to their essential role in the in homeostasis maintenance, kidneys are exposed to numerous insults of different nature, resulting in a large variety of renal injuries that can affect the lifestyle of patients to varying extents. Therefore, an early stage diagnosis of kidney damage is essential to be able to intervene immediately and efficiently. Diagnosis of kidney diseases is possible by checking markers of renal failure in blood and urine. Glomerular filtration rate (GFR), which describes how efficient is the renal filtration, is considered the best indicator of renal function and any changes of this parameter may reflect a pathological state ¹. However, since early kidney diseases usually do not have any symptoms, patients often have a delayed diagnosis, which results in a poor prognosis. An early detection and treatment of acute kidney injury (AKI) is extremely important to prevent its possible progression to chronic kidney disease or end-stage renal disease (ESRD) ². Regarding possible treatments, the only available options to date for ESRD are dialysis and/or renal transplantation, which are invasive for the patients and highly expensive for the public health care system ². It is therefore clear that alternative treatments for renal diseases are urgently needed.

In the next paragraphs, we will discuss about drug-induced kidney injuries (1.2) with focus on the antineoplastic drug cisplatin (1.3) and we will present stem cell therapy (1.4) as a possible treatment for cisplatin-induced kidney injury.

1.2. Drug-induced nephrotoxicity

Due to the kidneys' key role in plasma clearance, renal cells are directly exposed to all possible molecules present in the bloodstream, including drugs, some of which are known to have a nephrotoxic effect. Indeed, many different compounds can affect kidneys at different levels and with different modes of action. As shown in Figure 1, drugs can exert their nephrotoxicity by altering the kidney hemodynamics, obstructing excretory function or

directly harming renal cells³⁻⁵. The effects can be observable in terms of functional alterations, such as glomerular and/or tubular dysfunction, impaired renal endocrine function, inadequate blood pressure control and histopathological lesions^{5,6}. Although it is difficult to determine the real incidence, it has been estimated that approximately 20% of AKI in adult populations is attributed to drug-induced nephrotoxicity⁷⁻¹⁰.

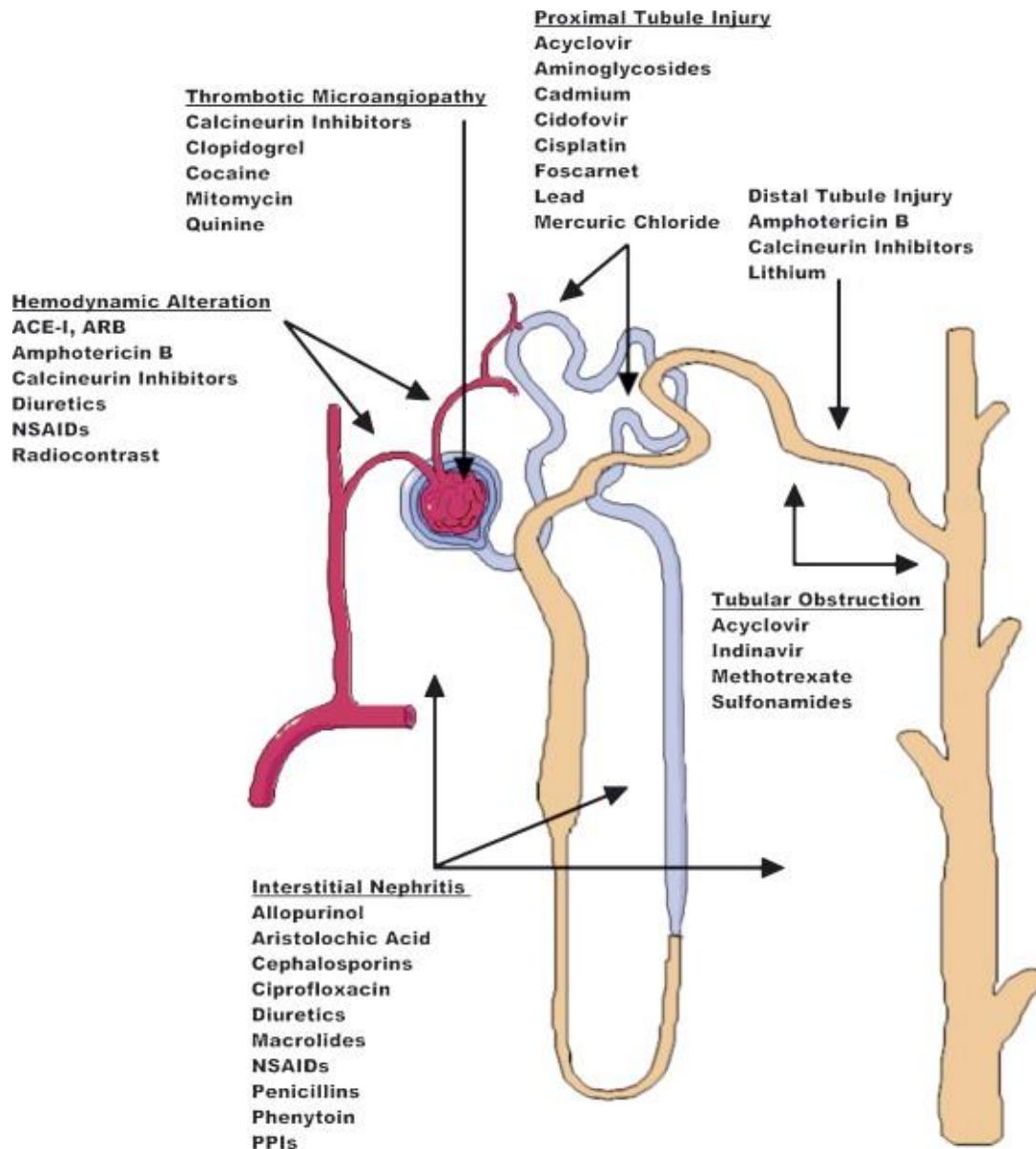


Figure 1 Common nephrotoxins and their site and mechanism of injury. ACE-I: angiotensin-converting enzyme inhibitors; ARB: angiotensin II receptor blockers; NSAID: nonsteroidal anti-inflammatory drugs⁴

Among different classes of drugs, chemotherapeutics represent a well-known example of nephrotoxic agents ¹¹. Indeed, the nephrotoxic side effect of chemotherapeutics is a limiting factor in cancer treatment, especially in patients where pre-existing and/or maybe subclinical renal injuries are present. Additionally, patients undergoing chemotherapy can develop several health complications throughout life and require, therefore, a constant follow-up. In this scenario, it is easy to understand that the diagnosis of an early stage kidney failure is essential for a good prognosis of the patients.

1.3. Chemotherapeutic-induced nephrotoxicity: cisplatin

Cis-diamminedichloroplatinum-(II), commonly called cisplatin, is a well-known and widely used chemotherapeutic drug. Synthesized for the first time at the beginning of the 19th century, its antineoplastic properties were discovered and demonstrated only one century later ¹²⁻¹⁴. In the 1970s, cisplatin was introduced in clinics ¹⁵ and approved by the U.S. Food and Drug Administration, becoming commercially available as Platinol[®] (Bristol-Myers Squibb) ¹⁶.

Cisplatin shows a remarkable and incomparable potency against certain types of neoplasms, such as testicular cancer, for the treatment of which shows 90% efficacy ¹⁷. According to the NIH National Cancer Institute database, cisplatin is nowadays used, alone or in combination with other drugs, to not only cure testicular malignancy but also for the treatment of ovarian, cervical, bladder, non-small cell lung and head and neck cancer, among others. Although cisplatin is nowadays considered as a gold standard for the treatment of solid tumors and hematological malignancies, its well-known side effects represent a big limitation for its application.

Cisplatin belongs to the 'not specific-targeted' class of antineoplastic drugs: once intravenously (iv) administrated, it destroys cancerous cells by interfering with their DNA replication. Indeed, once accumulated inside the cells, cisplatin is converted into a potent toxin capable of triggering cell damage ¹⁸. Cisplatin is a neutral inorganic compound consisting of a central ion of platinum linked to two chloride ions and two ammonia molecules. Due to the typical intracellular low

concentration of chloride ions, one or both cisplatin chloride ligands are replaced by water molecules generating a positively charged compound¹⁹ (Figure 2).

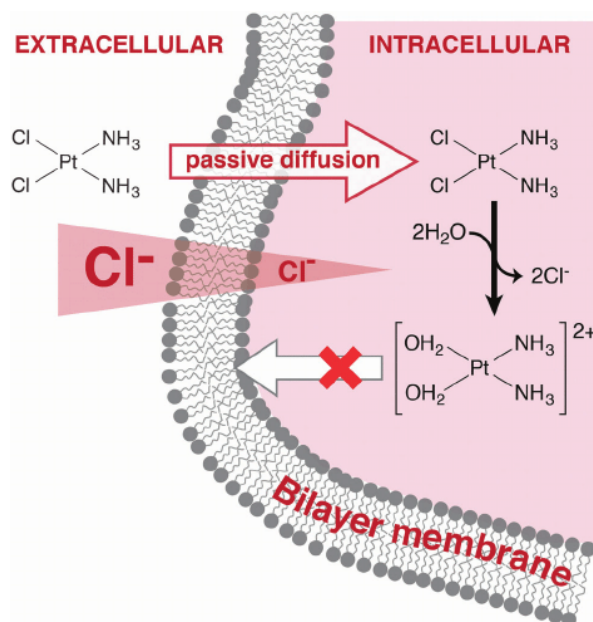


Figure 2 Mechanisms of cellular uptake and toxicity of cisplatin¹⁹

This new compound is now able to react with the nucleophilic molecules of the cells, including DNA, RNA and proteins. One of the key mechanisms involved in cisplatin cytotoxicity, is oxidative stress, which is known to mainly affect mitochondria²⁰. It has been suggested that cisplatin-induced excessive reactive oxygen species can induce cell death via apoptosis through both the extrinsic and intrinsic pathways²¹, necrosis²² and even autophagy²³

However, due to its not cell-specific action, cisplatin can exert a cytotoxic effect also on healthy tissues, at the renal, gastrointestinal, hepatic, hematological, cardiovascular and neurological level^{24, 25}. As widely reported in literature, kidneys are highly affected by cisplatin and the severity of nephrotoxicity is dose- and time-dependent and shows a cumulative effect^{26, 27}. It has been shown that up to 35% of patients who received a single dose of cisplatin experience impairment of renal function characterized by a decrease in GFR and an increase in serum creatinine and urea nitrogen²⁸⁻³⁰. The induced damage is often reversible, but a significant proportion of the affected patients exhibit a worsening of renal function and are developing a progressive loss of renal function³⁰. To understand the mechanisms behind its nephrotoxic

effect, it is necessary to elucidate what happens when this drug reaches the nephrons (Figure 3).

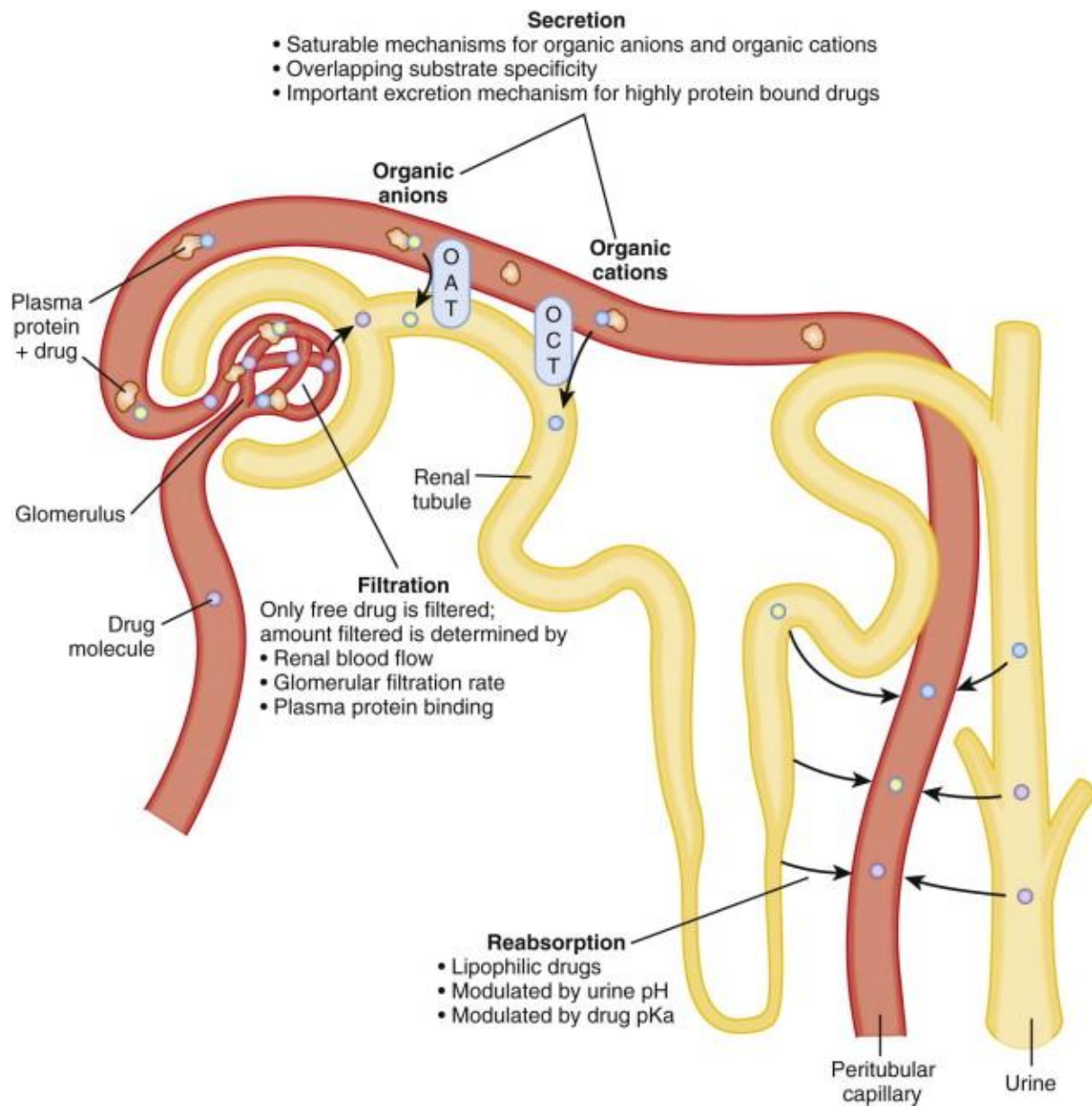


Figure 3 Renal drug excretion ³¹

After administration, cisplatin is mainly eliminated through the kidneys by glomerular filtration and secretion, with no evidence of tubular reabsorption ³⁰. Secretion of cisplatin is an active process mediated by the organic cationic transporter isoform 2, which is highly expressed in the basolateral membrane of proximal tubular cells ^{32, 33}. The presence of this transporter

explains why cisplatin accumulates in the kidneys in a more pronounced manner than in any other organ. This selective accumulation in the proximal tubular cells is so pronounced that a non-toxic amount of cisplatin in the blood can result in renal damage³⁴. Once in the proximal tubular cells, cisplatin leads to the activation of signaling pathways inducing injury, cell death and inflammatory response. All this translates into a loss of renal function and the occurrence of AKI. The typical renal histopathological changes induced by cisplatin include necrosis and degeneration of tubular epithelial cells, loss of brush border, dilation of tubular lumen, cytoplasmic vacuolization and infiltration of lymphocytes and macrophages^{30,35}.

In order to overcome cisplatin-induced nephrotoxicity during chemotherapy, cisplatin was also tested in combination with renoprotective agents³⁶. An alternative strategy was developing cisplatin analogues with the same anti-tumor efficacy and lesser toxic effects. However, only few platinum-based chemotherapeutic agents, such as carboplatin and oxaliplatin, have obtained approval after clinical trials, but even so, the use of cisplatin has not been fully replaced^{37,38}.

In animal experiments, cisplatin has been used for decades to create models of kidney injury. Especially in rodents, cisplatin-induced nephrotoxicity represents a simple and widely used model that has many similarities to human cisplatin nephrotoxic effect and that can therefore be used for assessing the putative therapeutic potential of different treatments³⁹.

1.4. Stem-cell therapy for the treatment of cisplatin-induced kidney injury

Within the last decades, the application of stem cells for the treatment of several diseases has become relevant. Exploiting their differentiation potential, stem cells are currently tested in a variety of pathologic conditions, including the field of nephrology. In cisplatin-induced nephrotoxicity models, different sources and doses of stem cells, applied with different timing and via different administration routes, have been tested and promising results in terms of survival rate, renal function and morphology have been achieved⁴⁰.

Noteworthy, both allogeneic and xenogeneic cells have been tested and, nowadays, an increasing number of studies involve the application of human stem cells in animal models, rising several debates and concerns. Undoubtedly, considering a possible translation to the clinical field, testing human cells in animals seems to be a reasonable approach.

Stem cells are known to have immune-modulatory properties, thanks to which they are able to escape and suppress the host immune system, making them suitable for transplantation across species ⁴¹. However, after xenogeneic stem cells administration, some studies reported both humoral and cellular responses ⁴². Additionally, in a recent study conducted by Lohan et al., immunomodulation of human stem cells were ineffective in a rat model of corneal transplantation because of interspecies incompatibilities. Indeed, the authors claim that human stem cells cannot be properly stimulated in a xenogeneic environment and therefore they cannot exert their immune modulatory action ⁴³. It is clear that the pronounced discordances observed in this area need to be clarified with further experiments.

Studying the mechanisms of action through which stem cells exert their therapeutic potential on a pathologic condition, scientists agree more and more on a possible paracrine action of the cells rather than their homing and engraftment in a particular organ ^{44, 45}. For this reason, the attention has been lately focused on the secretome, assuming that the therapeutic potential of stem cells is not due to the cells themselves but it is more ascribed to what they release into the medium where they grow ⁴⁶. Based on this finding, the use of conditioned medium derived from stem cells has become an alternative to the use of cell infusion, which is an important alternative approach when considering the risk/benefit ratio. However, besides the positive results achieved ⁴⁷, there is a study that demonstrates that different sources of CM do not ameliorate the condition of animals suffering kidney failure ⁴⁸. Once more, discrepancies need to be clarified.

In this controversial scenario, it seems that one possible observation is that the putative healing effects of stem cells and conditioned medium strictly vary based on cell source, dose, timing and severity of the kidney disease.

In a recent study, Schatton et al. identified in human dermis a particular non-hematopoietic cell subset that shows immune-regulatory functions similar to stem cells ⁴⁹. These dermal immune-

regulatory cells (DIRCs) are characterized by the expression of the ATP-binding cassette member B5 (ABCB5) peptide on their membrane and represent a unique dermal subpopulation. According to the authors, ABCB5 positive (ABCB5+) DIRCs may lead to promising results in cellular immunotherapy applications.

To the best of our knowledge, ABCB5+ cells and derived conditioned medium have not been applied for the treatment of nephrotoxicity yet. In the light of this, we decided to test whether ABCB5+ cells and derived conditioned medium may exert a therapeutic effect in the treatment of cisplatin-induced kidney failure.

Preliminary results of an ongoing study has demonstrated that local injection of ABCB5+ cells around a wound accelerates the healing process by triggering the resident macrophage polarization from a M1 pro-inflammatory to a M2 anti-inflammatory phenotype via paracrine release of IL-1RA (Ticeba, personal communication). Therefore, when ABCB5+ cells are co-cultured with macrophages, the healing effect produced by the two cell populations together is enhanced. We decided to test whether the conditioned medium derived from the aforementioned co-culture could ameliorate the conditions of animals suffering kidney injury.

2. Aims of the study

The aim of this study was to test whether human ABCB5⁺ cells and different derived conditioned media can exert a therapeutic effect in an animal model of kidney nephropathy.

First, a stable model of cisplatin-induced kidney injury in immunocompetent Sprague Dawley (SD) rats was established. The onset and progression of renal damage was evaluated through periodically measuring metabolic, plasmatic and urinary parameters and performing transcutaneous assessment of renal function.

The established model was then used to test the therapeutic potential of human ABCB5⁺ cells. This particular population of DIRC^s was purified from skin of healthy individuals of different sex, age and nationality by Ticeba-RHEACELL and was delivered as a ready-to-use solution. In order to overcome a possible trapping of the cells in the lungs and a subsequent pulmonary embolism, besides the classical intravenous (iv) administration route, ABCB5⁺ cells were also intraperitoneally (ip) injected and the outcomes were compared.

Based on the latest findings regarding the secretome and the possible application of stem cell derived conditioned medium as an alternative approach, we decided to test also the therapeutic potential of ABCB5⁺ cell derived conditioned medium (CM).

Additionally, exploiting the immune-modulatory effects that ABCB5⁺ have on macrophages, conditioned medium derived from a co-culture of ABCB5⁺ and macrophages was also tested in our cisplatin-induced nephrotoxicity model. In this case, the co-culture was stimulated with lipopolysaccharide (LPS) and interferon-gamma (IFN γ), factors that are known to trigger macrophages polarization into the M2 anti-inflammatory phenotype. This particular conditioned medium was addressed as coCM⁺.

Lastly, to test a possible effect of LPS and IFN- γ on stem cells only, ABCB5⁺ cells were cultured and stimulated without macrophages and the derived conditioned medium, referred as CM⁺, was also tested in our model.

All the media were iv administered to the animals and were delivered by Ticeba-RHEACELL as a ready-to-use solution.

In summary, a stable model of cisplatin-induced kidney injury was established in immunocompetent SD rats for testing the following treatments:

- ABCB5+ cells iv and ip administrated;
- conditioned media iv administrated and derived from:
 - o ABCB5+ cells (CM)
 - o ABCB5+ cells co-cultured with Macrophages and stimulated with LPS and IFN- γ (coCM+)
 - o ABCB5+ cells stimulated with LPS and IFN- γ (CM+)

The therapeutic potential of the aforementioned treatments was evaluated by analyzing:

- Urine and blood parameters;
- Metabolic parameters;
- Transcutaneous assessment of renal function;
- Histological evaluation;
- mRNA and miRNA expression profiling.

3. Animals, materials and methods

3.1. Animal experiments

All experiments were conducted in accordance with the German Animal Protection Law and approved by the local authority (Regierungspräsidium Nordbaden, Karlsruhe Germany in agreement with EU guideline 2010/63/EU. Male SD rats (Janvier- Labs), about 200 g were used in all the experiments. The establishment of kidney failure (section 3.5.) and the assessment of the therapeutic potential of ABCB5+ cells and CM (section 3.7.) involved 24 and 49 animals respectively. 73 animals in total were used. Before the start of any experiment, animals were acclimatized for 1 week. The first 2 days following cisplatin administration, animals were housed in pairs in individually ventilated cages to avoid cisplatin metabolites to be spread out.

3.2. Evaluation days

The animals' state of health was periodically checked and the evaluation days were organized as described: 16 hours before the evaluation, animals were placed into metabolic cages. Before and after this period, the following parameters were recorded: body weight (BW), diuresis, food and drink intake. On evaluation day, urine samples were collected early in the morning and thereafter, blood sampling was performed under anesthesia. Samples were processed as described in section 3.3. Animals were left to recover from the anesthesia for at least one hour. Afterwards, transcutaneous renal function was assessed as described in section 3.4.

3.3. Blood and urine collection

Blood samples were collected via ophthalmic venous plexus (orbital sinus) under anesthesia (5% isoflurane at 3 L/min airflow) in lithium-heparinized tubes using capillaries for blood collection. After centrifugation (5 minutes at 2000 g, 4°C) plasma was collected in 1.5 ml tubes and stored at -20°C until further analyses. Urine was collected overnight in individual metabolic cages for a period of 16 hours. Animals had free access to water and food during this time. At the end of each collection period, the urine volume was recorded and samples were centrifuged (78 g, 5 minutes) to remove precipitates. Centrifuged urine aliquots were placed in 2 ml tubes and stored at -20°C until further analyses. Plasma and urine chemical parameters were determined by using the Cobas c311 analyzer (Roche Diagnostics GmbH, Mannheim, Germany). Urinary albumin was determined by ELISA assay and osmolarity was analyzed using an osmometer (2020 Multi-Sample Osmometer, Advanced Instruments Inc., Norwood, MA).

3.4. Transcutaneous assessment of renal function

The transcutaneous assessment of renal function was performed by using a transdermal device (MediBeacon GmbH, Mannheim, Germany). The optical part of the device consists of two light-emitting diodes, with an emission in the near infrared region (excitation: 706nm, emission: 790nm), and a photodiode detecting the fluorescent light. Energy is supplied by a small lithium polymer rechargeable battery with a voltage of 3.7V and capacity of 50 mAh. The recorded digital data are stored in the internal memory of the device and are then downloaded onto a PC for the analysis⁵⁰⁻⁵³. To perform the transcutaneous measurement of renal function, the device and the connected battery were attached to a specifically designed double-sided adhesive patch and then fixed on the shaved back of the animal. The animal received a dose of 15mg/100 g BW of ABZWY-HP β CD (stock solution 160 mg/ml in Deltajonin) via tail-vein injection, and its emitted fluorescent signal was recorded by the device⁵⁴. Shaving, fixation of the device and dose administration were performed under short isoflurane anesthesia (5% isoflurane at 3 L/min air flow, decreasing to 2% isoflurane at 1.5 L/min air flow). The measurement was performed for at least 2 hours, during which the animal was completely awake and freely moving. The

recorded data represented the excretion curves of ABZWCY-HP β CD. To determine the half-life excretion of the administered ABZWCY-HP β CD, a 3-compartment model was applied using the open source freely-available software ‘GFRmeasure’ (<https://www.mathworks.com/products/compiler/matlab-runtime.html>).

3.5. Development of cisplatin-induced nephropathy model in SD rats

Kidney failure was induced by cisplatin administration. Cisplatin was purchased as a ready-to-use solution (TEVA, 1mg/ml solution) and it was administered via ip route under short isoflurane anesthesia (5% isoflurane at 3 L/min air flow, decreasing to 2% isoflurane at 1.5 L/min air flow). To induce kidney damage, a single dose of 7 mg/kg BW was chosen. Control animals received the same volume of sterile saline. 24 animals were used for the whole experiment (control n=3; cisplatin n=21). Six animals from the cisplatin group were excluded from the analysis because they died or were sacrificed before the end of the experiment. Therefore, 18 animals were finally included in the analysis (control n=3; cisplatin n=15, Table 1).

Animals	Control	Cisplatin
Total	3	21
Dead before day 15		6
Perfused on day 15	3	15

Table 1 Number of animals involved in the establishment of the cisplatin-induced nephrotoxicity model. Animals perfused on day 15 were included in the analysis

The day of the first cisplatin/saline administration was considered as day 0. Evaluation days were performed 3 days before the start of the experiment (baseline), and 2, 7 and 14 days after cisplatin/saline administration. Animals were sacrificed on day 15 by perfusion (0.9% saline heparin 5 IU/mL pH=7 for 3min at 280mbar, PFA 4% for 3min at 230mbar) under anesthesia

(Rompun 2% 5mg/Kg BW and Ketamin 10%, 100mg/Kg BW). The fresh left kidney was collected before perfusion and immediately snap-frozen in liquid nitrogen for subsequent mRNA extraction (section 3.10.). Other organs (right kidney, spleen, liver, pancreas, intestine, heart, lungs) were collected after perfusion and processed for subsequent histology and immunofluorescence analyses (section 3.9.). The experimental set-up is described in Figure 4.

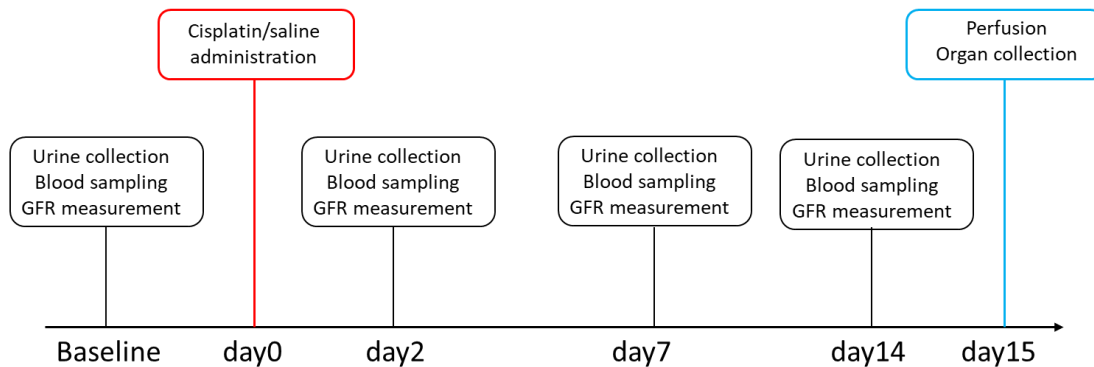


Figure 4 Experimental set-up for the establishment of cisplatin-induced nephropathy model in SD rats

3.6. ABCB5+ cells and conditioned media

Ready to use ABCB5+ cells and conditioned media were delivered from Ticeba-RHEACELL GmbH & Co. (Heidelberg, Germany). Conditioned media were obtained by collecting the supernatant of the following cell cultures:

- **CM**: ABCB5+ cell culture;
- **CM+**: ABCB5+ stimulated cell culture;
- **M+**: human monocyte cell line THP-1 cultured with PMA to induce macrophage differentiation. After stimulation, macrophages polarize to M1 pro-inflammatory macrophages;
- **coCM+**: ABCB5+ co-cultured with THP-1 derived macrophages. After stimulation and in presence of ABCB5+ cells, THP-1 derived macrophages polarize to M2 anti-inflammatory macrophages.

Stimulation consisted of IFN- γ and LPS for promoting macrophage polarization. Cells were stimulated with 50IU/ml IFN- γ on the seeding day (first day) and with 50IU/ml IFN- γ + 20ng/ml LPS on the day after. The third day, conditioned media were harvested and immediately frozen and stored at -20C until injection into the animals or subsequent analysis.

An overview of what has been just described is shown in Figure 5.

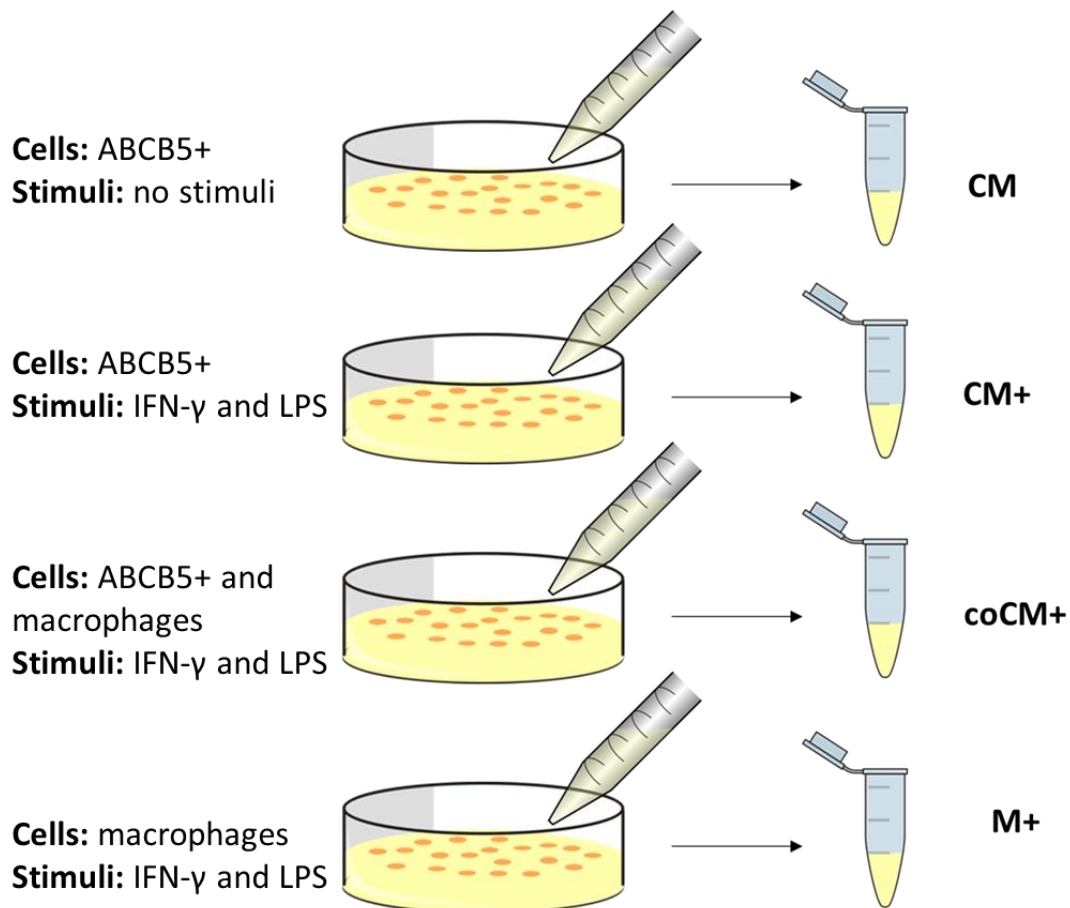


Figure 5 Conditioned media obtained by collecting the supernatant of ABCB5+ cells and/or macrophages with or without stimuli. IFN- γ : Interferon-gamma; LPS: lipopolysaccharide

3.7. Assessment of the therapeutic potential of human ABCB5+ cells and conditioned media in a cisplatin-induced nephropathy model

To assess the therapeutic potential of human ABCB5+ cells and conditioned media, the same experimental set-up used for the establishment of the cisplatin-induced nephrotoxicity model was used. Treatments were administrated on day 3.

More in detail, after baseline evaluation, on day 0 all animals received a single ip dose of cisplatin (7mg/kg BW). On day 2, blood and urine parameters were analyzed and the transcutaneous measurement of renal function was assessed in order to confirm whether the renal damage was properly induced. Thereafter, rats were randomly allocated to different groups according to the treatment received on day 3:

- 1) Group ivABCB5+: 2×10^6 ABCB5+ cells iv administrated;
- 2) Group ipABCB5+: 2×10^6 ABCB5+ cells ip administrated;
- 3) Group CM: 0.5ml of CM iv administrated;
- 4) Group CM+: 0.5ml of CM+ iv administrated;
- 5) Group coCM+: 0.5ml of coCM+ iv administrated;
- 6) Group vehicle: 0.5ml of fresh medium (RPMI1640 + L-Glutamine) iv administrated as a positive control.

The animals' health-status was evaluated on day 7 and 14, and the animals were sacrificed on day 15 as previously described in section 3.5. The experimental set-up is shown in Figure 6.

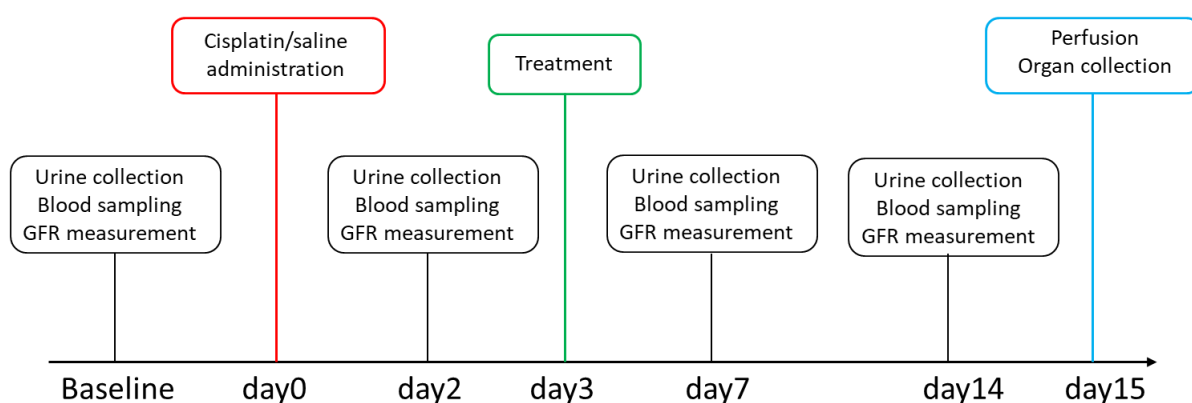


Figure 6 Experimental set-up for the assessment of the therapeutic potential of human ABCB5+ cells and conditioned media in a cisplatin-induced nephropathy model

49 animals were involved in the experiment (iv ABCB5+ n=12; ip ABCB5+ n=12; CM n=4; CM+ n=4, coCM n=12; vehicle n=5). Six animals (ip ABCB5+ n=1; CM n=1; CM+ n=1, coCM n=1; vehicle n=2) were excluded from the analysis because they died or were sacrificed before the end of the experiment. Therefore, 43 animals were finally included in the analysis (iv ABCB5+ n=12; ip ABCB5+ n=11; CM n=3; CM+ n=3, coCM n=11; vehicle n=3, Table 2).

Animals	ABCB5 ip	ABCB5 iv	CM	CM+	coCM+	Vehicle
Total	12	12	4	4	12	5
Dead before day 15			1	1	1	2
Perfused on day 15	11	12	3	3	11	3

Table 2 Number of animals involved in the assessment of the therapeutic potential of human ABCB5+ cells and conditioned media in the cisplatin-induced nephropathy model. Animals perfused on day 15 were included in the analysis

3.8. Statistical analysis

All statistical calculations regarding blood, urine and metabolic parameters as well as renal function values were performed using SAS JMP 13.0.0 (SAS Institute, Cary, NC, USA). Kruskal-Wallis tests were applied to evaluate the changes induced by cisplatin administration in the development of the model and the effect of the different therapies applied on injured animals. For all tests, nominal p-values <0.05 (*) or <0.005 (**) were considered as statistically significant.

3.9. Histology collection, staining, analysis and microscopy

On the day of the sacrifice, organs (right kidney, spleen, liver, pancreas, intestine, heart, lungs) were collected after perfusion and stored in 4% PFA for 24h. Fixed tissues were embedded in paraffin, cut (3µm) and stained with hematoxylin and eosin (H&E). H&E slices were used to detect morphological changes induced by cisplatin and full organ images were acquired using Axio Scan.Z1 microscope (ZEISS).

3.10. RNA Isolation

For gene expression analysis, frozen left kidney samples obtained from sacrificed animals were used. Total RNA was extracted by using the RNeasy mini kit (Qiagen) following the manufacturer's instructions. The mRNA purity and integrity was tested by capillary electrophoresis on an Agilent 2100 bioanalyzer (Agilent) and high quality was confirmed. The isolated RNA was used for gene expression analysis.

3.11. Affymetrix GeneChips gene expression analysis and bioinformatics evaluation

Gene expression profiling was performed using arrays of human RatGene-2_0-st-type from Affymetrix. From the RNA, biotinylated antisense cDNA was prepared according to the Affymetrix standard labelling protocol by using the GeneChip WT Plus Reagent Kit (Affymetrix, Santa Clara, USA) and the GeneChip Hybridization, Wash and Stain Kit (Affymetrix, Santa Clara, USA). The obtained cDNA was first hybridized on the chip with a GeneChip Hybridization oven 640, then dyed in the GeneChip Fluidics Station 450 and thereafter scanned with a GeneChip Scanner 3000. All of the equipment used was from the Affymetrix-Company (Affymetrix, High Wycombe, UK).

For array annotation, the Custom CDF Version 21 with ENTREZ based gene definitions was used (Dai et. al, 2005). The raw fluorescence intensity values were normalized applying quantile normalization and RMA background correction. For identification of differentially expressed genes, OneWay-ANOVA was performed using the software package SAS JMP10 Genomics, version 6, from SAS (SAS Institute, Cary, NC, USA). A false positive rate of $\alpha=0.05$ with FDR correction was taken as the level of significance.

Gene Set Enrichment Analysis (GSEA) was performed by using the software R v3.4.0 (R Core Team 2017) and RStudio: Integrated development environment for R (RStudio Boston, MA, USA). Pathways were obtained from Kyoto Encyclopedia of Genes and Genomes database (KEGG, <http://www.genome.jp/kegg>) version September 2018.

3.12. RNAseq gene and miRNAs expression and bioinformatics evaluation

New generation sequencing (NGS) gene expression profiling was performed with RNA sequencing (RNAseq) technology by BGI Tech Solutions Co. (Hong Kong) with BGISEQ-500 method. RNAseq data were analyzed and aligned by using R/Bioconductor and Rsubread software respectively. For annotation, the ENTREZ-based software package TxDb.Hsapiens.UCSC.hg19.knownGene was used and differential gene expression analysis was performed by a DESeq2 package. A false positive rate of $\alpha=0.05$ with FDR correction was taken as the level of significance. GSEA was performed by using the KEGG database version September 2018.

RNAseq technology also detects differentially expressed miRNA precursors. For miRNAs analysis, a false positive rate of $\alpha=0.05$ with FDR correction was taken as the level of significance. Putative target genes of differentially expressed miRNAs were predicted with the miRWalk program with a cutoff of binding p value=1⁵⁵. Putative target genes were compared with the differentially expressed genes found in the gene expression profiling. For functional interpretation of selected genes, the web-based online bioinformatics resource DAVID v6.8 (Database for Annotation, Visualization and Integrated Discovery) was used and BP-GO analysis was performed^{56,57}.

3.13. Cytokines assay

Simultaneous detection of 12 cytokines (IL2, IL4, IL5, IL6, IL10, IL12, IL13, IL17A, IFN γ , TNF α , G-CSF, TGF β 1) in different conditioned media was assessed with the human Th1/Th2/Th17 cytokine Multi-Analyte ELISArray Kit (Qiagen) by following the manufacturer's instructions. Samples from 3 different donors were evaluated and the assay was repeated twice independently. Due to the kit range, CM and CM+ were tested undiluted, while coCM+ and M+ were diluted 10 times. Results were obtained by using the infinite 200 PRO NanoQuant Microplate Readers (TECAN).

4. Results

4.1. Development and characterization of a cisplatin-induced nephrotoxicity model in SD rats

Cisplatin-induced nephrotoxicity model was established as described in section 3.5.

Briefly, at the beginning of the experiment (day 0), a single intraperitoneal dose of cisplatin (7 mg/kg BW) was administrated to SD rats in order to induce renal injury. For monitoring the animal's health state and for characterizing the induced damage, 3 days before (baseline) and 2, 7 and 14 days after cisplatin administration blood and urine were sampled for biochemical analyses, transcutaneous assessment of renal function was assessed and metabolic parameters were recorded. Kruskal-Wallis each paired comparison test of cisplatin-treated animals vs controls was applied and nominal p-values <0.05 (*) or <0.005 (**) were considered as statistically significant.

15 days after cisplatin administration, fresh left kidney was collected for gene expression analysis, while the other organs were collected after animal perfusion for histological evaluation.

4.1.1. Cisplatin effect on plasma parameters

Blood sampling was performed as described in section 3.3. Plasma biochemical results are summarized in Table 3.

Parameter	Group	Baseline	Day 2	Day 7	Day 14
Creatinine (mg/dl)	Control	0.23 ± 0.0	0.27 ± 0.0	0.28 ± 0.0	0.30 ± 0.0
	Cisplatin	0.26 ± 0.0	0.45 ± 0.0**	2.13 ± 1.5 **	0.83 ± 0.2*
Urea (mg/dl)	Control	29.8 ± 6.7	33.30 ± 9.2	34.53 ± 2.2	33.80 ± 4.1
	Cisplatin	35.36 ± 4.4	67.17 ± 4.1*	258.70 ± 195.9**	83.23 ± 30.5*
Glucose (mg/dl)	Control	153.66 ± 6.1	161.33 ± 4.6	154.33 ± 8.9	153.33 ± 8.3
	Cisplatin	149.06 ± 7.8	158.66 ± 18.2	160.33 ± 13.1	142.53 ± 6.9
Protein (mg/dl)	Control	55.66 ± 1.5	59.33 ± 2.3	59.00 ± 2.0	58.33 ± 1.5
	Cisplatin	55.53 ± 1.8	60.26 ± 2.1	55.66 ± 2.9	56.26 ± 3.1
Cholesterol (mg/dl)	Control	97.66 ± 28.4	100.00 ± 28.2	88.33 ± 18.4	87.66 ± 13.0
	Cisplatin	96.00 ± 12.5	140.20 ± 21.5*	113.20 ± 24.3	117.93 ± 15.7*

Triglycerides (mg/dl)	Control	90.00 ± 34.6	136.00 ± 26.2	121.66 ± 39.8	108.66 ± 30.4
	Cisplatin	94.40 ± 26.5	73.33 ± 27.0*	130.00 ± 37.8	127.33 ± 38.8
AST (U/l)	Control	48.3 ± 11.2	67.00 ± 17.5	54.00 ± 19.5	55.00 ± 5.2
	Cisplatin	52.8 ± 11.5	39.92 ± 6.7*	61.93 ± 35.8	51.20 ± 20.8
ALT (U/l)	Control	103.00 ± 11.9	92.33 ± 2.8	92.33 ± 14.0	100.00 ± 26.8
	Cisplatin	100.53 ± 5.3	104.46 ± 12.7	97.60 ± 18.5	91.13 ± 14.2
GGT (U/l)	Control	3.00 ± 0.0	3.00 ± 0.0	3.00 ± 0.4	3.00 ± 0.0
	Cisplatin	3.00 ± 0.0	3.66 ± 0.9	3.26 ± 0.1	3.00 ± 0.0
GLDH (U/l)	Control	8.22 ± 0.8	7.80 ± 0.1	7.68 ± 1.2	8.31 ± 2.2
	Cisplatin	8.60 ± 1.3	9.13 ± 2.1	19.2 ± 4.5	4.91 ± 1.2
Na (mmol/l)	Control	133.66 ± 6.4	141.00 ± 1.0	136.66 ± 7.5	143.50 ± 2.1
	Cisplatin	139.53 ± 4.5	140.13 ± 1.5	138.00 ± 4.2	139.36 ± 2.7
Ca (mmol/l)	Control	2.71 ± 0.0	2.80 ± 0.1	2.72 ± 0.0	2.71 ± 0.0
	Cisplatin	2.71 ± 0.0	2.73 ± 0.1*	2.75 ± 0.2*	2.84 ± 0.0*
K (mmol/l)	Control	4.72 ± 0.5	4.97 ± 0.3	4.41 ± 0.4	4.45 ± 0.6
	Cisplatin	4.95 ± 0.3	4.19 ± 0.3*	4.77 ± 0.5	5.55 ± 0.6
PO4 (mmol/l)	Control	2.55 ± 0.3	2.49 ± 0.1	2.31 ± 0.2	2.48 ± 0.1
	Cisplatin	2.75 ± 0.1	2.47 ± 0.2	2.20 ± 0.9	1.41 ± 0.5**

Table 3 Changes in plasma biochemistry in control (n= 3) and cisplatin-treated (n= 15) groups. Data are shown as mean ± SD. Values significantly different from control are indicated as *p< 0.05 and **p< 0.005

Already 2 days after cisplatin administration, both creatinine and urea increased by 1.6-fold and 2-fold respectively (creatinine p<0.005, urea p<0.05) compared to the corresponding controls and remained higher until day 14 (p<0.05). Particularly on day 7, we observed an increase of 7.6-fold for creatinine and 7.5-fold for urea (p<0.005) (Figure 7).

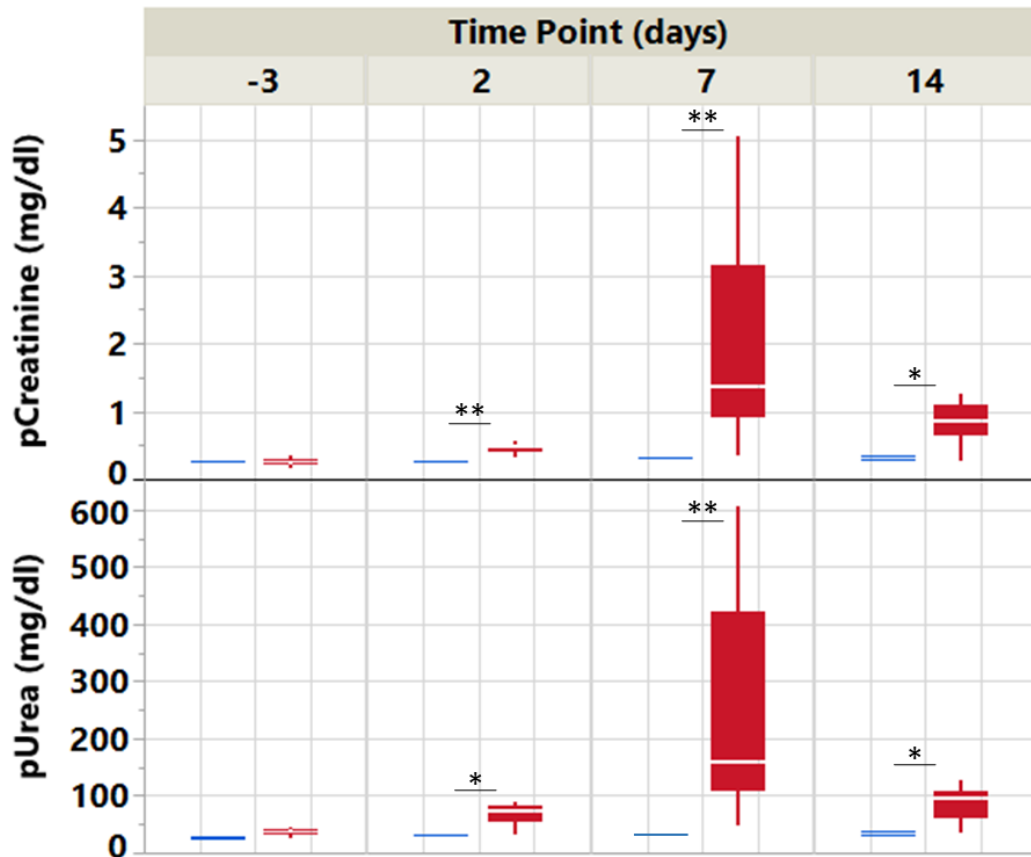


Figure 7 Effect of cisplatin administration in plasma creatinine and urea concentration. Control group n=3 in blue, cisplatin-treated group n=15 in red. Statistically significant differences are indicated as *p< 0.05 and **p< 0.005

Cisplatin also induced a 1.4-fold increase of plasma cholesterol already on day 2, which remained higher until day 14 (p<0.05) with respect to the control group. Additionally, the triglycerides levels halved on day 2 (p<0.05) in the cisplatin-treated animals, and then increased in the following days, by reaching a 1.2-fold increase on day 14 (Figure 8)

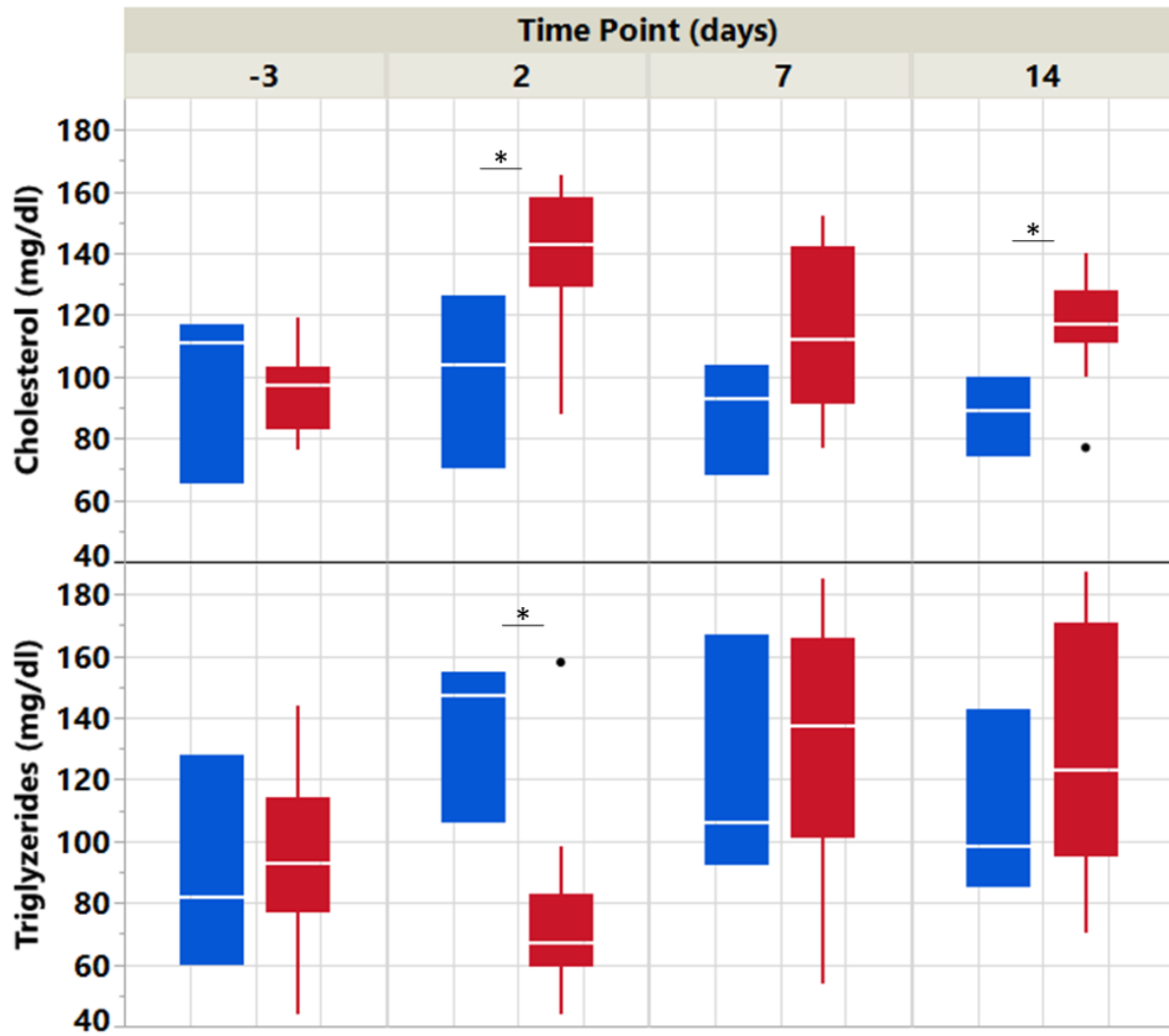


Figure 8 Effect of cisplatin administration in plasma cholesterol and triglycerides concentration. Control group n=3 in blue, cisplatin-treated group n=15 in red. Statistically significant differences are indicated as * $p < 0.05$

Plasma electrolyte levels were also affected by cisplatin. Indeed, hypokalemia on day 2 ($p < 0.05$) and hypophosphatemia on day 14 ($p < 0.005$) was recorded in the treated animals compared to the controls (Figure 9). Hypercalcemia was also observed from day 7 onwards ($p < 0.05$). In contrast, sodium level remained stable.

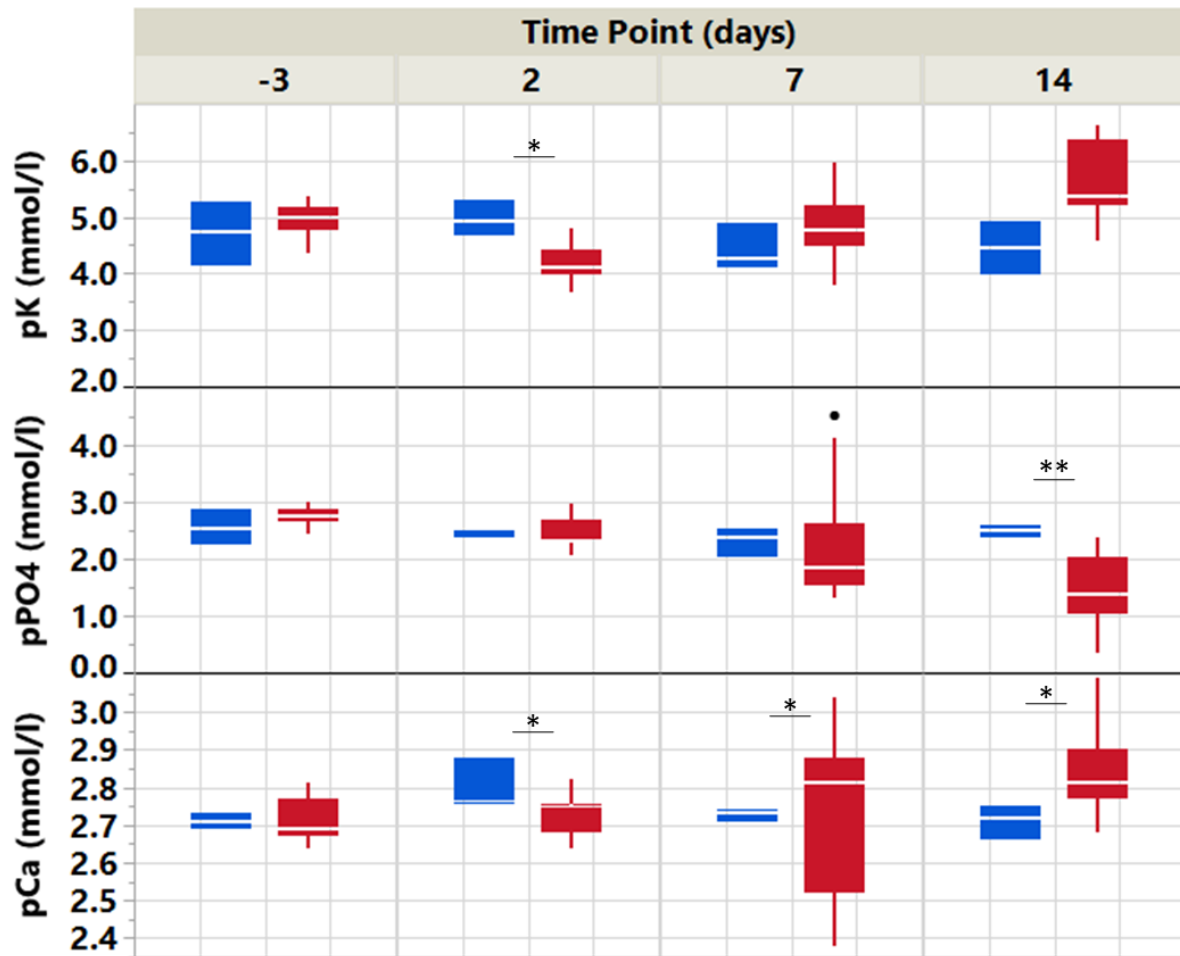


Figure 9 Effect of cisplatin administration in plasma potassium, phosphate and calcium concentration. Control group n=3 in blue, cisplatin-treated group n=15 in red. Statistically significant differences are indicated as * $p < 0.05$ and ** $p < 0.005$

Plasma levels of liver enzymes were also measured. A reduction by half in AST levels was recorded on day 2 ($p < 0.05$) in the treated animals compared to the controls. The AST value returned to basal levels on day 7. Additionally, GDHL levels increased by 2.5-fold on day 7 (not statistically significant) and halved on day 14. No differences in ALT and GGT levels were observed (Figure 10).

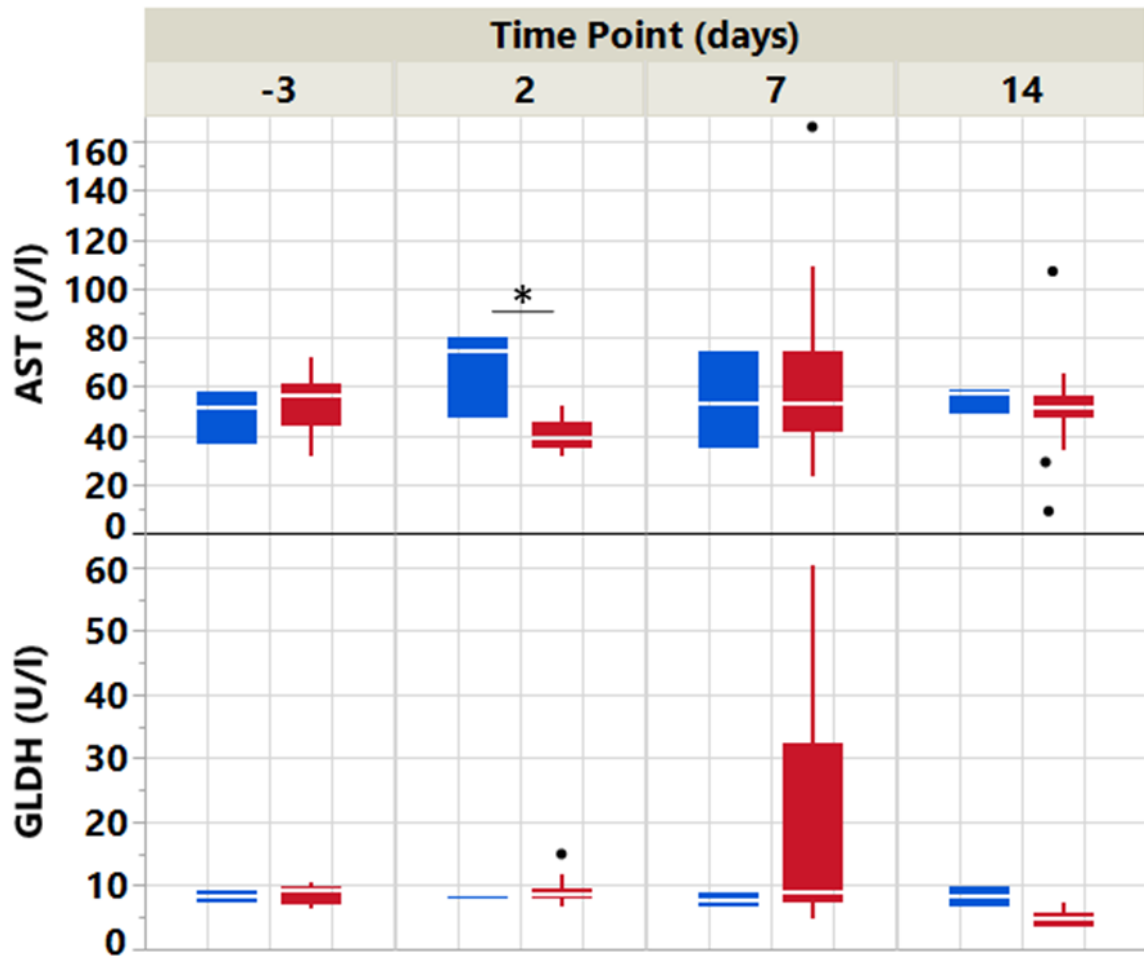


Figure 10 Effect of cisplatin administration in plasma AST and GLDH level. Control group n=3 in blue, cisplatin-treated group n=15 in red. Statistically significant differences are indicated as * $p < 0.05$

No statistically significant differences among the groups were found for plasma levels of glucose and proteins.

4.1.2. Cisplatin effect on urine parameters

Urine was collected overnight during 16 h as described in section 3.3. All urine parameters were normalized to the volume of urine produced in 16h. Urinary biochemical results are summarized in Table 4.

Parameter	Group	Baseline	Day 2	Day 7	Day 14
Creatinine (mg/16h)	Control	6.76 ± 1.6	8.53 ± 0.4	9.86 ± 1.1	11.13 ± 1.2
	Cisplatin	7.24 ± 1.4	8.19 ± 2.3	7.10 ± 2.2	7.94 ± 1.8*
Urea (mg/16h)	Control	477.39 ± 94.2	588.06 ± 116.9	661.29 ± 27.0	686.27 ± 40.5
	Cisplatin	431.60 ± 82.5	496.33 ± 129.7	616.61 ± 220.5	588.45 ± 82.1*
Glucose (mg/16h)	Control	3.75 ± 0.9	3.32 ± 0.2	3.68 ± 0.8	3.76 ± 0.5
	Cisplatin	3.33 ± 1.1	10.81 ± 6.9	63.37 ± 42.3*	100.76 ± 87.5*
Protein (mg/16h)	Control	6.76 ± 2.4	9.59 ± 2.5	11.46 ± 1.9	10.68 ± 2.7
	Cisplatin	8.12 ± 3.2	12.9 ± 1.1	8.85 ± 3.1	12.17 ± 4.6
Albumin (mg/16h)	Control	0.28 ± 0.1	0.18 ± 0.0	0.22 ± 0.0	0.23 ± 0.0
	Cisplatin	0.21 ± 0.1	2.71 ± 1.3**	4.92 ± 2.3**	4.24 ± 2.8**
Na (mmol/16h)	Control	1.82 ± 0.1	1.87 ± 0.1	2.05 ± 0.1	2.43 ± 0.2
	Cisplatin	2.08 ± 0.4	1.53 ± 1.0	1.71 ± 0.9	2.20 ± 0.7
Ca (mmol/16h)	Control	0.03 ± 0.0	0.03 ± 0.0	0.03 ± 0.0	0.03 ± 0.0
	Cisplatin	0.02 ± 0.0	0.03 ± 0.0	0.08 ± 0.0	0.18 ± 0.0*
K (mmol/16h)	Control	4.02 ± 0.2	4.42 ± 0.4	4.72 ± 0.3	4.46 ± 0.3
	Cisplatin	3.80 ± 0.5	2.52 ± 0.6**	2.62 ± 1.4	3.88 ± 1.4
PO4 (mmol/16h)	Control	0.16 ± 0.0	0.05 ± 0.0	0.04 ± 0.0	0.07 ± 0.0
	Cisplatin	0.13 ± 0.0	0.59 ± 0.3*	0.19 ± 0.1	0.05 ± 0.0

Table 4 Changes in urine biochemistry in control (n= 3) and cisplatin-treated (n= 15) groups. Values were normalized to the volume of urine produced in 16 hours. Data are shown as means ± SD. Values significantly different from control are indicated as *p< 0.05 and **p< 0.005

Cisplatin administration induced a significant albuminuria from day 2 onwards with respect to the corresponding controls (p<0.005). Specifically, albumin concentration increased by 15, 22 and 18-fold on day 2, 7 and 14 respectively. Additionally, cisplatin-treated animals also developed progressive glycosuria. Glucose levels in treated animals increased by 17.2-fold on day 7 (p<0.05) until 26.8-fold on day 14 (p<0.05) (Figure 11).

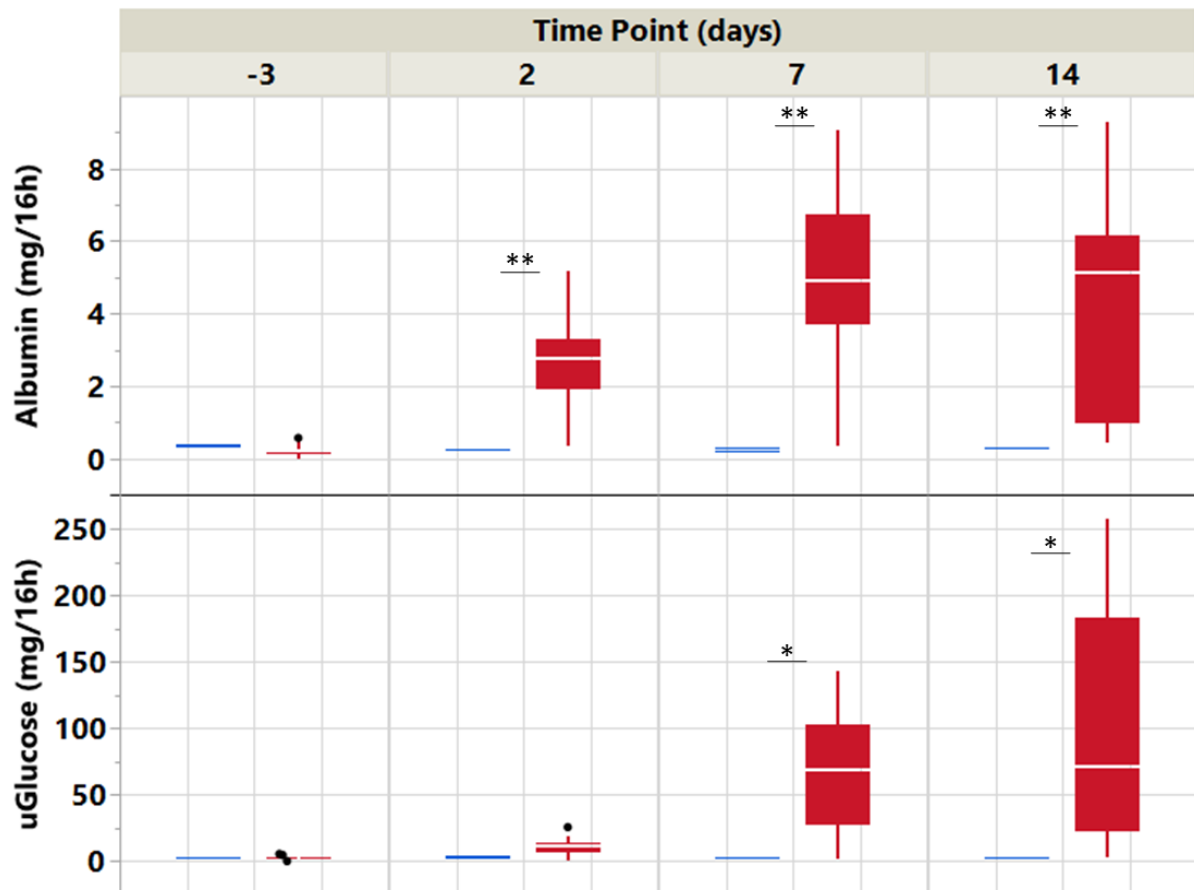


Figure 11 Albuminuria and glycosuria induced by cisplatin administration. Control group n=3 in blue, cisplatin-treated group n=15 in red. Values were normalized to the volume of urine produced in 16 hours. Statistically significant differences are indicated as *p< 0.05 and **p<0.005

Concerning the urine electrolytes, hypokalemia ($p<0.005$) and hyperphosphaturia ($p<0.05$) were observed from day 2 in the treated animals compared to the time-matched control. Both parameters returned to basic levels on day 14. Additionally, calcium concentration significantly increased in cisplatin-treated animals on day 14 ($p<0.05$) (Figure 12).

In contrast, sodium level in the urine remained stable in both groups.

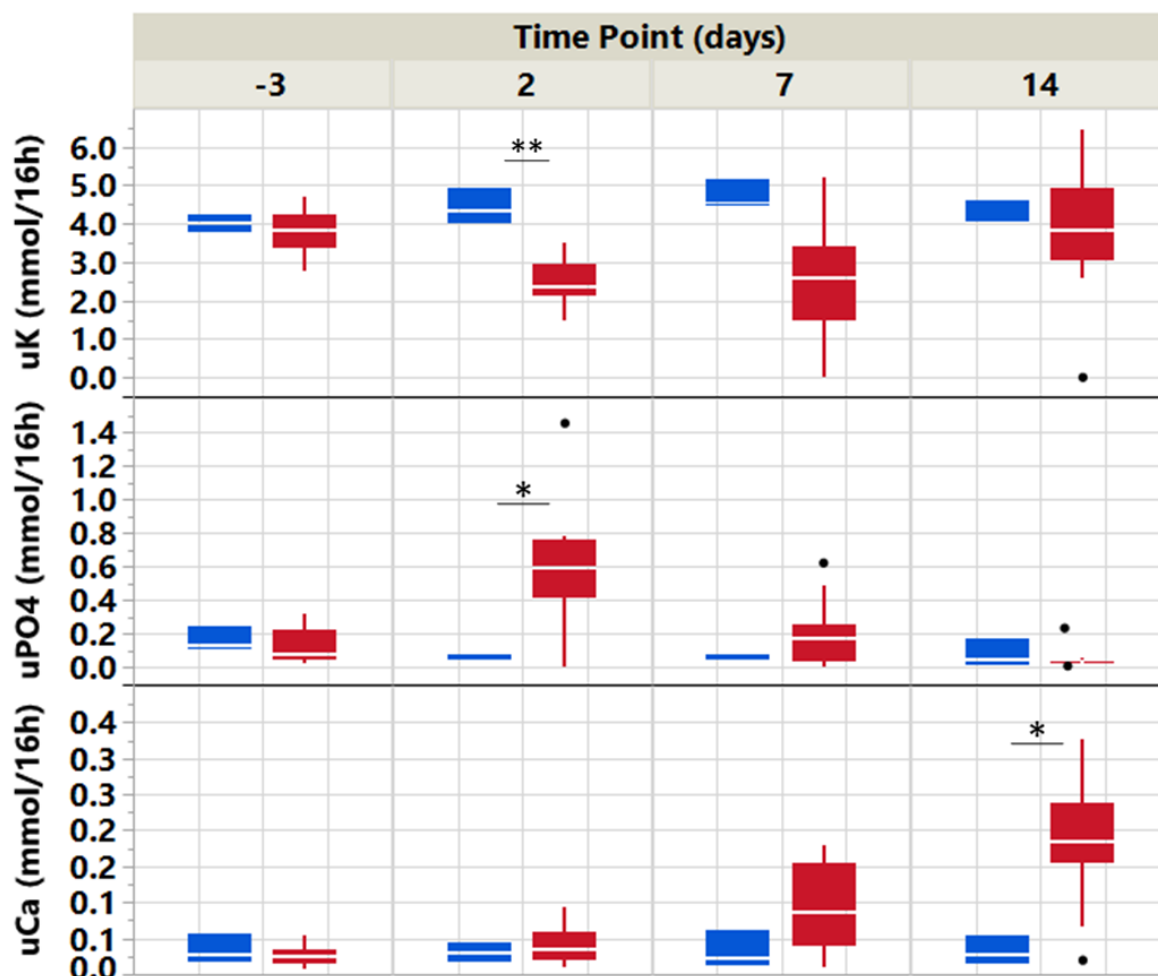


Figure 12 Effect of cisplatin administration in urine potassium phosphate and calcium concentrations. Control group n=3 in blue, cisplatin-treated group n=15 in red. Values were normalized to the volume of urine produced in 16 hours. Statistically significant differences are indicated as * $p < 0.05$ and ** $p < 0.005$

No statistically significant differences were found among the groups for urine levels of urea and protein.

4.1.3. Cisplatin effect on renal function

The transcutaneous assessment of renal function was performed as described in section 3.4. As shown in Table 5 and Figure 13, ABZWYC-HP β CD half-life significantly increased by 1.8-fold already 2 days after cisplatin administration ($p < 0.05$) and remained high until the end of the experiment, increasing by 2.1-fold on day 14. The observed changes in ABZWYC-HP β CD elimination curves represent the loss in renal function.

Parameter	Group	Baseline	Day 2	Day 7	Day 14
Half-life (min)	Control	39.80 ± 0.0	39.93 ± 1.2	33.10 ± 2.9	32.30 ± 2.1
	Cisplatin	38.67 ± 7.8	69.64 ± 10.3 *	68.01 ± 19.0	82.73 ± 38.3*

Table 5 Changes in ABZWCY-HP β CD half-life. Control group n=3 in blue, cisplatin-treated group n=15 in red. Data are shown as means \pm SD. Values significantly different from control are indicated as *p< 0.05 and **p< 0.005

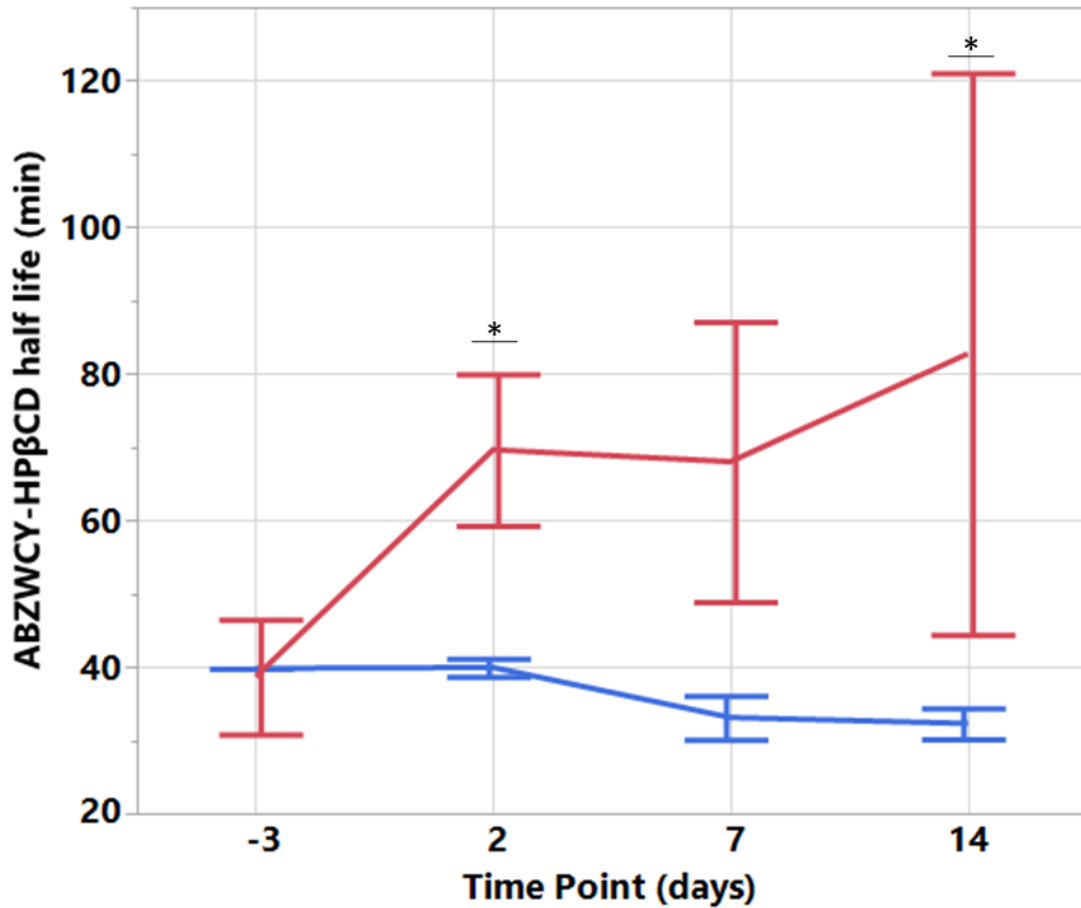


Figure 13 Transcutaneous assessment of renal function. Effect of cisplatin administration on ABZWCY-HP β CD half-life. Control group n=3 in blue, cisplatin-treated group n=15 in red. Data are shown as means \pm SD. Statistically significant differences are indicated as *p< 0.05

4.1.4. Cisplatin effect on body weight, diuresis, food and water intake

Before and after being in metabolic cages for 16 hours, changes in diuresis, BW, food and water intake were recorded. The values are summarized in Table 6

Parameter	Group	Baseline	Day 2	Day 7	Day 14
Diuresis (ml/16h)	Control	10.93 ± 1.9	10.5 ± 1.1	11.86 ± 1.1	14.50 ± 2.3
	Cisplatin	11.68 ± 2.0	16.1 ± 10.8	36.03 ± 10.0*	37.19 ± 2.4*
Water intake (ml/16h)	Control	30.83 ± 1.8	34.26 ± 2.0	33.90 ± 2.9	29.30 ± 5.9
	Cisplatin	26.38 ± 2.9*	23.38 ± 16.8	56.35 ± 18.7*	55.75 ± 12.5*
Body weight (g)	Control	360.33 ± 41.3	409.83 ± 22.0	435.33 ± 12.5	455.33 ± 18.0
	Cisplatin	366.53 ± 33.5	395.46 ± 37.1	376.80 ± 49.8*	386.26 ± 53.3*
Food intake (g/16h)	Control	20.96 ± 5.2	26.26 ± 2.6	24.86 ± 1.4	22.43 ± 4.6
	Cisplatin	19.54 ± 3.1	8.93 ± 5.8**	15.86 ± 5.3*	21.38 ± 3.0

Table 6 Changes in body weight, diuresis, food and water intake before and after metabolic cage allocation in control (n=3) and cisplatin-treated (n=15) groups. Data are shown as means ± SD. Values significantly different from control are indicated as *p< 0.05 and **p< 0.005

Diuresis visibly increased on day 7 and 14 by 3 and 2.5-fold respectively (p<0.05) in the cisplatin group compared to the control one. Accordingly, the water intake also increased by 1.6-fold on day 7 and significantly by 1.9-fold on day 14 (p<0.05) (Figure 14)

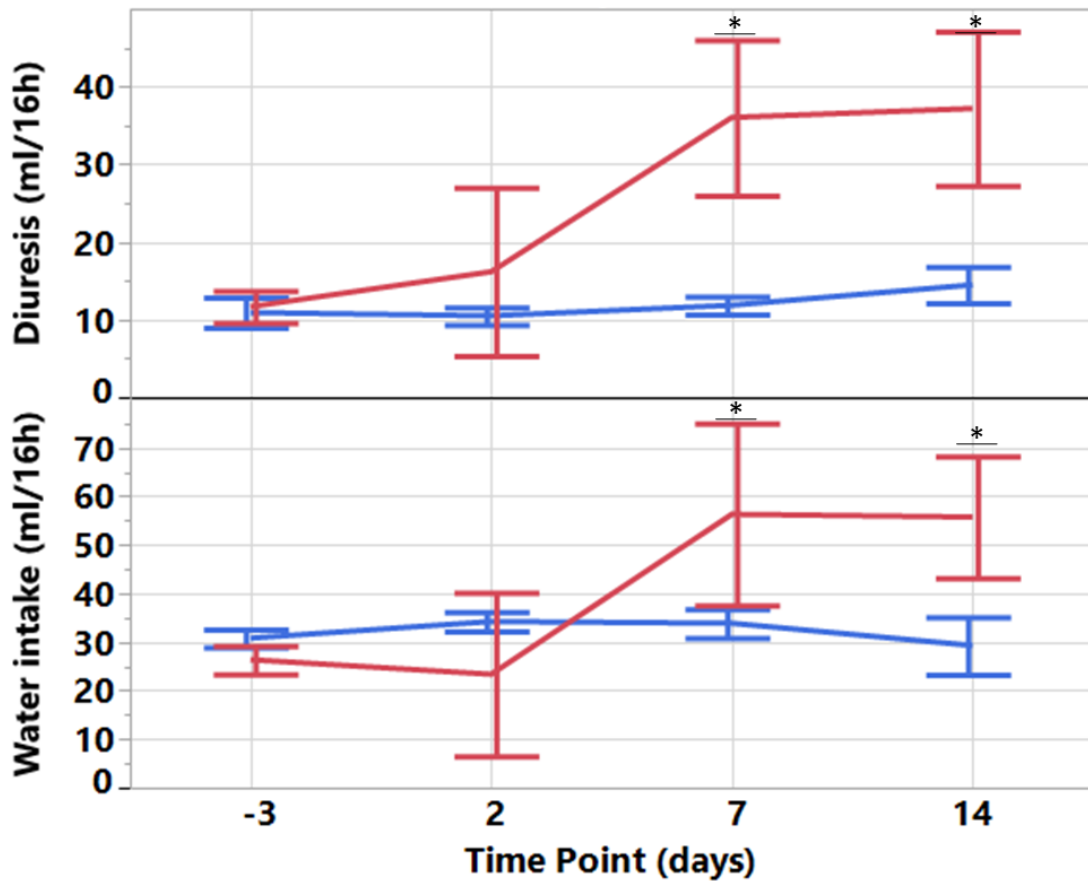


Figure 14 Effect of cisplatin on diuresis and water intake. Control group n=3 in blue, cisplatin-treated group n=15 in red. Data are shown as means \pm SD. Statistically significant differences are indicated as * $p < 0.05$

Already 2 days after cisplatin administration, animals ate less and stopped gaining weight ($p < 0.05$). On day 14, the loss of weight gain became evident. After the first week, the treated animals restarted eating, reaching the basal food intake values on day 14. In contrast, in control animals the food intake remained quite stable while the BW gain progressively increased over time with respect to baseline values (Figure 15)

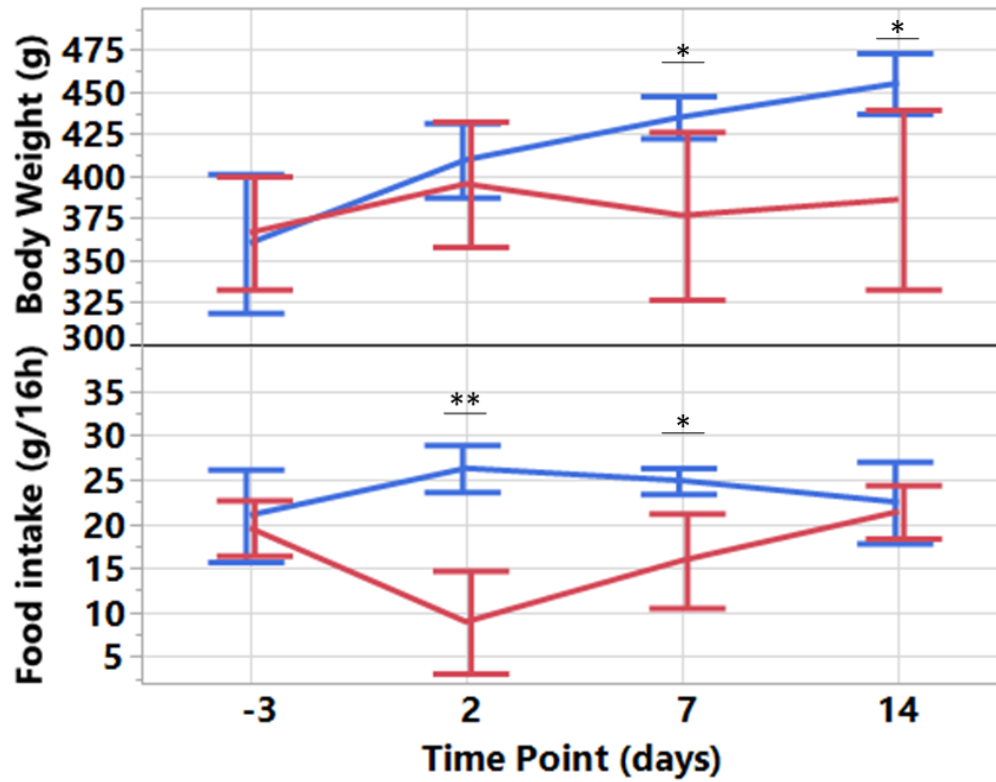


Figure 15 Effect of cisplatin on body weight and food intake. Control group n=3 in blue, cisplatin-treated group n=15 in red. Data are shown as means \pm SD. Statistically significant differences are indicated as * $p < 0.05$ and ** $p < 0.005$

4.1.5. Cisplatin effect on renal morphology

H&E kidney sections have revealed profound changes in the renal cytoarchitecture due to cisplatin administration (Figure 16 and Figure 17). The cortical region was the most affected area. Proximal tubules appeared highly degenerated with tubular cells detached from the basal membrane. Proximal tubule lumen appeared dilated (black asterisks) and was often filled with protein casts or dregs of extruded necrotic cells (green arrows and asterisks). Around the tubules, fibrotic tissue deposition and inflammatory cell infiltration were detected (yellow arrows). Due to the kidney's self-recovery capacity, flat regenerating distal tubular cells were also present. These histological observations indicate that the kidney injury model was successfully established.

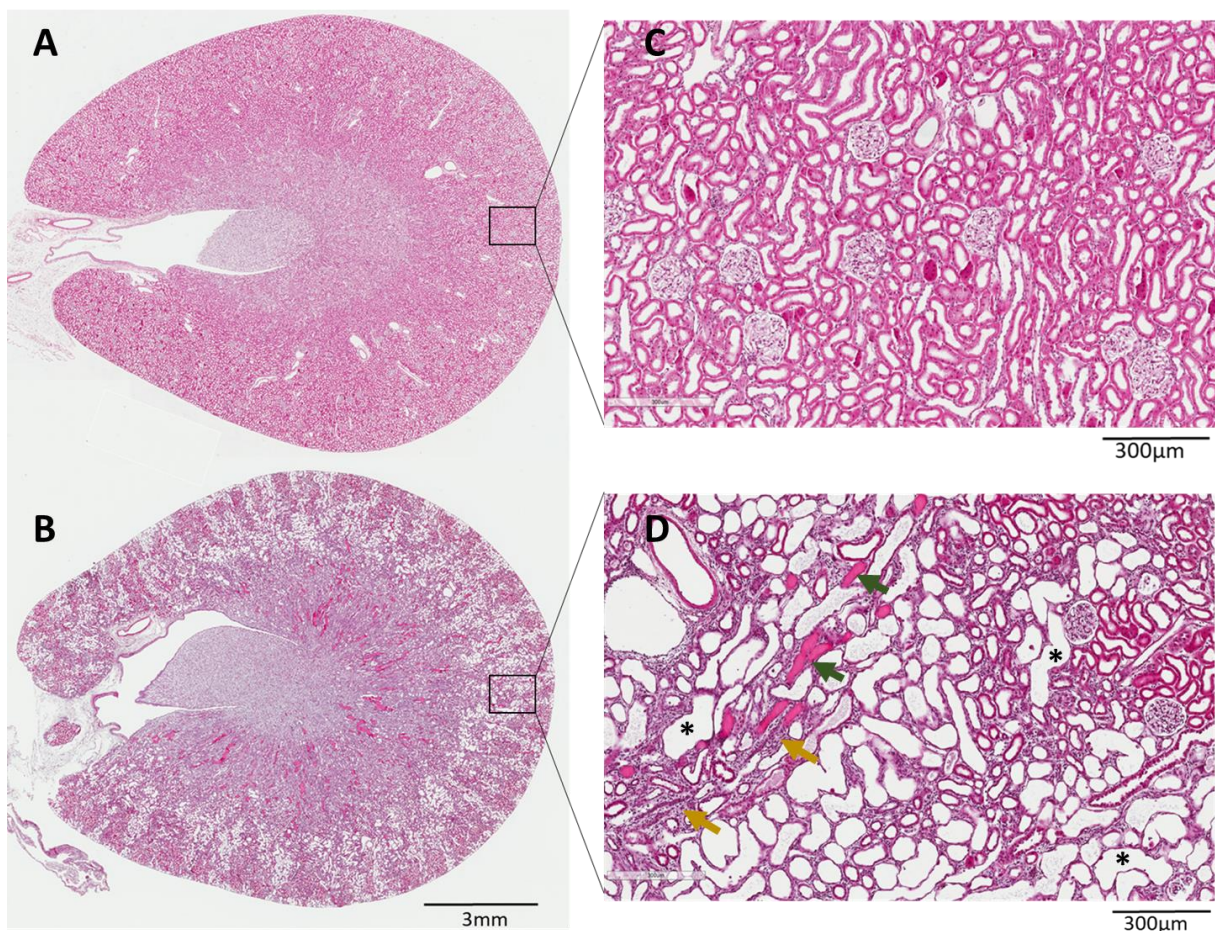


Figure 16 Effect of cisplatin on renal morphology. Whole kidney scan of a control (A) and a cisplatin-treated rat (B) and corresponding magnification of the corticomedullary region (C, D) showing the altered cytoarchitecture due to the induced damage. Black asterisks: proximal tubular dilatation; green arrows: protein casts; yellow arrows: new fibrotic tissue and inflammatory cell infiltrates. H&E staining. Images acquired with Axio Scan.Z1 microscope (ZEISS).

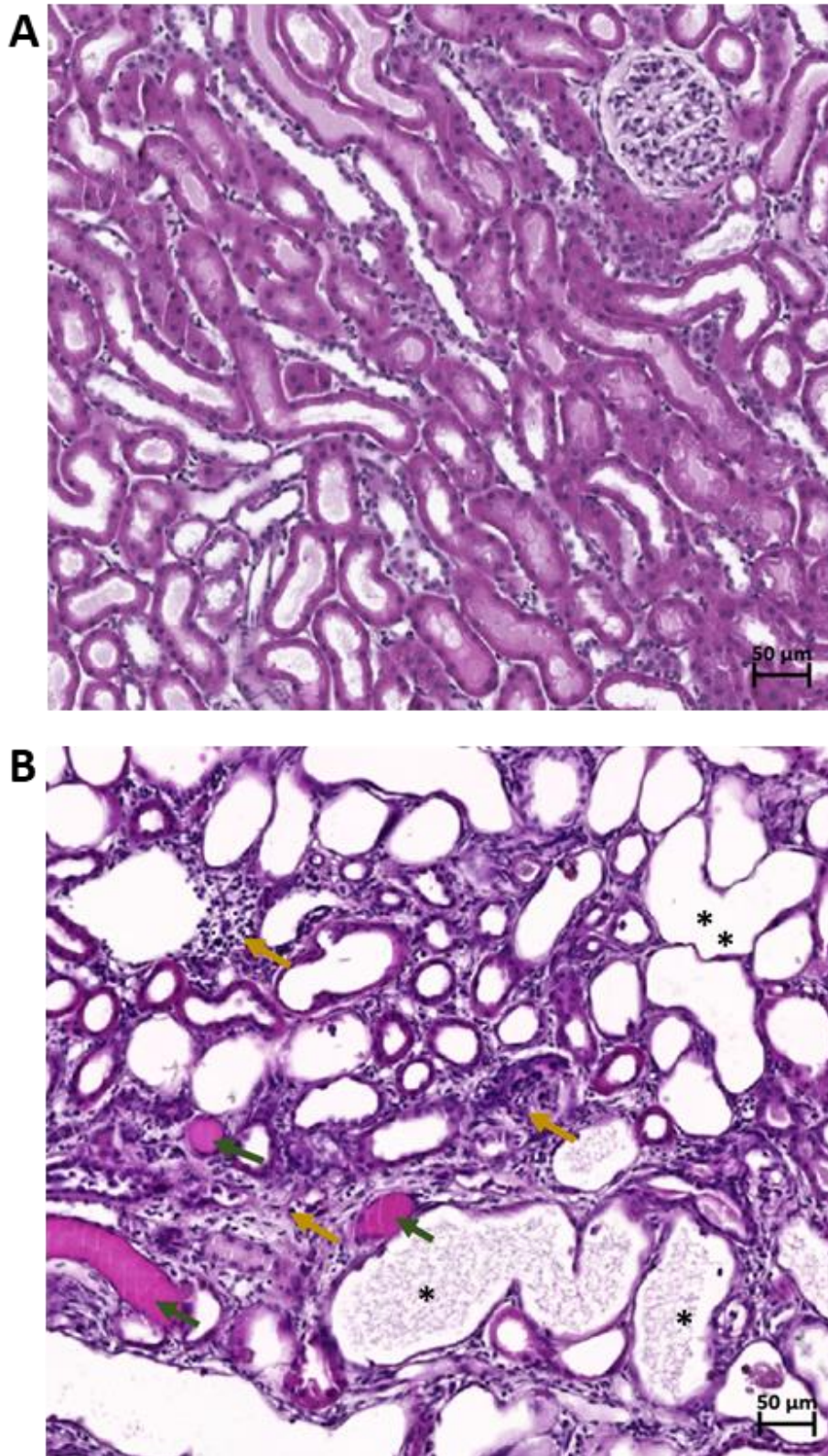


Figure 17 Effect of cisplatin on renal morphology. Magnification of the kidney cortical region of a cisplatin treated animal. Black asterisks: proximal tubular dilatation; green arrows: protein casts; yellow arrows: new fibrotic tissue and inflammatory cell infiltrates. H&E staining. Images acquired with Axio Scan.Z1 microscope (ZEISS).

4.2. Therapeutic effect of ABCB5+ cells and conditioned media in cisplatin-induced nephrotoxicity model in SD rats

Three days after cisplatin administration, the therapeutic potential of ABCB5+ cells and different conditioned media was tested. The following experimental groups were created: ivABCB5+, ipABCB5+, CM, CM+, coCM and vehicle. For monitoring the state of health of the animals and for characterizing any possible effect due to the treatments, blood and urine were sampled for biochemical analyses, renal function was assessed and metabolic parameters were recorded 3 days before (baseline) and 2, 7 and 14 days after cisplatin administration. Kruskal-Wallis each paired comparison test of treated animals vs cisplatin-treated animals was applied and nominal p-values <0.05 (*) or <0.005 (***) were considered as statistically significant. 15 days after cisplatin administration, fresh left kidney was collected for gene expression analysis, while the other organs were collected after animal perfusion for histological evaluation.

4.2.1. ABCB5+ cells/conditioned media effect on plasma parameters

Plasma sampling was performed as described in section 3.3. Plasma biochemical results are summarized in Table 7.

Parameter	Group	Baseline	Day 2	Day 7	Day 14
Creatinine (mg/dl)	Cisplatin	0.26 ± 0.0	0.45 ± 0.0	2.13 ± 1.5	0.83 ± 0.2
	iv ABCB5+	0.25 ± 0.0	0.47 ± 0.0	2.45 ± 1.7	1.04 ± 0.4
	ip ABCB5+	0.23 ± 0.0	0.46 ± 0.0	2.06 ± 1.4	1.40 ± 1.8
	CM	0.20 ± 0.0	0.33 ± 0.0*	0.54 ± 0.1*	0.52 ± 0.1
	CM+	0.17 ± 0.0	0.35 ± 0.0	0.89 ± 0.4	0.58 ± 0.1
	CoCM+	0.21 ± 0.0	0.37 ± 0.0**	1.43 ± 0.6	0.68 ± 0.1*
	Vehicle	0.24 ± 0.0	0.50 ± 0.0	1.37 ± 0.6	0.82 ± 0.1
Urea (mg/dl)	Cisplatin	35.36 ± 4.4	67.17 ± 4.1	258.70 ± 195.9	83.23 ± 30.5
	iv ABCB5+	34.60 ± 4.4	71.75 ± 10.9	267.35 ± 162.0	120.93 ± 85.7
	ip ABCB5+	36.03 ± 3.1	72.76 ± 9.8	258.67 ± 184.6	87.61 ± 32.9
	CM	34.30 ± 3.6	40.83 ± 5.3*	85.97 ± 33.4	56.43 ± 14.2
	CM+	35.03 ± 4.9	52.63 ± 0.1	140.07 ± 63.7	63.40 ± 5.4
	CoCM+	32.19 ± 4.6	60.63 ± 12.8	233.94 ± 81.0	74.54 ± 15.0
	Vehicle	33.50 ± 1.8	72.93 ± 11.9	161.67 ± 73.9	72.77 ± 22.4

Glucose (mg/dl)	Cisplatin	149.06 ± 7.8	158.66 ± 18.2	160.33 ± 13.1	142.53 ± 6.9
	iv ABCB5+	158.08 ± 18.1	164.08 ± 15.0	150.17 ± 18.5*	154.67 ± 12.1*
	ip ABCB5+	173.18 ± 38.0	153.72 ± 6.9	156.00 ± 18.5	141.09 ± 6.47
	CM	159.67 ± 4.5	166.33 ± 4.7	167.00 ± 13.9	158.00 ± 4.58*
	CM+	168.33 ± 9.0	167.33 ± 11.4	153.00 ± 4.3	147.67 ± 4.16
	CoCM+	156.54 ± 6.9	163.27 ± 13.2	158.09 ± 30.0	149.91 ± 13.8
	Vehicle	159.33 ± 9.9	159.33 ± 15.6	147.67 ± 8.9	155.33 ± 5.7*
Protein (mg/dl)	Cisplatin	55.53 ± 1.8	60.26 ± 2.1	55.66 ± 2.9	56.26 ± 3.1
	iv ABCB5+	55.50 ± 2.5	59.41 ± 1.9	55.75 ± 2.9	57.92 ± 2.3
	ip ABCB5+	56.72 ± 2.4	60.81 ± 2.7	54.54 ± 2.4	56.91 ± 1.7
	CM	54.00 ± 3.0	56.67 ± 1.5*	56.00 ± 2.6	57.33 ± 0.6
	CM+	56.67 ± 1.5	59.33 ± 2.1	57.00 ± 1.7	58.00 ± 0.0
	CoCM+	54.72 ± 2.1	58.18 ± 3.4	53.91 ± 4.7	55.54 ± 1.9
	Vehicle	58.33 ± 2.1	59.00 ± 4.3	54.33 ± 2.1	55.33 ± 4.7
Cholesterol (mg/dl)	Cisplatin	96.00 ± 12.5	140.20 ± 21.5	113.20 ± 24.3	117.93 ± 15.7
	iv ABCB5+	100.17 ± 10.5	142.42 ± 11.1	118.17 ± 13.9	129.58 ± 22.5
	ip ABCB5+	94.18 ± 14.0	148.36 ± 21.3*	105.82 ± 17.3	114.00 ± 17.2
	CM	107.67 ± 14.9	138.67 ± 17.6	90.33 ± 14.6	104.33 ± 10.5
	CM+	108.33 ± 15.3	144.67 ± 20.5	106.00 ± 24.9	109.67 ± 9.1
	CoCM+	107.36 ± 16.2	150.27 ± 11.8	117.64 ± 20.5	122.00 ± 14.2
	Vehicle	88.00 ± 8.5	135.67 ± 18.44	117.67 ± 21.4	122.00 ± 23.4
Triglycerides (mg/dl)	Cisplatin	94.40 ± 26.5	73.33 ± 27.0	130.00 ± 37.8	127.33 ± 38.8
	iv ABCB5+	115.58 ± 37.3	66.92 ± 11.1	124.67 ± 33.5	127.83 ± 33.1
	ip ABCB5+	118.00 ± 39.7	68.18 ± 10.0	127.18 ± 50.3	148.73 ± 45.3
	CM	131.67 ± 16.7	64.67 ± 3.2	215.00 ± 41.6*	178.00 ± 56.4
	CM+	122.33 ± 26.1	76.33 ± 29.9	182.33 ± 31.9	166.67 ± 37.9
	CoCM+	95.64 ± 29.5	70.54 ± 21.4	115.00 ± 36.4	159.73 ± 37.1
	Vehicle	151.67 ± 57.9	61.67 ± 12.7	156.67 ± 55.7	84.33 ± 21.5
AST (U/l)	Cisplatin	52.8 ± 11.5	39.92 ± 6.7	61.93 ± 35.8	51.20 ± 20.8
	iv ABCB5+	54.00 ± 12.7	37.83 ± 7.0	47.92 ± 16.2	49.17 ± 27.4
	ip ABCB5+	64.45 ± 15.0	43.36 ± 7.7	74.45 ± 25.7	58.27 ± 18.0
	CM	38.00 ± 6.2	39.67 ± 6.0	38.00 ± 32.5	51.33 ± 19.6
	CM+	45.33 ± 16.3	35.67 ± 3.8	67.00 ± 22.9	50.67 ± 33.0
	CoCM+	54.27 ± 13.2	41.45 ± 7.7	71.09 ± 12.6	59.54 ± 12.6
	Vehicle	78.00 ± 6.9	52.33 ± 10.2	76.33 ± 15.9	68.33 ± 33.2
ALT (U/l)	Cisplatin	100.53 ± 5.3	104.46 ± 12.7	97.60 ± 18.5	91.13 ± 14.2
	iv ABCB5+	88.08 ± 14.9	96.75 ± 16.1	90.17 ± 20.0	98.75 ± 30.6
	ip ABCB5+	97.73 ± 27.1	108.81 ± 14.9	98.64 ± 13.9	92.70 ± 13.5
	CM	86.00 ± 1.7	94.33 ± 19.3	87.00 ± 11.1	86.33 ± 2.3
	CM+	86.67 ± 9.6	92.00 ± 10.5	81.33 ± 4.9	81.00 ± 7.2
	CoCM+	87.09 ± 6.6	107.45 ± 23.4	97.09 ± 14.1	80.36 ± 10.2
	Vehicle	88.67 ± 9.9	150.33 ± 50.6	125.67 ± 37.2	101.33 ± 17.7

GGT (U/l)	Cisplatin	3.00 ± 0.0	3.66 ± 0.9	3.26 ± 0.1	3.00 ± 0.0
	iv ABCB5+	3.00 ± 0.0	3.00 ± 0.0	3.17 ± 1.3	3.00 ± 0.0
	ip ABCB5+	3.00 ± 0.0	3.00 ± 0.0	3.54 ± 1.3	3.63 ± 1.3*
	CM	3.00 ± 0.0	3.00 ± 0.0	3.00 ± 0.0	3.00 ± 0.0
	CM+	3.00 ± 0.0	3.00 ± 0.0	3.00 ± 0.0	3.00 ± 0.0
	CoCM+	3.00 ± 0.0	3.00 ± 0.0	3.00 ± 0.0	3.00 ± 0.0
	Vehicle	3.00 ± 0.0	3.00 ± 0.0	2.67 ± 0.6	3.00 ± 0.0
GLDH (U/l)	Cisplatin	8.60 ± 1.3	9.13 ± 2.1	19.2 ± 4.5	4.91 ± 1.2
	iv ABCB5+	7.50 ± 3.5	9.22 ± 1.9	19.94 ± 30.2	6.48 ± 2.7
	ip ABCB5+	6.60 ± 1.4	9.74 ± 1.6	16.72 ± 16.5	6.51 ± 3.9
	CM	6.54 ± 0.5	8.99 ± 1.0	5.18 ± 0.9*	4.93 ± 1.1
	CM+	6.56 ± 0.8	12.24 ± 6.3	7.31 ± 3.4	4.19 ± 0.3
	CoCM+	6.89 ± 1.0	10.58 ± 4.1	12.50 ± 3.9	3.67 ± 0.4*
	Vehicle	6.22 ± 2.0	8.33 ± 1.6	11.99 ± 4.5	6.45 ± 0.7
Na (mmol/l)	Cisplatin	139.53 ± 4.5	140.13 ± 1.5	138.00 ± 4.2	139.36 ± 2.7
	iv ABCB5+	142.75 ± 1.4	140.75 ± 1.2	139.33 ± 2.2	142.00 ± 3.1
	ip ABCB5+	142.45 ± 0.9	141.82 ± 1.2**	141.64 ± 4.4*	141.45 ± 2.5
	CM	139.33 ± 0.6	143.00 ± 1.0*	144.33 ± 3.2*	143.67 ± 0.6*
	CM+	138.00 ± 1.0	141.67 ± 1.1	142.67 ± 2.1*	142.33 ± 3.2
	CoCM+	140.82 ± 1.5	138.82 ± 2.4*	141.36 ± 4.9	140.82 ± 3.6
	Vehicle	143.67 ± 2.9	140.33 ± 2.1	139.67 ± 1.5	140.00 ± 2.6
Ca (mmol/l)	Cisplatin	2.71 ± 0.0	2.73 ± 0.0	4.75 ± 7.6	2.84 ± 0.0
	iv ABCB5+	2.71 ± 0.1	2.72 ± 0.0	2.89 ± 0.2	2.88 ± 0.1
	ip ABCB5+	2.71 ± 0.1	2.75 ± 0.1	2.80 ± 0.1	2.80 ± 0.1
	CM	2.71 ± 0.1	2.67 ± 0.1	2.74 ± 0.1	2.85 ± 0.1
	CM+	2.73 ± 0.0	2.69 ± 0.0	2.81 ± 0.1	2.88 ± 0.0
	CoCM+	2.71 ± 0.0	2.70 ± 0.0	2.74 ± 0.1	2.88 ± 0.1
	Vehicle	2.76 ± 0.0	2.73 ± 0.0	2.84 ± 0.1	2.69 ± 0.1
K (mmol/l)	Cisplatin	4.95 ± 0.3	4.19 ± 0.3	4.77 ± 0.5	5.55 ± 0.6
	iv ABCB5+	5.20 ± 0.3	4.14 ± 0.2	5.34 ± 0.4*	5.90 ± 0.6
	ip ABCB5+	5.37 ± 0.4	4.28 ± 0.2	5.08 ± 0.4	5.43 ± 0.5
	CM	5.11 ± 0.3	4.38 ± 0.5	5.13 ± 0.3	5.59 ± 0.3
	CM+	5.69 ± 0.2	4.19 ± 0.1	5.63 ± 0.1*	6.45 ± 0.5
	CoCM+	5.26 ± 0.2	4.15 ± 0.3	4.99 ± 0.6	5.84 ± 0.6
	Vehicle	5.14 ± 0.3	4.26 ± 0.2	4.94 ± 0.2	5.77 ± 0.7
PO4 (mmol/l)	Cisplatin	2.75 ± 0.1	2.47 ± 0.2	2.20 ± 0.9	1.41 ± 0.5
	iv ABCB5+	2.51 ± 0.3	2.46 ± 0.2	2.07 ± 1.0	1.32 ± 0.3
	ip ABCB5+	2.57 ± 0.4	2.51 ± 0.2	1.89 ± 0.6	1.34 ± 0.6
	CM	2.64 ± 0.2	2.70 ± 0.1	1.47 ± 0.4	1.99 ± 0.4
	CM+	2.71 ± 0.1	2.73 ± 0.1	1.46 ± 0.2	1.70 ± 0.5
	CoCM+	2.44 ± 0.1	2.47 ± 0.2	1.65 ± 0.5	1.23 ± 0.3
	Vehicle	2.33 ± 0.3	2.40 ± 0.3	1.74 ± 0.2	1.61 ± 0.6

Table 7 Changes in plasma biochemistry in the experimental groups (cisplatin n=15; iv ABCB5+ n=12; ip ABCB5+ n=11; CM n=3; CM+ n=3; CoCM+ n=11; Vehicle n=3). Data are shown as means \pm SD. Values significantly different from cisplatin group are indicated as * $p < 0.05$ and ** $p < 0.005$

On day 7, plasma creatinine decreased by 3.9 ($p < 0.05$), 2.4 and 1.5 times in animals treated with CM, CM+ and co-CM+ respectively when compared to the cisplatin treated group, and remain low on day 14. Plasma urea decreased on day 7 by 3 and 1.8 times in animals treated with CM and CM+ respectively and remain low on day 14 when compared to the cisplatin treated group. No particular changes were found in animals who received ABCB5+ cells compared to cisplatin treated animals (Figure 18).

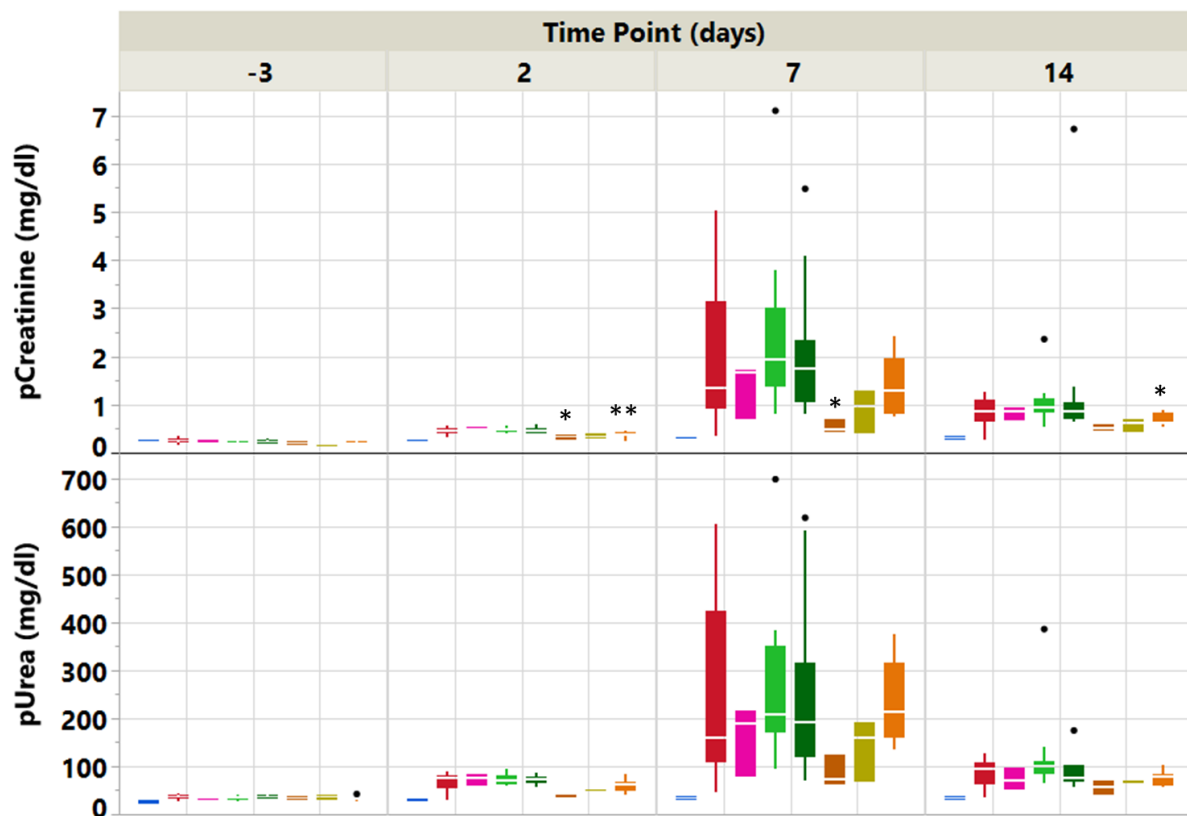


Figure 18 Effect of different treatments on a cisplatin-induced nephrotoxicity model in plasma creatinine and urea concentration. Statistically significant differences (treatment vs cisplatin) are indicated as * $p < 0.05$ and ** $p < 0.005$.

Control n=3; Cisplatin n=15; iv ABCB5+ n=12; ip ABCB5+ n=11; CM n=3; CM+ n=3; coCM+ n=11; vehicle n=3;

Among the hepatic enzymes, GLDH levels decreased on day 7 by 3.7 ($p < 0.05$) and 2.6 times in animals treated with CM and CM+ respectively. On day 14, GLDH levels were found significantly decreased by 1.3 times in co-CM+ treated animals compared to the cisplatin model. No changes were found in animals who received ABCB5+ cells compared to cisplatin treated animals (Figure 19).

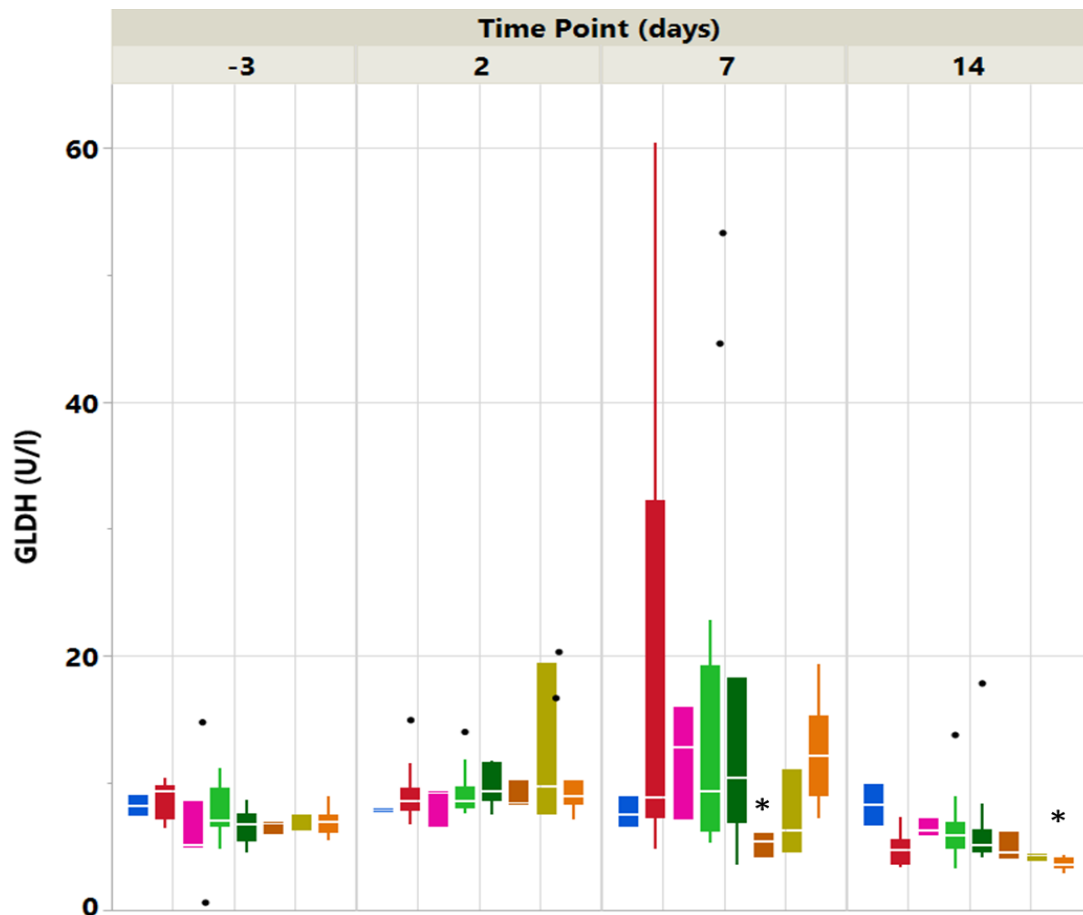


Figure 19 Effect of different treatments on a cisplatin-induced nephrotoxicity model in plasma GLDH level. Statistically significant differences (treatment vs cisplatin) are indicated as * $p < 0.05$ and ** $p < 0.005$.

Control n=3; Cisplatin n=15; iv ABCB5+ n=12; ip ABCB5+ n=11; CM n=3; CM+ n=3; coCM+ n=11; vehicle n=3;

Plasma triglycerides significantly increase on day 7 ($p < 0.05$) in animals treated with CM compared with the cisplatin treated group.

No other significant changes of other plasma parameters were observed.

Animals who received the vehicle did not show any particular differences in plasma parameters compared to the cisplatin-treated animals.

4.2.2. ABCB5+ cells/conditioned media effect on urine parameters

Urine was collected as described in section 3.3. Urine biochemistry results are summarized in Table 8.

Parameter	Group	Baseline	Day 2	Day 7	Day 14
Creatinine (mg/16h)	Cisplatin	7.24 ± 1.4	8.19 ± 2.3	7.10 ± 2.2	7.94 ± 1.8
	iv ABCB5+	7.51 ± 1.6	7.92 ± 1.9	7.01 ± 2.0	7.04 ± 1.5
	ip ABCB5+	7.51 ± 1.2	6.86 ± 1.5	6.99 ± 1.3	7.15 ± 1.4
	CM	5.39 ± 0.6	9.94 ± 2.5	8.35 ± 1.4	8.09 ± 1.4
	CM+	4.87 ± 0.5	6.22 ± 0.5*	7.11 ± 0.6	7.24 ± 1.1
	CoCM+	5.51 ± 0.7	5.53 ± 1.3**	6.94 ± 1.5	5.31 ± 1.8**
	Vehicle	8.0 ± 1.9	8.69 ± 1.0	8.23 ± 1.1	8.88 ± 2.8
Urea (mg/16h)	Cisplatin	431.60 ± 82.5	496.33 ± 129.7	616.61 ± 220.5	588.45 ± 82.1
	iv ABCB5+	460.11 ± 106.6	430.26 ± 109.26	537.44 ± 159.9	560.55 ± 89.4
	ip ABCB5+	446.76 ± 155.2	438.63 ± 45.52	555.73 ± 93.1	546.64 ± 114.2
	CM	379.38 ± 39.2	655.66 ± 205.9	993.00 ± 302.8	540.42 ± 66.0
	CM+	409.05 ± 21.7	417.28 ± 117.1	638.72 ± 125.7	548.10 ± 83.3
	CoCM+	421.85 ± 81.0	350.14 ± 94.4**	721.38 ± 192.7	485.28 ± 167.3
	Vehicle	424.89 ± 163.2	447.56 ± 88.9	584.9 ± 180.6	512.14 ± 72.4
Glucose (mg/16h)	Cisplatin	3.33 ± 1.1	10.81 ± 6.9	63.37 ± 42.3	100.76 ± 87.5
	iv ABCB5+	4.08 ± 1.0	8.01 ± 3.8	81.39 ± 47.3	89.80 ± 73.6
	ip ABCB5+	4.05 ± 0.8	6.18 ± 4.5	61.49 ± 25.7	98.12 ± 117.4
	CM	2.17 ± 1.8	1.99 ± 2.1	4.75 ± 4.8*	0.87 ± 0.1**
	CM+	2.44 ± 1.9	5.35 ± 6.0	39.88 ± 31.4	78.24 ± 118.4
	CoCM+	3.56 ± 0.8	4.29 ± 3.7*	56.56 ± 29.6	50.95 ± 56.8
	Vehicle	3.67 ± 0.5	10.72 ± 2.7	39.91 ± 28.9	80.57 ± 65.5
Protein (mg/16h)	Cisplatin	8.12 ± 3.2	12.9 ± 1.1	8.85 ± 3.1	12.17 ± 4.6
	iv ABCB5+	7.80 ± 3.2	12.11 ± 4.5	9.32 ± 3.8	10.41 ± 4.1
	ip ABCB5+	8.96 ± 3.3	11.34 ± 3.6	9.18 ± 2.6	14.18 ± 5.0
	CM	4.41 ± 1.5	9.42 ± 2.4	10.22 ± 6.5	10.03 ± 1.5
	CM+	5.16 ± 1.1	10.95 ± 3.4	9.94 ± 0.8	11.67 ± 2.7
	CoCM+	6.04 ± 2.8	12.50 ± 19.6*	8.41 ± 2.0	8.56 ± 4.9
	Vehicle	9.73 ± 4.7	16.13 ± 7.2	9.43 ± 1.8	15.03 ± 1.2

Albumin (mg/16h)	Cisplatin	0.21 ± 0.1	2.71 ± 1.3	4.92 ± 2.3	4.24 ± 2.8
	iv ABCB5+	0.25 ± 0.1	2.67 ± 0.7	4.68 ± 1.8	4.67 ± 3.1
	ip ABCB5+	0.21 ± 0.0	2.63 ± 0.8	5.05 ± 1.7	5.03 ± 3.0
	CM	0.21 ± 0.0	1.44 ± 0.1	3.43 ± 3.2	1.08 ± 0.7
	CM+	0.20 ± 0.1	2.26 ± 0.9	3.13 ± 0.4	2.01 ± 1.4
	CoCM+	0.23 ± 0.1	1.79 ± 0.5*	4.82 ± 1.4	2.28 ± 2.3
	Vehicle	0.30 ± 0.1	2.59 ± 0.7	3.60 ± 1.0	4.09 ± 2.8
Na (mmol/16h)	Cisplatin	2.08 ± 0.4	1.53 ± 1.0	1.71 ± 0.9	2.20 ± 0.7
	iv ABCB5+	1.94 ± 0.4	1.13 ± 0.4	1.57 ± 0.7	2.48 ± 0.7
	ip ABCB5+	1.85 ± 0.3	1.11 ± 0.3	1.46 ± 0.6	2.24 ± 0.3
	CM	1.92 ± 0.0	1.54 ± 0.5	1.25 ± 0.8	2.73 ± 0.7
	CM+	2.03 ± 0.4	1.20 ± 0.1	1.19 ± 0.8	2.83 ± 0.5
	CoCM+	2.16 ± 0.6	1.07 ± 0.3	1.08 ± 0.5*	2.04 ± 0.8
	Vehicle	1.81 ± 0.8	1.17 ± 0.1	1.01 ± 0.1	1.99 ± 0.8
Ca (mmol/16h)	Cisplatin	0.02 ± 0.0	0.03 ± 0.0	0.08 ± 0.0	0.18 ± 0.0
	iv ABCB5+	0.02 ± 0.0	0.04 ± 0.0	0.11 ± 0.0	0.19 ± 0.1
	ip ABCB5+	0.02 ± 0.0	0.04 ± 0.0	0.10 ± 0.0	0.19 ± 0.1
	CM	0.02 ± 0.0	0.10 ± 0.1	0.09 ± 0.0	0.19 ± 0.1
	CM+	0.03 ± 0.0	0.04 ± 0.0	0.11 ± 0.1	0.18 ± 0.1
	CoCM+	0.03 ± 0.0	0.04 ± 0.0	0.08 ± 0.0	0.22 ± 0.1
	Vehicle	0.01 ± 0.0	0.03 ± 0.0	0.10 ± 0.0	0.18 ± 0.1
K (mmol/16h)	Cisplatin	3.80 ± 0.5	2.52 ± 0.6	2.62 ± 1.4	3.88 ± 1.4
	iv ABCB5+	3.76 ± 0.9	2.27 ± 0.5	2.42 ± 0.8	3.76 ± 0.8
	ip ABCB5+	3.84 ± 0.6	1.90 ± 0.6*	2.51 ± 0.8	4.26 ± 0.8
	CM	4.08 ± 0.3	2.91 ± 0.7	3.54 ± 0.6	6.15 ± 0.4*
	CM+	4.06 ± 0.2	2.14 ± 0.2	2.89 ± 1.3	5.50 ± 0.8
	CoCM+	4.07 ± 0.9	1.88 ± 0.6*	2.16 ± 0.9	3.49 ± 1.1
	Vehicle	3.42 ± 1.0	2.74 ± 0.5	2.72 ± 0.6	4.63 ± 1.4
PO4 (mmol/16h)	Cisplatin	0.13 ± 0.0	0.59 ± 0.3	0.19 ± 0.1	0.05 ± 0.0
	iv ABCB5+	0.11 ± 0.1	0.57 ± 0.1	0.16 ± 0.1	0.05 ± 0.0
	ip ABCB5+	0.14 ± 0.1	0.55 ± 0.1	0.14 ± 0.1	0.04 ± 0.0
	CM	0.10 ± 0.0	0.67 ± 0.1	0.15 ± 0.1	0.05 ± 0.0
	CM+	0.17 ± 0.1	0.60 ± 0.1	0.09 ± 0.1	0.03 ± 0.0*
	CoCM+	0.07 ± 0.0	0.46 ± 0.1	0.21 ± 0.1	0.03 ± 0.0
	Vehicle	0.14 ± 0.1	0.57 ± 0.1	0.20 ± 0.1	0.05 ± 0.0

Table 8 Changes in urine biochemistry in the experimental groups (cisplatin n=15; iv ABCB5+ n=12; ip ABCB5+ n=11; CM n=3; CM+ n=3; CoCM+ n=11; Vehicle n=3). Values were normalized to the volume of urine produced in 16 hours. Data are shown as means ± SD. Values significantly different from cisplatin group are indicated as *p < 0.05 and **p < 0.005.

Urine albumin levels decreased from day 7 onward in animals treated with all kind of conditioned media. On day 14, albuminuria decreased by 4.2, 2.1 and 1.8 times in animals treated with CM, CM+ and co-CM+ respectively when compared to the cisplatin treated group. No changes were found in animals who received ABCB5+ cells compared to the cisplatin treated animals (Figure 20).

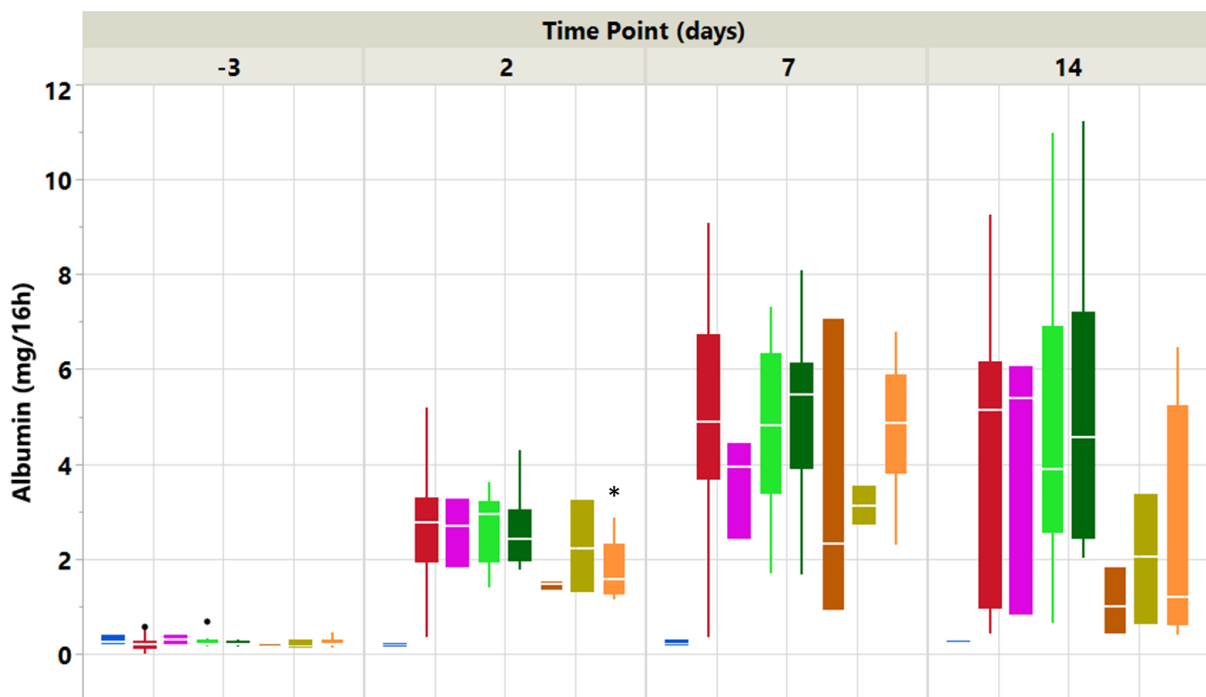


Figure 20 Albuminuria found by different treatments on a cisplatin-induced nephrotoxicity mode. Values were normalized to the volume of urine produced in 16 hours. Statistically significant differences (treatment vs cisplatin) are indicated as * $p < 0.05$ and ** $p < 0.005$.

■ Control n=3; ■ Cisplatin n=15; ■ iv ABCB5+ n=12; ■ ip ABCB5+ n=11; ■ CM n=3; ■ CM+ n=3; ■ coCM+ n=11; ■ vehicle n=3;

Only in CM treated animals, glycosuria significantly decreased on day 7 ($p < 0.05$) and 14 ($p < 0.005$) (Figure 21).

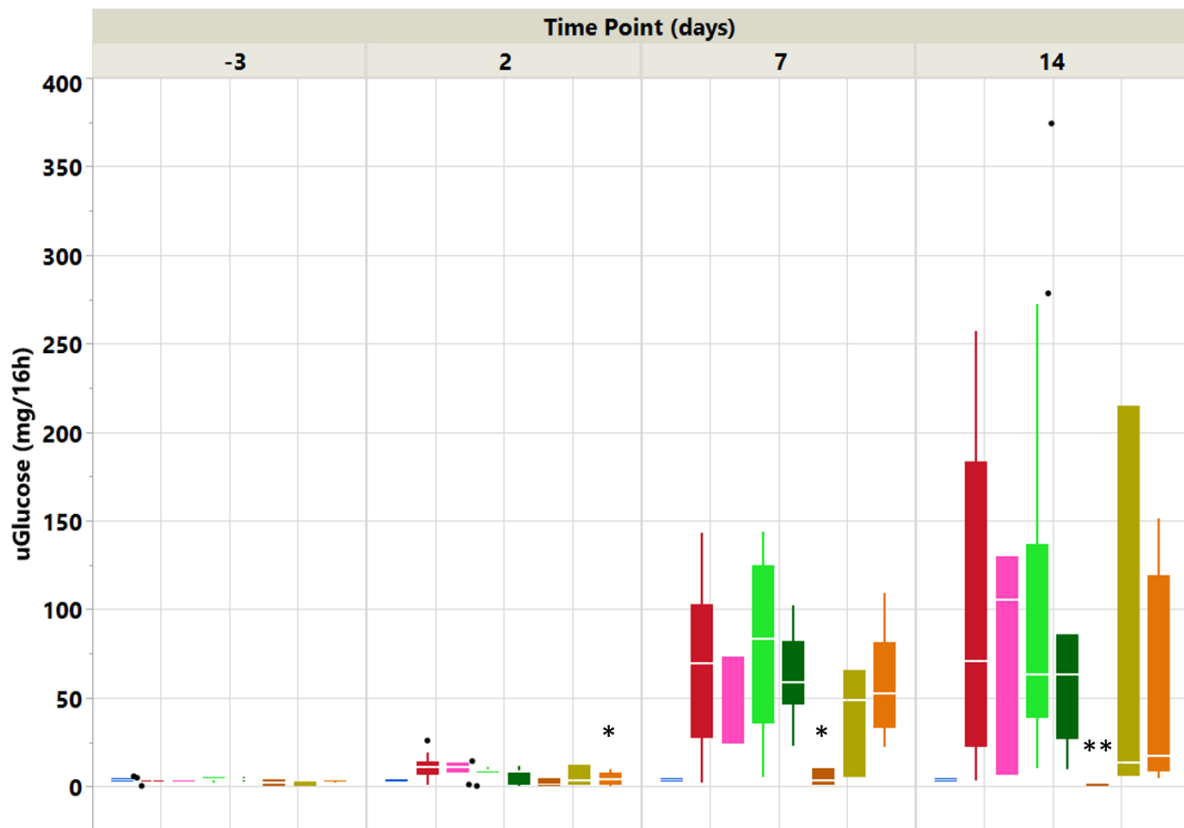


Figure 21 Glycosuria found by different treatments on a cisplatin-induced nephrotoxicity model. Values were normalized to the volume of urine produced in 16 hours. Statistically significant differences (treatment vs cisplatin) are indicated as * $p < 0.05$ and ** $p < 0.005$.

Control n=3; Cisplatin n=15; iv ABCB5+ n=12; ip ABCB5+ n=11; CM n=3; CM+ n=3; coCM+ n=11; vehicle n=3;

No other significant changes of other urine parameters were observed.

Animals who received the vehicle did not show any particular differences in urine parameters compared to the cisplatin-treated animals.

4.2.3. ABCB5+ cells/conditioned media effect on renal function

Transcutaneous assessment of renal function was performed as described in section 3.4. Values of ABZWCY-HP β CD half-life are summarized in Table 9.

Parameter	Group	Baseline	Day 2	Day 7	Day 14
Half-life (min)	Cisplatin	38.67 \pm 7.8	69.64 \pm 10.3	68.01 \pm 19.1	82.73 \pm 38.3
	iv ABCB5+	32.44 \pm 6.7	69.62 \pm 25.9	129.19 \pm 63.2*	100.64 \pm 22.9
	ip ABCB5+	32.12 \pm 6.6	70.11 \pm 18.1	109.50 \pm 40.7*	101.48 \pm 26.8
	CM	31.10 \pm 6.2	29.40 •	61.27 \pm 4.1	68.87 \pm 19.6
	CM+	31.33 \pm 6.9	60.10 •	38.55 \pm 0.2	72.37 \pm 22.7
	CoCM+	32.04 \pm 4.5	59.38 \pm 19.24	115.81 \pm 33.0*	69.15 \pm 20.5
	Vehicle	26.00 \pm 14.9	69.13 \pm 30.12	100.80 \pm 24.4	84.00 \pm 3.8

Table 9 Changes in ABZWCY-HP β CD half-life. Experimental groups: cisplatin n=15; iv ABCB5+ n=12; ip ABCB5+ n=11; CM n=3; CM+ n=3; CoCM+ n=11; vehicle n=3. Data are shown as means \pm SD. Values significantly different from control are indicated as *p< 0.05 and **p< 0.005. • data of only one animal

On day 7, animals treated with ABCB5+ cells and coCM+ showed a higher ABZWCY-HP β CD half-life when compared to the cisplatin treated animals (p<0.05), while the CM+ group had a 1.8-times smaller ABZWCY-HP β CD half-life. One week later, animals treated with the 3 different conditioned media had a similar ABZWCY-HP β CD excretion time, which was lower than in the control, while animals treated with ABCB5+ cells maintained a high ABZWCY-HP β CD half-life (Figure 22).

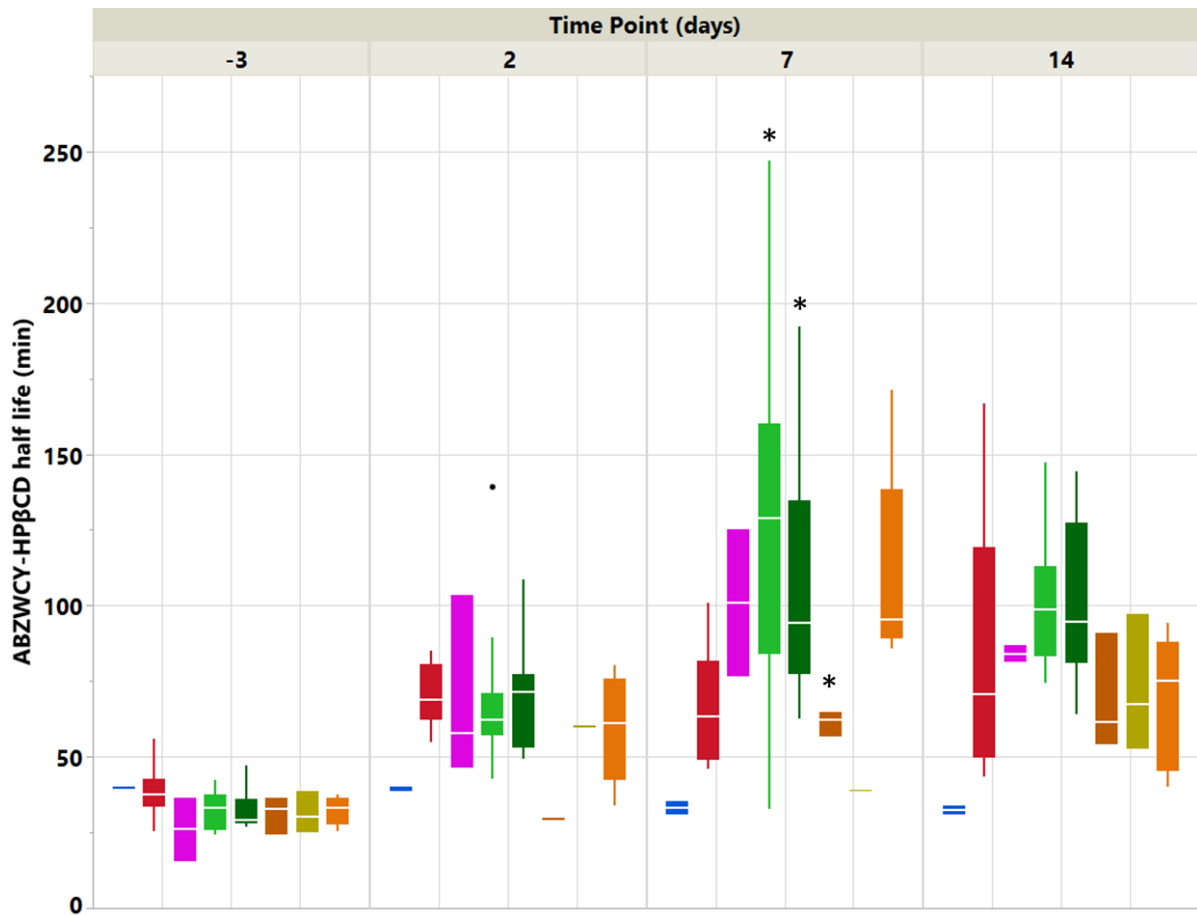


Figure 22 Transcutaneous assessment of renal function (ABZWCY-HPβCD half-life). Effect of different treatments on a cisplatin-induced nephrotoxicity model. Statistically significant differences (treatment vs cisplatin) are indicated as * $p < 0.05$ and ** $p < 0.005$.

Control n=3; Cisplatin n=15; iv ABCB5+ n=12; ip ABCB5+ n=11; CM n=3; CM+ n=3; coCM+ n=11; vehicle n=3;

4.2.4. ABCB5+ cells/conditioned media effect on body weight, diuresis, food and water intake

Before and after being in metabolic cages for 16 hours, changes in diuresis, BW, food and water intake were recorded. The values are summarized in Table 10.

Parameter	Group	Baseline	Day 2	Day 7	Day 14
Diuresis (ml/16h)	Cisplatin	11.68 ± 2.0	16.18 ± 10.8	36.03 ± 10.0	37.19 ± 9.9
	iv ABCB5+	13.55 ± 3.5	16.38 ± 13.5	40.50 ± 15.3	43.10 ± 7.3
	ip ABCB5+	10.85 ± 1.7	16.81 ± 12.8	35.85 ± 3.8	38.18 ± 4.6
	CM	10.46 ± 2.2	30.30 ± 14.4	43.20 ± 7.6	34.70 ± 7.6
	CM+	10.37 ± 1.7	16.00 ± 8.5	31.63 ± 3.9	30.03 ± 2.4
	CoCM+	11.41 ± 3.4	21.23 ± 20.8	43.91 ± 17.9	32.38 ± 9.7
	Vehicle	14.13 ± 3.6	12.63 ± 3.9	39.80 ± 6.6	36.67 ± 7.4
Water intake (ml/16h)	Cisplatin	26.38 ± 2.9	23.38 ± 16.8	56.35 ± 18.7	55.75 ± 12.5
	iv ABCB5+	29.16 ± 4.7	21.50 ± 15.3	60.27 ± 13.4	61.09 ± 9.3
	ip ABCB5+	25.50 ± 4.2	22.44 ± 13.6	51.69 ± 6.3	60.06 ± 6.8
	CM	28.67 ± 5.5	38.33 ± 15.3	78.67 ± 9.3*	58.67 ± 10.7
	CM+	25.33 ± 4.7	19.67 ± 9.9	53.00 ± 11.3	47.33 ± 4.6
	CoCM+	24.97 ± 5.6	27.52 ± 24.2	57.76 ± 25.8	59.28 ± 11.1
	Vehicle	25.00 ± 7.9	18.80 ± 4.13	64.47 ± 5.7	60.90 ± 11.9
Body weight (g)	Cisplatin	366.53 ± 33.5	395.47 ± 37.1	376.80 ± 49.9	386.27 ± 53.3
	iv ABCB5+	371.41 ± 32.7	375.25 ± 53.7	340.25 ± 59.4	361.50 ± 63.7
	ip ABCB5+	339.00 ± 39.7	358.91 ± 47.2	328.73 ± 54.9*	355.45 ± 57.9
	CM	295.67 ± 3.5	326.00 ± 14.0*	338.00 ± 29.5	382.67 ± 24.7
	CM+	278.00 ± 8.1	294.67 ± 16.6**	291.67 ± 26.1*	337.67 ± 17.5
	CoCM+	292.18 ± 16.4	325.27 ± 16.8**	288.64 ± 30.2**	341.27 ± 28.3*
	Vehicle	377.33 ± 33.0	378.67 ± 48.7	360.33 ± 49.9	384.33 ± 58.1

Food intake (g/16h)	Cisplatin	19.54 ± 3.1	8.93 ± 5.8	15.87 ± 5.3	21.39 ± 3.0
	iv ABCB5+	21.69 ± 4.6	9.55 ± 3.5	15.47 ± 4.9	21.69 ± 3.2
	ip ABCB5+	20.04 ± 3.7	8.77 ± 1.5	15.68 ± 3.9	22.14 ± 3.0
	CM	20.00 ± 8.2	11.33 ± 4.2	23.33 ± 0.6*	26.33 ± 3.0*
	CM+	22.00 ± 1.0	10.00 ± 1.0	21.00 ± 2.6	24.33 ± 4.0
	CoCM+	19.74 ± 3.5	8.47 ± 1.8	14.24 ± 6.4	23.99 ± 3.2
	Vehicle	22.80 ± 3.4	9.70 ± 0.6	17.17 ± 3.0	22.00 ± 2.7

Table 10 Changes in body weight, diuresis, food and water intake before and after metabolic cage allocation. Experimental groups: cisplatin n=15; iv ABCB5+ n=12; ip ABCB5+ n=11; CM n=3; CM+ n=3; CoCM+ n=11; vehicle n=3. Data are shown as means ± SD. Values significantly different from control are indicated as *p< 0.05 and **p< 0.005.

Loss of weight gain, in a range of 20-30 g, was recorded between day 2 and 7 in animals who received ABCB5+ cells and coCM+. Animals who received CM and CM+ gained weight or maintained a quite stable weight (CM p<0.05). Accordingly, in these groups the food intake, which decreased on day 2, was higher than in the other animal groups (CM p<0.05).

4.2.5. ABCB5+ cells/conditioned media effect on renal morphology

Whole kidney scans displayed in Figure 23 show changes in the renal cytoarchitecture of animals treated with ABCB5+ cells and conditioned media. Animals that received ABCB5+ cells, both ip and iv, did not show any visible differences from the cisplatin treated animals. The cortical and juxtamedullary region was the most affected area with dilated proximal tubuli in the cortical region and protein cast accumulations mostly in the papillary region. Animals treated with conditioned media showed less severe damage in terms of affected area and protein cast accumulations. CM treated animals resulted to be affected mainly in the juxtamedullary region.

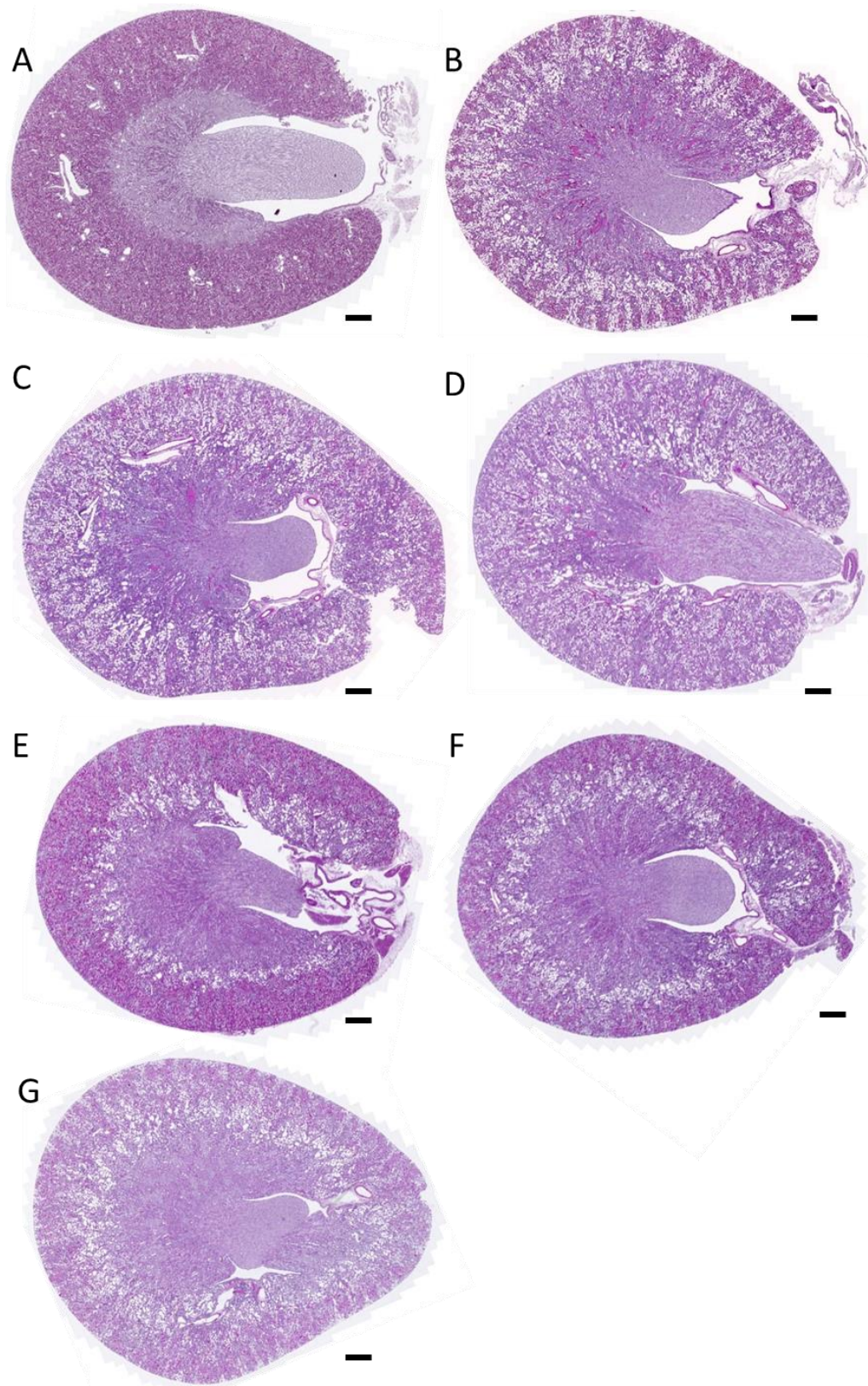


Figure 23 Effect of ABCB5+ cells and conditioned media on renal morphology. Whole kidney scan showing changes in the cytoarchitecture. A: control; B: cisplatin; C: ipABCB5+; D: ivABCB5+; E: CM; F: CM+; G: coCM+. H&E staining. Scale bars: 1mm. Images acquired with Axio Scan.Z1 microscope (ZEISS).

4.3. Gene expression analysis

Gene expression analysis of renal tissue obtained from sacrificed animals was performed. The analysis was first performed with both microarray and RNAseq, showing reliable results with both approaches. However, due to its innovative and more sensitive methodology, and for the possibility to additionally performed miRNAs profiling, RNAseq was chosen over microarray for subsequent analyses.

4.3.1. Cisplatin effect on gene expression: microarray vs RNAseq analysis

Distribution and batch normalization of the data were first performed. PCA and cluster analysis of 3 healthy and 3 cisplatin-treated animals showed 2 distinct clusters with both microarray and RNAseq. (Figure 24).

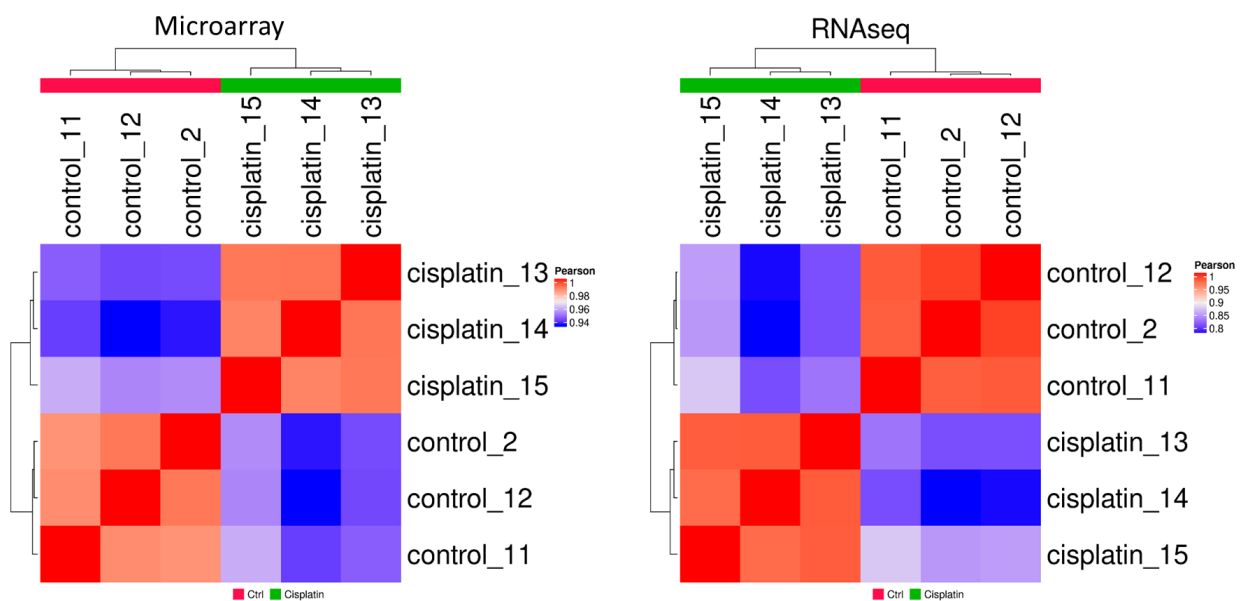


Figure 24 Heatmap showing cluster analysis of treated (cisplatin, n=3) and untreated (control, n=3) animals with both microarray (on the left) and RNAseq (on the right)

From the 21569 genes screened in the microarray, 6651 were significant differentially expressed (3656 upregulated and 2995 downregulated genes) in the cisplatin-treated animals compared to the controls (adj. $p < 0.05$). Similarly, from the 17322 genes screened, 6333 differentially expressed genes (3310 upregulated and 3023 downregulated genes) were detected with RNAseq. The Venn diagram in Figure 25 shows that 4087 genes were found with both microarray and RNAseq technology. Linear regression fitted for \log_2 fold change (\log_2FC) cisplatin vs control of the common genes determined via microarray and RNAseq was performed and showed a correlation with $R\text{-square} = 0.82$ and $p\text{-value} < 0.0001$ (Figure 25).

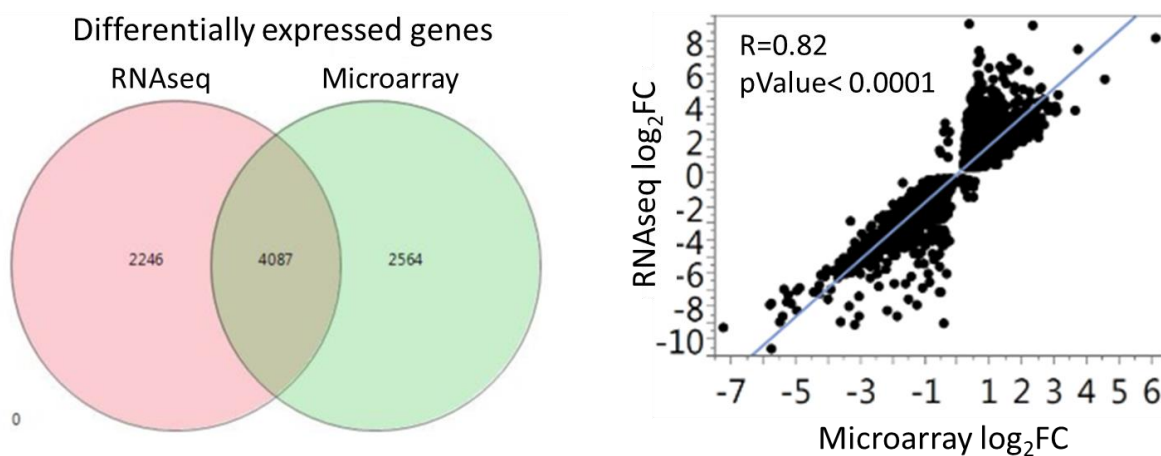


Figure 25 Venn diagram of differentially expressed genes with RNAseq and microarray (left). Linear regression fitted for \log_2FC of selected common genes determined via microarray and RNAseq technology (right). R: R-square.

Successively, GSEA using the KEGG database was performed. Conventionally, considering a list of differentially expressed ranked genes organized in gene set, a positive (or negative) NES indicate the position of a pathway at the top (or at the bottom) of the gene list, meaning that the genes which belong to that pathway are highly (or low) expressed. From 123 selected significant pathways, 73 pathways were commonly detected with both microarray and RNAseq and showed similar NES values, indicating reliability of the results obtained by using the two techniques (Table 11).

KEGG pathway	Sub category	NES	NES
		Microarray	RNAseq
Carbon metabolism	1.0 Global and overview maps	-2.6	-2.5
Oxocarboxylic acid metabolism	1.0 Global and overview maps	-1.7	-1.7
Fatty acid metabolism	1.0 Global and overview maps	-2.0	-2.0
Biosynthesis of amino acids	1.0 Global and overview maps	-2.1	-2.0
Glycolysis / Gluconeogenesis	1.1 Carbohydrate metabolism	-2.1	-2.0
Citrate cycle (TCA cycle)	1.1 Carbohydrate metabolism	-2.2	-2.3
Pentose and glucuronate interconversions	1.1 Carbohydrate metabolism	-1.9	-2.0
Ascorbate and aldarate metabolism	1.1 Carbohydrate metabolism	-2.1	-2.2
Pyruvate metabolism	1.1 Carbohydrate metabolism	-2.5	-2.2
Glyoxylate and dicarboxylate metabolism	1.1 Carbohydrate metabolism	-2.5	-2.2
Propanoate metabolism	1.1 Carbohydrate metabolism	-2.5	-2.1
Butanoate metabolism	1.1 Carbohydrate metabolism	-2.4	-1.9
Metabolism of xenobiotics by cyt P450	1.11 Xenobiotics metabolism	-2.0	-2.1
Drug metabolism - cytochrome P450	1.11 Xenobiotics metabolism	-2.2	-2.2
Drug metabolism - other enzymes	1.11 Xenobiotics metabolism	-1.5	-2.1
Oxidative phosphorylation	1.2 Energy metabolism	-2.4	-2.5
Fatty acid elongation	1.3 Lipid metabolism	-1.9	-1.9
Fatty acid degradation	1.3 Lipid metabolism	-2.4	-2.2
Steroid hormone biosynthesis	1.3 Lipid metabolism	-1.9	-1.9
Glycerolipid metabolism	1.3 Lipid metabolism	-2.1	-1.8
Biosynthesis of unsaturated fatty acids	1.3 Lipid metabolism	-1.7	-1.8
Glycine, serine and threonine met	1.5 Amino acid metabolism	-2.8	-2.2
Cysteine and methionine metabolism	1.5 Amino acid metabolism	-2.2	-2.0
Valine, leucine and isoleucine degradation	1.5 Amino acid metabolism	-2.8	-2.3
Lysine degradation	1.5 Amino acid metabolism	-1.5	-2.0
Arginine and proline metabolism	1.5 Amino acid metabolism	-2.4	-1.8
Histidine metabolism	1.5 Amino acid metabolism	-2.2	-1.9
Tyrosine metabolism	1.5 Amino acid metabolism	-1.9	-1.9
Tryptophan metabolism	1.5 Amino acid metabolism	-2.4	-2.2
beta-Alanine metabolism	1.6 Metabolism of other amino acids	-2.5	-2.2
Selenocompound metabolism	1.6 Metabolism of other amino acids	-2.1	-1.8
Glutathione metabolism	1.6 Metabolism of other amino acids	-2.2	-2.0
Glycosaminoglycan biosynthesis	1.7 Glycan biosynthesis and metabolism	1.7	1.8
Nicotinate and nicotinamide metabolism	1.8 Metabolism of cofactors and vitamins	-1.9	-1.6
Pantothenate and CoA biosynthesis	1.8 Metabolism of cofactors and vitamins	-1.9	-1.8
Folate biosynthesis	1.8 Metabolism of cofactors and vitamins	-1.8	-1.9
Retinol metabolism	1.8 Metabolism of cofactors and vitamins	-1.7	-1.9
Porphyrin and chlorophyll metabolism	1.8 Metabolism of cofactors and vitamins	-1.8	-1.9
Terpenoid backbone biosynthesis	1.9 Metabolism of terpenoids and polyketides	-1.7	-1.6
Spliceosome	2.1 Transcription	1.7	1.7
Aminoacyl-tRNA biosynthesis	2.2 Translation	-1.8	-1.7
MAPK signaling pathway	3.2 Signal transduction	2.0	1.4
Rap1 signaling pathway	3.2 Signal transduction	2.0	1.3
NF-kappa B signaling pathway	3.2 Signal transduction	2.5	1.9
PI3K-Akt signaling pathway	3.2 Signal transduction	2.2	1.4
Notch signaling pathway	3.2 Signal transduction	1.9	1.8
Hippo signaling pathway	3.2 Signal transduction	2.1	1.4
Jak-STAT signaling pathway	3.2 Signal transduction	2.2	1.6
TNF signaling pathway	3.2 Signal transduction	2.3	1.9
Cytokine-cytokine receptor interaction	3.3 Signaling molecules and interaction	2.2	2.1
ECM-receptor interaction	3.3 Signaling molecules and interaction	2.3	1.7
Cell adhesion molecules (CAMs)	3.3 Signaling molecules and interaction	2.3	2.2
Phagosome	4.1 Transport and catabolism	2.3	1.8
Peroxisome	4.1 Transport and catabolism	-2.7	-2.3
Regulation of actin cytoskeleton	4.2 Cell motility	2.3	1.4
Cell cycle	4.3 Cell growth and death	2.3	2.0
p53 signaling pathway	4.3 Cell growth and death	2.1	1.9
Apoptosis	4.3 Cell growth and death	2.3	1.6
Focal adhesion	4.4 Cellular community	2.5	1.6

Chemokine signaling pathway	5.1 Immune system	2.3	1.7
Complement and coagulation cascades	5.1 Immune system	1.8	1.6
Platelet activation	5.1 Immune system	2.0	1.5
Antigen processing and presentation	5.1 Immune system	2.2	1.9
Toll-like receptor signaling pathway	5.1 Immune system	2.2	1.8
NOD-like receptor signaling pathway	5.1 Immune system	1.9	1.5
Hematopoietic cell lineage	5.1 Immune system	2.1	2.0
Natural killer cell mediated cytotoxicity	5.1 Immune system	2.5	1.9
T cell receptor signaling pathway	5.1 Immune system	2.3	1.5
B cell receptor signaling pathway	5.1 Immune system	2.4	1.7
Fc gamma R-mediated phagocytosis	5.1 Immune system	2.4	1.6
Leukocyte transendothelial migration	5.1 Immune system	2.3	1.7
Intestinal immune network for IgA prod.	5.1 Immune system	1.9	1.8
Renin-angiotensin system	5.2 Endocrine system	-1.6	-1.7

Table 11 GSEA analysis using KEGG database sorted by subcategory: significant (adjusted p-value < 0.05) differentially expressed pathways (cisplatin vs control). For each pathway the normalized enrichment score (NES) obtained with microarray and RNAseq are given. Downregulated pathways are displayed in green, upregulated pathways in red. KEGG main categories: 1 metabolism; 2 genetic information processing; 3 environmental information processing; 4 cellular processes; 5 organismal system.

An overview of what was discussed so far is shown in Table 12.

	Cisplatin vs control	Microarray	RNAseq
Genes	Significant differentially expressed	6651	6333
	Significant upregulated	3656	3310
	Significant downregulated	2995	3023
Pathways	Detected	298	305
	Significant	201	139
	Selected	111	85

Table 12 Overview of differentially expressed genes and pathways in cisplatin vs control found with microarray and RNAseq; significance was attributed for an adjusted p-value < 0.05

Based on the reliable results discussed so far and due to the innovative and more sensitive method used in the RNAseq technique, we chose RNAseq over microarray for the following analyses.

4.3.2. Cisplatin effect on gene expression: RNAseq analysis

The GSEA analysis showed 49 significant differentially expressed pathways. As shown in Table 13, cisplatin led to upregulation of apoptosis and p53 signaling pathways. The renal tissue metabolism is downregulated and so the translational activity and protein processing.

KEGG pathway	Main category	Sub category	NES RNAseq
Metabolic pathways	1. Metabolism	1.0 Global and overview maps	-2.31
Carbon metabolism	1. Metabolism	1.0 Global and overview maps	-2.46
Fatty acid metabolism	1. Metabolism	1.0 Global and overview maps	-1.97
Biosynthesis of amino acids	1. Metabolism	1.0 Global and overview maps	-1.96
Oxocarboxylic acid metabolism	1. Metabolism	1.0 Global and overview maps	-1.69
Metabolism of xenobiotics by cytochrome P450	1. Metabolism	1.11 Xenobiotics biodegradation and metabolism	-2.1
Drug metabolism (982)	1. Metabolism	1.11 Xenobiotics biodegradation and metabolism	-2.22
Drug metabolism (983)	1. Metabolism	1.11 Xenobiotics biodegradation and metabolism	-2.13
Aminoacyl-tRNA biosynthesis	2. Genetic Information Processing	2.2 Translation	-1.7
Protein processing in endoplasmic reticulum	2. Genetic Information Processing	2.3 Folding sorting and degradation	-1.79
Peroxisome	4. Cellular Processes	4.1 Transport and catabolism	-2.3
p53 signaling pathway	4. Cellular Processes	4.3 Cell growth and death	1.87
Apoptosis	4. Cellular Processes	4.3 Cell growth and death	1.62
Renin-angiotensin system	5. Organismal Systems	5.2 Endocrine system	-1.67

Table 13 GSEA analysis using KEGG database sorted by subcategory: significant (adjusted p-value < 0.05) differentially expressed pathways (cisplatin vs control). For each pathway the normalized enrichment score (NES) is given. Downregulated pathways are displayed in green (light green: $-1.5 > \text{NES} > 0$; green: $-2 > \text{NES} > -1.5$; dark green: $\text{NES} > -2$), upregulated pathways in red (light red: $1.5 > \text{NES} > 0$; red: $2 > \text{NES} > 1.5$; dark red: $\text{NES} > 2$).

In contrast, upregulation of DNA replication, cell cycle, ribosome and spliceosome assembly, and of several pathways involved in extracellular matrix (ECM) remodeling was found (Table 14).

KEGG pathway	Main category	Sub category	NES RNAseq
DNA replication	2. Genetic Information Processing	2.4 Replication and repair	1.68
Ribosome	2. Genetic Information Processing	2.2 Translation	1.63
Spliceosome	2. Genetic Information Processing	2.1 Transcription	1.7
Phagosome	4. Cellular Processes	4.1 Transport and catabolism	1.78
Cell cycle	4. Cellular Processes	4.3 Cell growth and death	2.03
Glycosaminoglycan biosynthesis	1. Metabolism	1.7 Glycan biosynthesis and metabolism	1.79
Cell adhesion molecules (CAMs)	3. Environmental Information Processing	3.3 Signaling molecules and interaction	2.24
Cytokine-cytokine receptor interaction	3. Environmental Information Processing	3.3 Signaling molecules and interaction	2.06
ECM-receptor interaction	3. Environmental Information Processing	3.3 Signaling molecules and interaction	1.73
Neuroactive ligand-receptor interaction	3. Environmental Information Processing	3.3 Signaling molecules and interaction	1.28
Regulation of actin cytoskeleton	4. Cellular Processes	4.2 Cell motility	1.35
Focal adhesion	4. Cellular Processes	4.4 Cellular community	1.55

Table 14 GSEA analysis using KEGG database sorted by subcategory: significant (adjusted p-value < 0.05) differentially expressed pathways (cisplatin vs control). For each pathway the normalized enrichment score (NES) is given. Upregulated pathways are displayed in red (light red: $1.5 > \text{NES} > 0$; red: $2 > \text{NES} > 1.5$; dark red: $\text{NES} > 2$).

Additionally, upregulation of immune system and signal transduction pathways were observed (Table 15).

KEGG pathway	Main category	Sub category	NES RNAseq
NF-kappa B signaling pathway	3. Environmental Information Processing	3.2 Signal transduction	1.85
TNF signaling pathway	3. Environmental Information Processing	3.2 Signal transduction	1.93
JAK-STAT signaling pathway	3. Environmental Information Processing	3.2 Signal transduction	1.59
Notch signaling pathway	3. Environmental Information Processing	3.2 Signal transduction	1.79
MAPK signaling pathway	3. Environmental Information Processing	3.2 Signal transduction	1.36
PI3K-Akt signaling pathway	3. Environmental Information Processing	3.2 Signal transduction	1.35
Hippo signaling pathway	3. Environmental Information Processing	3.2 Signal transduction	1.4
Rap1 signaling pathway	3. Environmental Information Processing	3.2 Signal transduction	1.26
Antigen processing and presentation	5. Organismal Systems	5.1 Immune system	1.9
Toll-like receptor signaling pathway	5. Organismal Systems	5.1 Immune system	1.83
Natural killer cell mediated cytotoxicity	5. Organismal Systems	5.1 Immune system	1.93
Leukocyte transendothelial migration	5. Organismal Systems	5.1 Immune system	1.69
Chemokine signaling pathway	5. Organismal Systems	5.1 Immune system	1.72
B cell receptor signaling pathway	5. Organismal Systems	5.1 Immune system	1.68
NOD-like receptor signaling pathway	5. Organismal Systems	5.1 Immune system	1.54
Fc gamma R-mediated phagocytosis	5. Organismal Systems	5.1 Immune system	1.62
Complement and coagulation cascades	5. Organismal Systems	5.1 Immune system	1.59
Platelet activation	5. Organismal Systems	5.1 Immune system	1.49
T cell receptor signaling pathway	5. Organismal Systems	5.1 Immune system	1.5
Th1 and Th2 cell differentiation	5. Organismal Systems	5.1 Immune system	1.91
Th17 cell differentiation	5. Organismal Systems	5.1 Immune system	1.73
C-type lectin receptor signaling pathway	5. Organismal Systems	5.1 Immune system	1.61
IL-17 signaling pathway	5. Organismal Systems	5.1 Immune system	1.46

Table 15 GSEA analysis using KEGG database sorted by subcategory: significant (adjusted p-value < 0.05) differentially expressed pathways (cisplatin vs control). For each pathway the normalized enrichment score (NES) is given. Upregulated pathways are displayed in red (light red: $1.5 > \text{NES} > 0$; red: $2 > \text{NES} > 1.5$; dark red: $\text{NES} > 2$).

4.3.3. ABCB5+ cells/conditioned media effect on gene expression: RNAseq analysis

Cluster analysis of 21 RNAseq samples showed that, among the seven experimental groups, two distinct clusters could be distinguished. As shown in the heatmap (Figure 26), control animals and 2 over 3 animals treated with CM and CM+ clustered together, while all animals treated with ABCB5+ cells and coCM+ bunched with the cisplatin-treated animals.

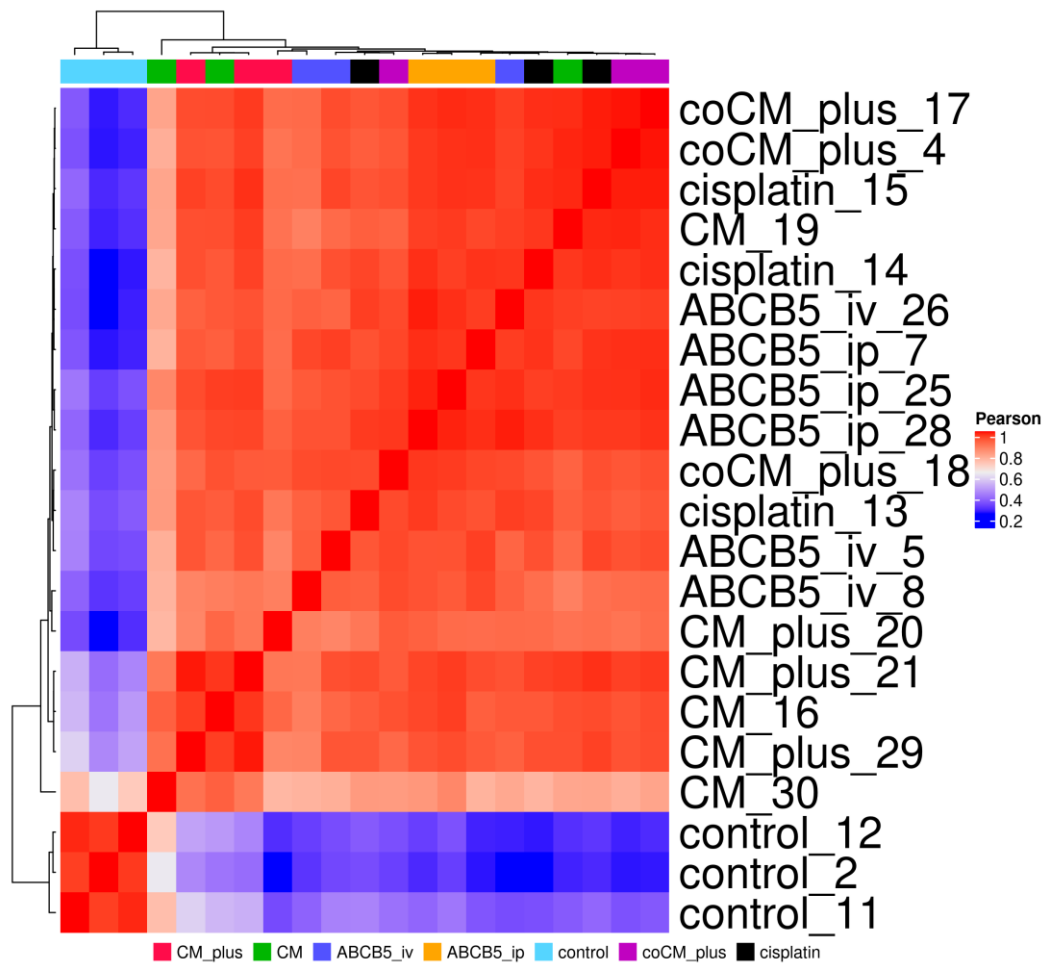


Figure 26 Heatmap showing cluster analysis of the experimental groups (n=3 per experimental group) with RNAseq. Numbers in the legend correspond to the animal numbers

For GSEA analysis, pairwise comparisons of each treatment group to the cisplatin were performed. A total of 126 significant (adj p-value < 0.05) differently expressed pathways were found. For some pathways, a different trend of expression in the different experimental groups was observed. An overview of up and down regulated pathways in the different groups is shown in Figure 27.

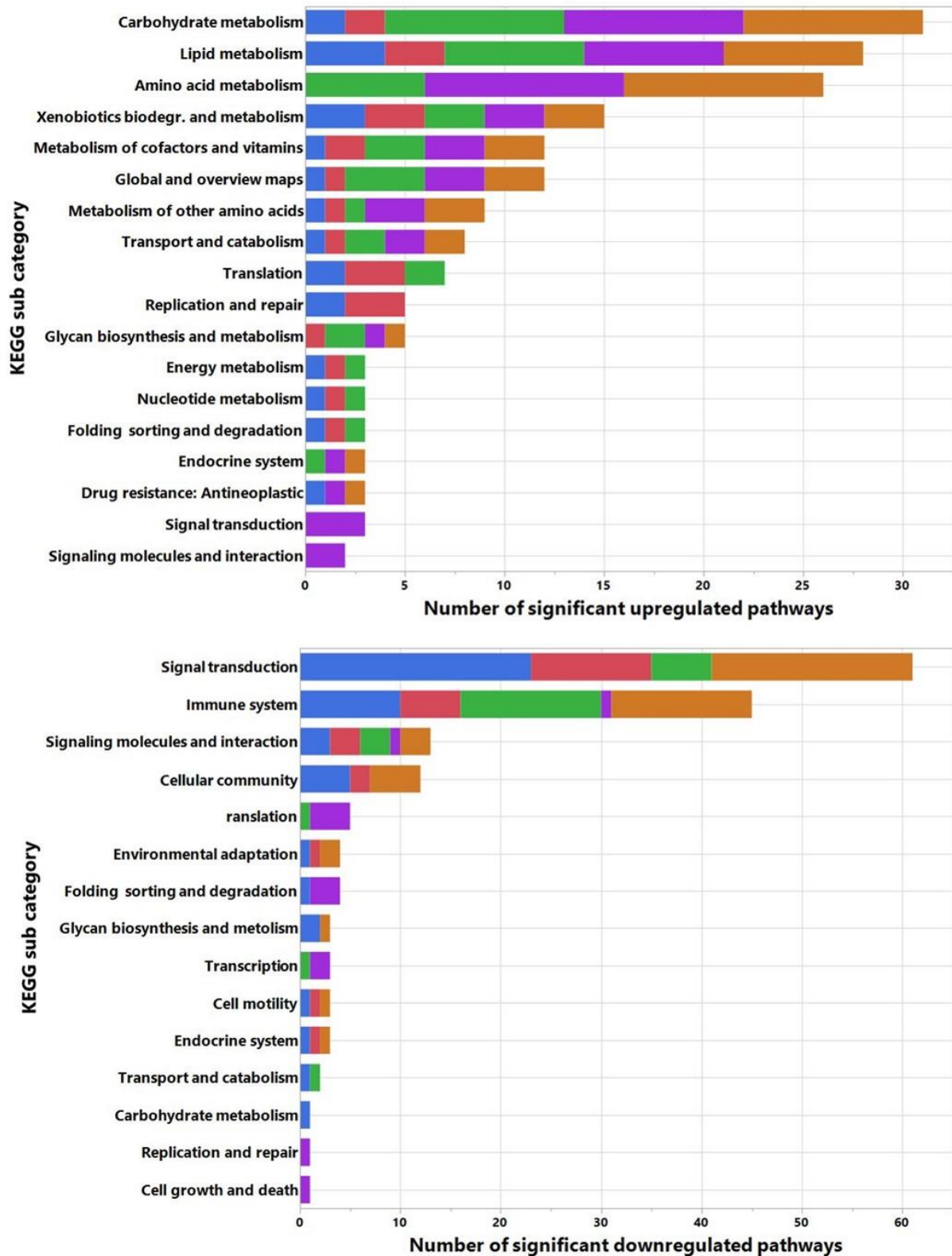


Figure 27 GSEA analysis using KEGG database: number of significant (adjusted p-value < 0.05) upregulated (upper figure) and downregulated (lower figure) pathways in the treatment groups.

■ ip ABCB5+ n=11; ■ iv ABCB5+ n=12; ■ coCM+ n=11; ■ CM n=3; ■ CM+ n=3;

More details can be found in tables 14-17.

Upregulation of xenobiotic degradation and metabolism pathways were found in the animals treated with any therapy. Overall, upregulation of several metabolic pathways was mainly found in the animals treated with CM and coCM+ (Table 16).

Main category: 1. Metabolism

KEGG pathway	Sub category	NES	NES	NES	NES	NES
		ABCBS5 ip vs cisplatin	ABCBS5 iv vs cisplatin	CM vs cisplatin	CM+ vs cisplatin	coCM+ vs cisplatin
Metabolic pathways	1.0 Global and overview maps	1.34	1.47	2.07	1.62	2.18
Carbon metabolism	1.0 Global and overview maps	1.04	1.02	2.03	1.88	2.25
Biosynthesis of amino acids	1.0 Global and overview maps	0.99	0.71	1.75	1.69	1.9
2-Oxocarboxylic acid metabolism	1.0 Global and overview maps	-0.42	0.65	1.53	1.55	1.82
Glycolysis Gluconeogenesis	1.1 Carbohydrate metabolism	1.08	1.03	1.64	1.69	2.11
Pyruvate metabolism	1.1 Carbohydrate metabolism	1.19	0.94	1.84	1.88	1.98
Glyoxylate and dicarboxylate metabolism	1.1 Carbohydrate metabolism	1.14	0.68	2.28	2.28	2.01
Citrate cycle (TCA cycle)	1.1 Carbohydrate metabolism	-0.78	0.67	1.93	1.9	1.96
Pentose phosphate pathway	1.1 Carbohydrate metabolism	1.31	1.43	1.73	1.38	1.92
Amino sugar and nucleotide sugar metabolism	1.1 Carbohydrate metabolism	1.01	0.76	1.33	0.84	1.71
Propanoate metabolism	1.1 Carbohydrate metabolism	-0.58	0.54	1.6	1.63	1.74
Ascorbate and aldarate metabolism	1.1 Carbohydrate metabolism	1.67	1.84	2.35	1.61	1.7
Pentose and glucuronate interconversions	1.1 Carbohydrate metabolism	1.77	1.72	2.34	1.46	1.67
Inositol phosphate metabolism	1.1 Carbohydrate metabolism	-1.46	0.73	0.92	1.01	-1.38
Fructose and mannose metabolism	1.1 Carbohydrate metabolism	1.09	0.8	1.39	1.79	1.27
Butanoate metabolism	1.1 Carbohydrate metabolism	0.72	-0.74	1.62	1.66	1.1
Drug metabolism (2)	1.11 Xenobiotics biodegradation and metabolism	2.43	2.17	2.42	1.85	2.45
Metabolism of xenobiotics by cytochrome P450	1.11 Xenobiotics biodegradation and metabolism	1.98	1.73	2.38	1.97	2.22
Drug metabolism (3)	1.11 Xenobiotics biodegradation and metabolism	2.08	1.68	2.37	1.86	2.11
Oxidative phosphorylation	1.2 Energy metabolism	1.81	2.03	1.14	-1	2.65
Fatty acid degradation	1.3 Lipid metabolism	1.1	1.1	1.97	1.92	1.9
Linoleic acid metabolism	1.3 Lipid metabolism	1.94	1.56	1.29	0.76	1.93
Arachidonic acid metabolism	1.3 Lipid metabolism	1.63	1.17	1.47	1.29	1.82
Steroid hormone biosynthesis	1.3 Lipid metabolism	1.86	1.54	2.1	1.32	1.72
Fatty acid elongation	1.3 Lipid metabolism	1.21	1.65	1.65	0.87	1.68
alpha-Linolenic acid metabolism	1.3 Lipid metabolism	1.48	1.53	1.23	1.27	1.68
Glycerolipid metabolism	1.3 Lipid metabolism	1.24	1.24	1.76	1.71	1.5
Steroid biosynthesis	1.3 Lipid metabolism	0.96	0.79	1.67	1.13	1.39
Glycerophospholipid metabolism	1.3 Lipid metabolism	1.05	1.59	1.04	0.96	1.18
Biosynthesis of unsaturated fatty acids	1.3 Lipid metabolism	1.2	1.26	1.83	1.4	1.18
Pyrimidine metabolism	1.4 Nucleotide metabolism	1.68	1.73	1.1	-1.08	1.91
Glycine, serine and threonine metabolism	1.5 Amino acid metabolism	1.42	-0.66	2.42	2.15	2.16
Valine, leucine and isoleucine degradation	1.5 Amino acid metabolism	1.09	0.8	1.95	1.79	1.81
Tyrosine metabolism	1.5 Amino acid metabolism	1.24	0.73	1.83	1.57	1.91
Cysteine and methionine metabolism	1.5 Amino acid metabolism	0.89	0.6	1.82	1.58	1.77
Phenylalanine metabolism	1.5 Amino acid metabolism	0.71	-0.67	1.77	1.57	1.62
Tryptophan metabolism	1.5 Amino acid metabolism	-0.67	-1.06	2.23	2.19	1.5
Arginine and proline metabolism	1.5 Amino acid metabolism	-0.94	-1.29	1.87	1.58	1.42
Alanine, aspartate and glutamate metabolism	1.5 Amino acid metabolism	0.68	-0.7	1.73	1.59	1.24
Histidine metabolism	1.5 Amino acid metabolism	-0.74	-1.03	1.96	1.45	1.15
Lysine degradation	1.5 Amino acid metabolism	-1.28	-1.03	1.88	1.53	-1.05
Glutathione metabolism	1.6 Metabolism of other amino acids	1.79	1.57	2.06	1.64	2.12
beta-Alanine metabolism	1.6 Metabolism of other amino acids	-0.59	-1.49	1.93	1.75	1.43
Selenocompound metabolism	1.6 Metabolism of other amino acids	1.32	1.26	1.86	1.34	1.34
Other glycan degradation	1.7 Glycan biosynthesis and metabolism	1.74	1.43	1.83	1.56	1.78
Mucin type O-glycan biosynthesis	1.7 Glycan biosynthesis and metabolism	-1.73	-1.31	0.92	1.11	-1.74
Glycosaminoglycan degradation	1.7 Glycan biosynthesis and metabolism	1.12	0.86	1.59	2.04	1.73
Glycosaminoglycan biosynthesis	1.7 Glycan biosynthesis and metabolism	-1.82	-1.57	-1.51	1.3	-1.36
Porphyrin and chlorophyll metabolism	1.8 Metabolism of cofactors and vitamins	1.92	1.6	2.2	1.17	2.04
Retinol metabolism	1.8 Metabolism of cofactors and vitamins	1.48	1.21	2.23	1.24	1.83
One carbon pool by folate	1.8 Metabolism of cofactors and vitamins	0.54	-0.76	1.48	1.18	1.61
Folate biosynthesis	1.8 Metabolism of cofactors and vitamins	1.3	0.72	1.77	1.35	1.3

Table 16 GSEA analysis using KEGG database sorted by subcategory: significant (adjusted p-value < 0.05) differentially expressed pathways (treatment vs cisplatin). For each pathway the normalized enrichment score (NES) is given. Downregulated pathways are displayed in green (light green: $-1.5 > NES > 0$; green: $-2 > NES > -1.5$; dark green: $NES > -2$), upregulated pathways in red (light red: $1.5 > NES > 0$; red: $2 > NES > 1.5$; dark red: $NES > 2$).

Translation, proteasome and ribosome biogenesis are unregulated in animals treated with ABCB5 cells and coCM+. Additionally, the DNA replication and reparation activity is upregulated in ABCB5 cells groups. In contrast, these pathways are downregulated in thje CM and CM+ groups (Table 17).

Main category: 2. Genetic information processing

KEGG pathway	Sub category	NES	NES	NES	NES	NES
		ABCB5 ip vs cisplatin	ABCB5 iv vs cisplatin	CM vs cisplatin	CM+ vs cisplatin	coCM+ vs cisplatin
Basal transcription factors	2.1 Transcription	1.36	1.14	-0.95	-1.76	1.03
Spliceosome	2.1 Transcription	1.33	0.79	-1.48	-2.2	-0.64
Ribosome	2.2 Translation	2.74	2.55	-2.02	-2.43	2.22
Aminoacyl-tRNA biosynthesis	2.2 Translation	1.17	1.58	1.18	-0.85	1.68
Ribosome biogenesis in eukaryotes	2.2 Translation	1.47	1.41	0.67	-1.8	1.3
RNA transport	2.2 Translation	1.5	1.27	-0.67	-1.9	0.89
mRNA surveillance pathway	2.2 Translation	1.21	1.17	0.8	-1.62	0.81
Proteasome	2.3 Folding sorting and degradation	1.97	1.73	-0.85	-1.99	2.02
RNA degradation	2.3 Folding sorting and degradation	0.83	1.03	-1.24	-1.62	-1.13
Protein export	2.3 Folding sorting and degradation	-0.87	-0.8	-0.69	-1.8	0.71
Protein processing in endoplasmic reticulum	2.3 Folding sorting and degradation	-1.78	-1.26	0.79	-1.39	-0.81
DNA replication	2.4 Replication and repair	1.57	1.39	-0.88	-1.14	1.29
Mismatch repair	2.4 Replication and repair	1.48	1.63	-0.8	-1.34	1.23
Nucleotide excision repair	2.4 Replication and repair	1.56	1.24	-0.84	-1.65	1.11

Table 17 GSEA analysis using KEGG database sorted by subcategory: significant (adjusted p-value < 0.05) differentially expressed pathways (treatment vs cisplatin). For each pathway the normalized enrichment score (NES) is given. Downregulated pathways are displayed in green (light green: -1.5 > NES > 0; green: -2 > NES > -1.5; dark green: NES > -2), upregulated pathways in red (light red: 1.5 > NES > 0; red: 2 > NES > 1.5; dark red: NES > 2).

A strong downregulation of signaling pathways was observed in the animals treated with ipABC56+, ivABC5+ and coCM+, while no significant changes were found in the CM and CM+ groups. Interestingly, the downregulation of the cytokine-cytokine receptor interaction pathway was found in all groups (Table 18).

Main category: 3. Environmental information processing

KEGG pathway	Sub category	NES	NES	NES	NES	NES
		ABC5 ip vs cisplatin	ABC5 iv vs cisplatin	CM vs cisplatin	CM+ vs cisplatin	coCM+ vs cisplatin
MAPK signaling pathway	3.2 Signal transduction	-2	-1.88	-1.3	1.18	-1.95
Rap1 signaling pathway	3.2 Signal transduction	-2.09	-1.88	-0.97	1.47	-1.83
Calcium signaling pathway	3.2 Signal transduction	-1.87	-1.89	-1.33	0.76	-1.77
cGMP-PKG signaling pathway	3.2 Signal transduction	-2.22	-2.13	-1.2	1.11	-2.1
cAMP signaling pathway	3.2 Signal transduction	-1.8	-1.6	-1.44	0.85	-1.95
PI3K-Akt signaling pathway	3.2 Signal transduction	-1.88	-1.84	-0.91	1.17	-1.91
Wnt signaling pathway	3.2 Signal transduction	-1.96	-1.61	-1.15	-0.73	-1.89
JAK-STAT signaling pathway	3.2 Signal transduction	-1.54	-1.66	-1.19	-0.77	-1.83
TNF signaling pathway	3.2 Signal transduction	-1.62	-1.42	-1.69	-1.26	-2.08
Ras signaling pathway	3.2 Signal transduction	-1.81	-1.62	-0.96	0.97	-1.68
NF-kappa B signaling pathway	3.2 Signal transduction	-1.57	-1.46	-1.84	-1.03	-1.92
FoxO signaling pathway	3.2 Signal transduction	-1.46	-1.04	0.78	-0.85	-1.63
Hippo signaling pathway	3.2 Signal transduction	-2.23	-1.71	-1.03	1.17	-1.55
Hedgehog signaling pathway	3.2 Signal transduction	-1.91	-1.51	0.98	1.6	-1.8
Phosphatidylinositol signaling system	3.2 Signal transduction	-1.32	0.82	0.95	1.13	-1.63
Phospholipase D signaling pathway	3.2 Signal transduction	-1.57	-1.36	-0.92	1.17	-1.47
HIF-1 signaling pathway	3.2 Signal transduction	-1.62	-1.49	-1.43	-0.78	-1.54
Sphingolipid signaling pathway	3.2 Signal transduction	-1.58	-1.02	-0.96	-0.68	-1.49
ErbB signaling pathway	3.2 Signal transduction	-1.58	0.81	1.05	1.35	-1.54
Hippo signaling pathway	3.2 Signal transduction	-1.98	-1.92	-0.9	1.04	-1.64
TGF-beta signaling pathway	3.2 Signal transduction	-1.72	-1.15	-0.84	0.91	-1.39
mTOR signaling pathway	3.2 Signal transduction	-1.43	0.85	1.06	1.2	-1.28
AMPK signaling pathway	3.2 Signal transduction	-1.43	-0.87	1.09	1.28	-1.29
Notch signaling pathway	3.2 Signal transduction	-1.51	-1.34	-1.07	1.42	-0.93
Cytokine-cytokine receptor interaction	3.3 Signaling molecules and interaction	-1.38	-1.71	-1.94	-1.48	-1.89
ECM-receptor interaction	3.3 Signaling molecules and interaction	-1.76	-2.02	-1.27	0.98	-1.93
Cell adhesion molecules (CAMs)	3.3 Signaling molecules and interaction	-1.51	-1.27	-1.63	0.79	-1.43
Neuroactive ligand-receptor interaction	3.3 Signaling molecules and interaction	-1.14	-1.56	-1.41	0.77	-1.23

Table 18 GSEA analysis using KEGG database sorted by subcategory: significant (adjusted p-value < 0.05) differentially expressed pathways (treatment vs cisplatin). For each pathway the normalized enrichment score (NES) is given. Downregulated pathways are displayed in green (light green: $-1.5 > NES > 0$; green: $-2 > NES > -1.5$; dark green: $NES > -2$), upregulated pathways in red (light red: $1.5 > NES > 0$; red: $2 > NES > 1.5$; dark red: $NES > 2$).

Downregulation of pathways involved in the immune system was mainly observed in the ipABCB5+, coCM+ and CM groups. Pathways involved in the regulation of actin cytoskeleton and cellular junctions were found downregulated in ipABCB5+, ivABCB5+ and coCM+ (Table 19).

Main category: 4. Cellular processes - 5. Organismal systems - 6. Human diseases

KEGG pathway	Sub category	NES	NES	NES	NES	NES
		ABCBS ip vs cisplatin	ABCBS iv vs cisplatin	CM vs cisplatin	CM+ vs cisplatin	coCM+ vs cisplatin
Lysosome	4.1 Transport and catabolism	1.21	1.31	1.69	1.3	1.83
Peroxisome	4.1 Transport and catabolism	1.52	1.49	2.18	1.73	1.83
Endocytosis	4.1 Transport and catabolism	-1.35	-0.82	-0.93	1.09	-1.17
Phagosome	4.1 Transport and catabolism	-1.12	-1.08	-1.39	-1.26	-0.81
Regulation of actin cytoskeleton	4.2 Cell motility	-2.09	-1.81	-1.23	1.1	-2.04
Cell cycle	4.3 Cell growth and death	1.22	1.03	-0.66	-1.6	0.88
Focal adhesion	4.4 Cellular community	-2.46	-2.1	-1.09	1.12	-2.25
Signaling pathways regulating pluripot. of stem cells	4.4 Cellular community	-1.8	-1.15	-0.96	1.51	-1.64
Adherens junction	4.4 Cellular community	-2.16	-1.41	0.7	1.2	-1.78
Gap junction	4.4 Cellular community	-1.83	-1.52	-0.88	1.18	-1.55
Tight junction	4.4 Cellular community	-1.72	-1.12	-1.08	-0.87	-1.33
Platelet activation	5.1 Immune system	-1.89	-1.89	-1.6	-0.76	-2.06
Chemokine signaling pathway	5.1 Immune system	-1.65	-1.56	-1.87	-1.15	-2.08
Hematopoietic cell lineage	5.1 Immune system	-1.25	-1.51	-1.86	-1.71	-2.01
Natural killer cell mediated cytotoxicity	5.1 Immune system	-1.52	-1.48	-1.72	-1.5	-1.98
B cell receptor signaling pathway	5.1 Immune system	-1.68	-1.45	-1.74	-1.11	-2.14
Toll-like receptor signaling pathway	5.1 Immune system	-1.51	-1.35	-1.64	-1	-2.03
T cell receptor signaling pathway	5.1 Immune system	-1.57	-1.19	-1.69	-1.03	-2.24
Fc epsilon RI signaling pathway	5.1 Immune system	-1.17	-1.1	-1.55	-0.98	-1.89
NOD-like receptor signaling pathway	5.1 Immune system	-1.15	-0.94	-1.56	-1.3	-1.48
Leukocyte transendothelial migration	5.1 Immune system	-1.7	-1.34	-1.36	-0.85	-1.5
Complement and coagulation cascades	5.1 Immune system	-1.25	-1.88	-1.12	0.93	-1.27
Antigen processing and presentation	5.1 Immune system	-1.19	-0.92	-1.63	-0.98	0.93
C-type lectin receptor signaling pathway	5.1 Immune system	-1.47	-1.48	-1.74	-1.25	-2.02
Th17 cell differentiation	5.1 Immune system	-1.62	-1.36	-1.69	-1.07	-2.1
Th1 and Th2 cell differentiation	5.1 Immune system	-1.61	-1.26	-1.78	-0.9	-2.15
IL-17 signaling pathway	5.1 Immune system	-1.07	-0.85	-2.06	-1.49	-1.62
Renin secretion	5.2 Endocrine system	-1.68	-1.65	-0.73	0.78	-1.72
Renin-angiotensin system	5.2 Endocrine system	0.73	-0.92	2.04	1.11	1.69
Circadian entrainment	5.9 Environmental adaptation	-1.54	-1.48	0.75	1.16	-1.7
Circadian rhythm	5.9 Environmental adaptation	-1.42	-1.35	0.78	0.88	-1.53
Platinum drug resistance	6.12 Drug resistance: Antineoplastic	1.25	1.56	1.77	1.27	1.26

Table 19 GSEA analysis using KEGG database sorted by subcategory: significant (adjusted p-value < 0.05) differentially expressed pathways (treatment vs cisplatin). For each pathway the normalized enrichment score (NES) is given. Downregulated pathways are displayed in green (light green: -1.5 > NES > 0; green: -2 > NES > -1.5; dark green: NES > -2), upregulated pathways in red (light red: 1.5 > NES > 0; red: 2 > NES > 1.5; dark red: NES > 2)

4.4. miRNA expression analysis

Thanks to the ability of RNAseq technology to detect miRNAs, we were able to perform miRNA expression analysis on renal tissue obtained from sacrificed animals.

4.4.1. Cisplatin effect on miRNA expression

miRNA expression analysis was performed according to the workflow shown in Figure 28.

1. miRNAs selection

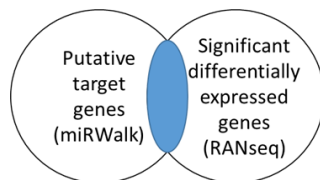
Only significant (adj $p < 0.05$) differentially expressed miRNAs found with RNAseq were selected

2. Target genes prediction

miRNA target genes were predicted by using the program miRWalk (cutoff: binding p value=1)

3. Target genes selection

Only target genes in common with the significant differentially expressed genes found in the transcriptomic analysis (RNAseq) were selected



4. BP-GO analysis

For BP-GO analysis, selected target genes were analyzed with the program DAVID

Figure 28 miRNA expression analysis: workflow

In the cisplatin treated animals, the expression of 14 miRNAs was found significantly changed (adj. $p < 0.05$); 6 miRNAs were downregulated, whereas 8 were upregulated (Table 20).

Log₂ fold change (cisplatin/control) of differentially expressed miRNAs ($p < 0.05$)			
Downregulated miRNAs		Upregulated miRNAs	
miRNA	Log₂FC	miRNA	Log₂FC
mir-5132	-2.79	mir-3120	2.97
mir-1199	-2.58	mir-155	2.87
mir-196b	-1.99	mir-214	2.83
mir-6321	-1.78	mir-142	2.71
mir-10a	-0.98	mir-147	2.32
mir-3064	-0.58	mir-6328	1.78
		mir-21	1.69
		mir-678	1.34

Table 20 List of significant differentially expressed miRNAs ($p < 0.05$) obtained with RNAseq analysis. Log₂ fold change (Log₂FC) of cisplatin vs control is shown.

The top five upregulated (mir-5132, mir-1199, mir-196b, mir-6321, mir-10a) and downregulated (mir-3120, mir-155, mir-214, mir-142, mir-147) miRNAs were selected for the subsequent analysis. By using the miRWalk program with a cutoff of binding p value=1, the putative target genes of the 10 aforementioned miRNAs were predicted.

The analysis showed 6192 and 5196 target genes of the five top downregulated and upregulated miRNAs respectively. The putative genes were compared with the 6333 significant (adj. $p < 0.05$) differentially expressed genes found in the RNAseq analysis. Genes in common between the two groups were selected.

As a result, 2185 and 1898 overlapping genes of the downregulated and upregulated miRNAs respectively were selected and used for the further analysis (Figure 29).

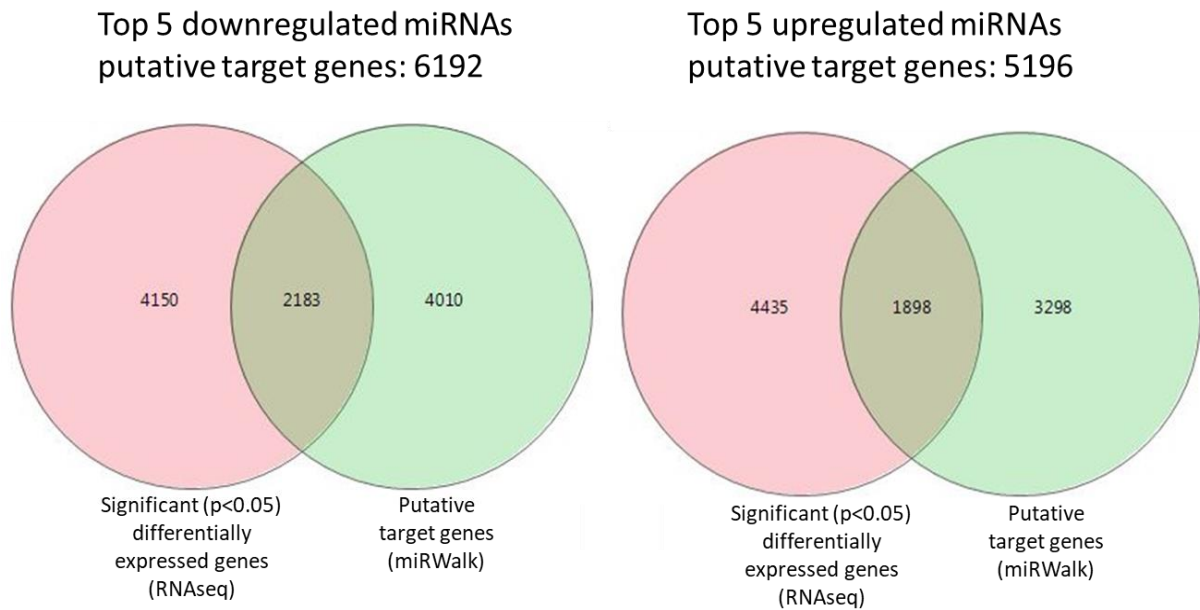


Figure 29 Selection of top 5 downregulated and upregulated miRNAs target genes. The Venn diagrams show the intersection between the putative target genes obtained by miRWalk and the differentially expressed genes found with RNAseq. Genes in common between the two groups were selected.

To elucidate their biological functions, the selected miRNA target genes were analyzed with the DAVID program, where BP-GO analysis was performed. The top 5 downregulated and upregulated miRNA selected target genes resulted in 290 and 207 significant ($p < 0.05$) BP-GO terms respectively. Only terms of interest with a cutoff of adj. $p \text{ value} \leq 0.1$ were selected. However, being the term GO:0043065 (positive regulation of apoptotic processes) of interest for our study, it was added to the list, albeit it had an adj. $p \text{ value} = 0.11$. All selected GO terms are shown in Table 21

Downregulated miRNAs target genes involved in BP-GOs

Term	Gene count	Percentage covered	adj. p value (FDR)
GO:0030335~positive regulation of cell migration	52	2.4	0.00
GO:0010628~positive regulation of gene expression	72	3.3	0.00
GO:0014070~response to organic cyclic compound	55	2.5	0.02
GO:0008285~negative regulation of cell proliferation	69	3.2	0.03
GO:0071456~cellular response to hypoxia	33	1.5	0.05
GO:0045944~positive regulation of transcription from RNA polymerase II promoter	153	7.0	0.08
GO:0043065~positive regulation of apoptotic process	62	2.8	0.11

Upregulated miRNAs target genes involved in BP-GOs

Term	Gene count	Percentage covered	adj. p value (FDR)
GO:0030335~positive regulation of cell migration	43	2.3	0.00
GO:0006468~protein phosphorylation	80	4.2	0.02
GO:0042493~response to drug	83	4.4	0.02
GO:0001822~kidney development	33	1.7	0.03
GO:0008285~negative regulation of cell proliferation	62	3.3	0.07
GO:0034162~toll-like receptor 9 signaling pathway	6	0.3	0.09

Table 21 Involvement of significant differentially expressed miRNA target genes in BP-GO terms (adj. p value ≤ 0.1 ; GO0043065 adj. p value=0.11). miRNA target genes and BP-GO terms were obtained with the miRWalk and DAVID programs respectively. For each BP-GO term, the number and the percentage of genes counted are given. Adj. p value is also reported

4.4.2. ABCB5+ cells/conditioned media effect on miRNA expression

ABCB5+ cells and derived conditioned media also affected miRNAs expression. The analysis was performed by following the workflow shown in Figure 28. Table 22 illustrates the differentially expressed miRNAs found in the different groups. 6 differentially expressed miRNAs were found in ipABCB5+ treated animals (downregulated: miR-7a-1, miR-632; upregulated: miR-3562, miR-3596b, miR-let-7d, miR-3594), 6 in CM+ (downregulated: miR-147, miR-155, miR-7a-1; upregulated: miR-5132, miR-196b, miR-3594), 2 in CM (upregulated: miR-5132, miR-186) and 1 in coCM+ (downregulated: miR-142) and ivABCB5+ (upregulated: miR-6318). Five over 14 differentially expressed miRNAs found in the cisplatin-induced nephrotoxicity model were found oppositely regulated in animals treated with CM (miR-5132), coCM+ (miR-142) and CM+ (miR-5132, miR-196b, miR-147, miR-155).

Log fold change of significant differentially expressed miRNAs ($p < 0.05$) in cisplatin model (cisplatin/control) and treated animals (treatment/cisplatin)

miRNA	LogFC					
	cisplatin model	ipABCB5+	ivABCB5+	CM	CM+	coCM+
miR-5132	-2.79			1.96	1.91	
miR-196b	-1.99				0.93	
miR-147	2.32				-1.50	
miR-142	2.71					-1.21
miR-155	2.87				-1.46	
miR-7a-1		-1.59			-1.46	
miR-186				1.26		
miR-6318			0.99			
miR-632		-1.73				
miR-3562		0.88				
miR-3596b		1.30				
miR-let-7d		1.30				
miR-3594		2.36			2.22	

Table 22 List of significant differentially expressed miRNAs ($p < 0.05$) obtained with RNAseq analysis. Positive and negative log fold change (LogFC) values are displayed in red and green respectively.

We checked for putative target genes of the miRNAs and we selected only the ones that overlaps with the differentially expressed genes found in each experimental group by RNAseq gene expression profiling. An overview is reported in Table 23.

Treatment	Downregulated miRNA target genes	Upregulated miRNA target genes	Sign (adj p<0.05) differentially expressed genes	Downregulated miRNA selected target genes	Upregulated miRNA selected target genes
lv ABCB5+	-	1988	23	-	2
lp ABCB5+	1658	6530	13	0	2
CM	-	4310	419	-	91
CM+	2410	6266	85	7	28
coCM+	677	-	15	-	0

Table 23 Number of miRNAs target genes before and after selection. Putative target genes, obtained with the miRWalk program, were compared with the significant differentially expressed genes found with RNAseq analysis. Only overlapping genes were selected

As result, only upregulated miRNAs found in CM treated animals showed a sufficient number of selected target genes to perform BP-GO analysis, which was carried out by using the DAVID database. The analysis did not show any significance at the adjusted but only at the nominal p value ($p < 0.05$). The obtained BP-GO terms are reported in Table 24.

CM treated animals
Upregulated miRNAs target genes involved in BP-GOs

Term	Gene count	Percentage covered	p value
GO:0055114~oxidation reduction	10	1.5	0.00
GO:0009611~response to wounding	6	0.9	0.03
GO:0044271~nitrogen compound biosynthetic process	6	0.9	0.01
GO:0006631~fatty acid metabolic process	5	0.7	0.01
GO:0006732~coenzyme metabolic process	4	0.6	0.03
GO:0001655~urogenital system development	4	0.6	0.03
GO:0016053~organic acid biosynthetic process	4	0.6	0.03
GO:0046394~carboxylic acid biosynthetic process	4	0.6	0.03
GO:0009309~amine biosynthetic process	4	0.6	0.01
GO:0043648~dicarboxylic acid metabolic process	4	0.6	0.00
GO:0030308~negative regulation of cell growth	3	0.4	0.04

Table 24 Involvement of upregulated miRNA target genes in BP-GOs terms (p value<0.05). miRNA target genes and BP-GO terms were obtained with the miRWalk and DAVID programs respectively. For each BP-GO term, the number and the percentage of genes counted are given. p value is also reported

4.5. Cytokines assay on conditioned media

By using an ELISA array, conditioned media were tested for the following 12 cytokines: IL2, IL4, IL5, IL6, IL10, IL12, IL13, IL17A, IFN γ , TNF α , G-CSF, TGF β 1. The result showed changes among the groups in TGF β 1, TNF α , IL6 and G-CSF levels. IL6 and G-CSF levels were higher in coCM+ compared to the other conditioned media. Higher levels of TGF β 1 and TNF α were found in M+ when compared to the other conditioned media (**Error! Reference source not found.**).

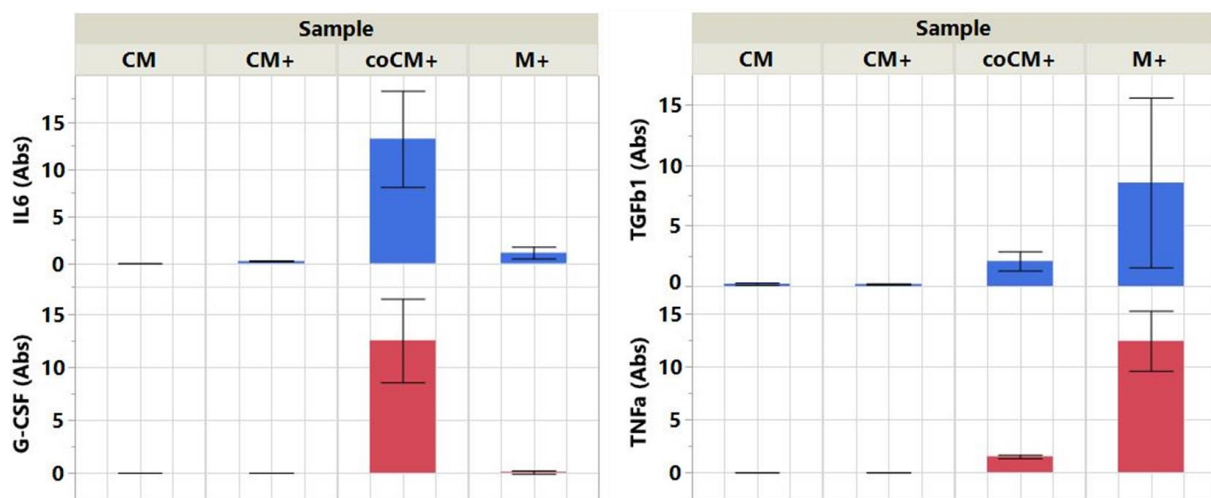


Figure 30 ELISA of 4 secreted cytokines: IL6, TNF α , G-CSF and TGF β 1. Data are corrected for the negative control and adjusted for the dilution factor. All samples were assayed in duplicate and values are shown are means \pm SD from 2–3 independent tests

5. Discussion

Nowadays, stem cells therapy represents the most promising approach for the treatment of several pathologies in different medical fields, including nephrology. Several studies described the application of different types and sources of stem cells for treating various renal diseases but up to now, no consensus about the best source, type, dose and administration route to be used has been achieved.

The aim of this study was to test the therapeutic potential of human skin derived ABCB5+ cells and different cell-derived conditioned media on renal injury.

For this purpose, a stable model of cisplatin-induced kidney damage was established in immunocompetent rats. The progression of the renal damage was evaluated by periodically measuring plasmatic and urinary parameters, performing transcutaneous assessment of renal function and checking the metabolic parameters. The established model was then used to test the therapeutic potential of ABCB5+ cells and different cell-derived conditioned media.

This study has demonstrated that ABCB5+ derived conditioned medium (CM) showed therapeutic potential both at functional and genomic level in treating cisplatin-induced nephrotoxicity.

5.1. Cisplatin-induced nephrotoxicity model in immunocompetent SD rats

Kidney failure in immunocompetent SD rats was induced by cisplatin, the nephrotoxic side effect of which is well known and documented^{36, 58}. Although cisplatin has been used for decades to establish kidney injury in animal models, there is no apparent agreement about the dose that has to be used to induce the damage or about the evaluation points that have to be chosen for monitoring the disease progress³⁹. What is known is that the severity of cisplatin-induced damage is dose and time dependent^{59, 60}. Previous studies have shown that a single ip dose of cisplatin was sufficient to induce renal impairment and that the maximum stage of tubular necrosis was reached 7 days after cisplatin administration^{61, 62}. In this study, a single ip dose of 7mg/kg BW was chosen and evaluations were made before cisplatin administration and 2, 7 and 14 days after.

Although injecting cisplatin in the peritoneum could appear an easy procedure to perform, several issues regarding both the handling and the administration of cisplatin have been encountered.

Indeed, platinum drugs are known to be relatively poorly soluble and choosing the best solvent and drug concentration is of high importance. As shown in Figure 2, cisplatin becomes active in the intracellular low chloride environment after replacing one or both of its chloride ligands with water molecules, a phenomenon known as 'aquation'¹⁹. For this reason, cisplatin has to be dissolved in saline solution with a high chloride concentration in order to prevent its aquation prior to administration. Solvents like DMSO, which reacts with cisplatin forming various complexes, or PBS, which provides an alkaline environment that leads to the hydrolysis of the drug, have to be avoided⁶³. Another important aspect to take into account is the light sensitivity of cisplatin, which makes simple routine actions, such as weighing the drug on a scale, more complicated. Therefore, it is recommended to dissolve cisplatin in saline solution to a final concentration of 0.5 mg/ml, avoiding working under direct light. After failing several times in inducing kidney injury in our animals, probably because of an incorrect handling and/or solubilization of the drug, we decided to use a ready-to-use cisplatin solution provided by the company TEVA⁶⁴.

To induce renal damage in rodents, cisplatin is usually ip administrated. Although it seems a simple procedure, ip injection needs to be precisely performed in order not to puncture vital organs such as the cecum, which causes pain and sometimes peritonitis. Moreover, if cisplatin is administrated intra-caecum rather than ip, animals do not develop kidney injury. It is known that the cecum is most commonly located in the left part of the abdominal cavity. However, a study conducted on rats has demonstrated that the position of the caecum varies among species, litters and gender⁶⁵. Therefore, a correct ip injection represents a critical point for the induction of renal damage. In order to overcome a possible intra-caecum puncture, we decided to perform ip injection under short isoflurane anesthesia and by using a butterfly cannula rather than a normal needle. In this way, while the animal is lying on its back, we could lift the abdominal wall and introduce the cannula under the skin fold. A free movement of the cannula was the sign that we were in the peritoneum and that we could then inject the drug. Eventually, after several trials, we were able to perform a correct ip injection.

For monitoring the progression of the disease, blood and urine parameters were analyzed. Plasma creatinine and urea are worldwide accepted as gold standard markers of renal damage, even though several studies showed that their levels were not always found altered at the same stage of the disease. Indeed, some previous studies showed increased plasma creatinine and urea levels detectable already 2 days after cisplatin administration⁶⁶, while in other studies they were not detectable until 5 days after cisplatin administration⁶⁰. Notably, it has to be also taken into account that plasma creatinine lacks sensitivity and its level can also be affected by non-renal factors such as gender, age, physical activity, muscle mass and liver function⁶⁷⁻⁷⁰. The experiment performed here showed that the single intraperitoneal dose of cisplatin used was sufficient to induce renal damage. Indeed, already 2 days after the administration of cisplatin, animals showed a 1.6 and 2-fold increase of plasma creatinine and urea respectively when compared to the healthy not treated animals. These parameters remain altered until the end of the experiment, with a peak on day 7 when an increase of 7.6-fold for creatinine and 7.5-fold for urea was observed (Figure 7).

Other plasma parameters, which were found altered in this model, were cholesterol and triglycerides. Cholesterol increased by 1.4-fold compared to the control animals already on day 2 and it remained high until the end of the experiment. Differently, triglycerides halved on day 2 and then increased in the following days, by reaching a 1.2-fold increase on day 14 in the cisplatin-treated animals compared to the time-matched controls (Figure 8). Hypercholesterolemia and hyperlipidemia had been previously described in cisplatin-treated rats⁷¹ and it has been explained as a consequence of the excessive production of reactive oxygen species during the induced damage³⁵. Additionally, accumulation of cholesterol in kidney affected by renal injury was seen and it has been proposed to be part of a “renal stress response”^{72, 73}.

Electrolyte deficiencies after cisplatin treatment were widely described in literature^{74, 75}. We analyzed plasma and urinary levels of calcium, potassium, sodium and phosphate, unfortunately, we did not measure magnesium. It is known that cisplatin induces renal magnesium wasting which can lead to hypocalcemia and hypercalciuria⁷⁶. We observed an early hypocalcemia on day 2 and a following hypercalcemia on day 7 and 14. Hypercalciuria was observed on day 14. Being magnesium a cofactor of ATP, hypomagnesemia leads to

potassium and phosphate wasting^{74, 77}. In this model, hypokalemia, hypophosphaturia and a marked decrease in urinary potassium was detected on day 2. Hypophosphaturia was observed on day 14. In contrast to the other electrolytes wasting, sodium level remained stable in both urine and plasma (Figure 9).

In this model, urine analyses showed no proteinuria, even though kidney injury is usually associated with a loss of proteins. Previous studies in rats have shown proteinuria 4/5 days after cisplatin administration, which resolved spontaneously in the next days^{60, 61}. Therefore, it could be possible that there was proteinuria between day 2 and 7 but was not detected. Conversely, abundant albuminuria, which is typically associated to proximal tubular dysfunction⁷⁸, was recorded from day 2 onwards with respect to the corresponding controls. Damaged proximal tubular cells also fail in reabsorbing glucose, leading to glycosuria⁷⁹. In our model, urinary glucose level progressively increased by 17.2-fold on day 7 until 26.8-fold on day 14. Glycosuria was not associated to glycemia, accordingly with the typical scenario of tubular dysfunction (Figure 11).

Urine volume is another parameter that has to be considered when referring to kidney injury. Polyuria, indeed, was already largely described in literature as a consequence of cisplatin therapy⁸⁰. In the model here described, diuresis triplicated on day 7 and visibly remained high until the end of the experiment, along with a significant increase of water intake from day 7 onwards (Figure 14).

Concerning BW, it is well known that cisplatin induces anorexia⁸¹. Accordingly, already 2 days after cisplatin administration, animals decreased the amount of food intake, which was reflected by a decrease in weight gain on day 7 and 14. While control animals progressively gained weight, cisplatin-treated animals visibly appeared more fatigued and weaker than the time-matched controls (Figure 15).

Besides its well documented nephrotoxic effect, cisplatin-induced hepatotoxicity has also been reported^{82, 83}. To test whether in our model cisplatin affects liver, plasma levels of the hepatic enzymes were also measured. In a previous study⁸⁴, increased plasma levels of AST and ALT were recorded in rats already 2 days after cisplatin administration. Differently, we observed a

reduction in AST levels on day 2 in the treated animals compared to the controls, which was probably due to outliers in the control group. No differences were observed in ALT and GGT levels. However, we observed an increase by 2.5-fold on GDHL levels on day 7 but the result was not statistically significant (Figure 10). A possible explanation to this apparently incongruent result could be addressed to the cisplatin dose used in our experiment. Indeed, significant increases of hepatic enzymes were found in studies in which high doses of cisplatin were used. In oncology, the cisplatin dose that can be administrated for cancer therapy has to be low to minimize the nephrotoxic side effect, which usually occurs at a lower dose than the one which could lead to hepatotoxicity⁸². Therefore, we probably did not see severe changes in liver enzymes because we did not use a very high cisplatin dose, apparently needed for liver damage.

Besides plasma and urine analyses, the progress of the diseases was also evaluated by a transcutaneous measurement of renal function^{51, 52, 54}. Briefly, the ABZWCY-HP β CD fluorescent dye was iv injected into the animals and its excretion curve was transcutaneously measured with a specific device. Nowadays, this represents an innovative, precise, not invasive analysis for measuring the renal function. The results indicate that ABZWCY-HP β CD half-life in healthy rats of this strain is between 32 to 39 minutes. Data showed that already 2 days after cisplatin administration, ABZWCY-HP β CD half-life increased by 1.8-fold, and doubled after 14 days, indicating that the renal function is extremely compromised (Figure 13).

Histological kidney sections also showed the nephrotoxic effect of cisplatin. Indeed, it is well known that cisplatin accumulates in the renal proximal tubules, where it causes the main damage^{26, 32, 85, 86}. Accordingly to what is described in literature^{84, 87}, we observed the expected histological changes due to cisplatin treatment, with predominant proximal tubular degeneration and formation of casts in the lumen due to proteins and detached tubular cells (Figure 16 and Figure 17). We did not observe cisplatin-induced glomerular damage, which could be recorded after long-term exposure to cisplatin^{88, 89}.

Gene expression analysis was performed with RNAseq technology. To the best of our knowledge (NCBI GEO Series, keyword: cisplatin, <https://www.ncbi.nlm.nih.gov/geo/browse/?view=series&search=cisplatin&tax=10116&zsort>

[=date&display=20](#)), this is the first study that analyzed changes in gene expression in a cisplatin-induced nephrotoxicity model in SD rats by using RNAseq.

Cluster analysis showed that the two experimental groups distinctly clustered and showed 6333 differentially expressed genes in the cisplatin treated animals when compared to the controls. The GSEA analysis, which analyzes sets of genes describing pathways, revealed 49 significant differentially expressed pathways in the cisplatin treated animals when compared to the controls.

We observed that cisplatin promoted the upregulation of apoptosis and p53 signaling pathways, which lead to tissue degeneration (Table 13). In line with our result, the activation of p53 after cisplatin administration and the consequent increase of caspase cascade that leads to apoptosis has been largely described in literature⁹⁰⁻⁹⁴. Cisplatin-induced up-regulation of death receptors and their ligands, such as TNFR1, TNFR2, TNF α , Faslg and Fas, which are responsible for the extrinsic pathway of the programmed cell death, has also been reported⁹⁵⁻⁹⁷. Accordingly, in our model all the aforementioned receptors and ligands were found upregulated.

TNF α plays an important role during cisplatin-induced nephrotoxicity, not only in terms of apoptosis induction, but also in relation to inflammation, due to its ability to activate pro-inflammatory molecules^{95,98}. Indeed, we found upregulated pathways related to cytokine and chemokine activity. Furthermore, our model showed upregulation of immune system pathways, such as leucocytes recruitment and activation, indicating an ongoing inflammatory response. Accordingly, we also observed immune cells infiltrate in the kidney histological sections (Figure 16 and Figure 17).

As reported in literature, also the renin-angiotensin system (RAS) was affected by cisplatin (Table 13). Indeed, beside the well-known circulatory RAS, it has also been identified an intra-tubular RAS⁹⁹⁻¹⁰². As mentioned before, we know that cisplatin selectively accumulates in the proximal tubular cells, where it triggers apoptosis. As we expected, in our cisplatin-induced nephrotoxicity model we observed a downregulation of the renal RAS due to tubular cell death. Changes in the cell cycle of renal cells after cisplatin administration have also been investigated. It is known that after DNA damage, p53 induces the expression of p21, which interacts with cdk2 and causes G1 phase arrest¹⁰³. Accordingly, in our model we found an upregulation of

the cell cycle pathway, where both p53 and p21 appear to be highly upregulated (Table 14). Worthy to be mentioned, a p53-independent activation of p21 has also been reported¹⁰⁴. Studies have demonstrated that the activation of p21 after cisplatin administration is a protective strategy that kidney cells apply to avoid DNA-damaged cells from entering the cell cycle^{105, 106}.

Concerning signaling activity, several pathways, such as MAPK, JAK/STAT, NFkB, PI3K-AKT, which are known to be involved in the regulation of apoptosis, cell cycle, immune cell recruitment and cell interaction, were found upregulated (Table 15). Changes in the regulation of these pathways in relation to cisplatin-induced nephrotoxicity have been largely investigated for decades¹⁰⁷⁻¹¹¹.

Pathways related to metabolism, including carbon, fatty acid, amino acid and oxocarboxylic acid metabolic pathways, were found downregulated (Table 13). A possible explanation could be the cisplatin-induced cell death, which is also evident in the histological sections, where the nude basal membrane of the tubuli is clearly visible. The only metabolic pathway found upregulated in our model is the one relating to the glycosaminoglycan (GAG) biosynthesis. GAGs are polysaccharides that can be expressed on the cell surface or be part of the ECM. By interacting with many different proteins, GAGs can be involved in several biological functions involving tissue development and homeostasis^{112, 113}. GAGs are well known to take part in the wound healing process, during which the degraded tissue is replaced with a new functional one¹¹⁴. Therefore, we assume that these molecules are conducting an ongoing regenerative process. Indeed, it has to be taken into account that we are analyzing the gene expression profile of renal tissue 14 days after cisplatin administration and that, at that time, a regenerative process can occur. Supporting this hypothesis, several pathways involved in DNA replication, ribosome and spliceosome assembly, ECM remodeling and cell junctions were also found upregulated.

The GSEA results described so far seem to define two different phenomena happening in the kidney at the same time: tissue degeneration, due to cisplatin, and tissue regeneration, due to the kidney intrinsic self-recovery ability¹¹⁵. Nowadays, it is still poorly understood what mediates the renal regeneration, but the latest results address this ability to the renal epithelium cells that have survived the injury and that can either transdifferentiate in other cells or

dedifferentiate and acquire mitotic properties¹¹⁶⁻¹¹⁸. The role of the immune system, mainly dendritic cells and M2 macrophages, has also been addressed to induce renal regeneration¹¹⁹⁻¹²².

Besides the mRNA expression profiling just described, RNAseq technology also allows to perform miRNAs expression analysis. Indeed, we were able to identify miRNA precursors differentially expressed in our model, which can be used to predict their putative targets. miRNAs are involved in the post-transcriptional regulation of gene expression and a single miRNA can regulate hundreds of genes¹²³⁻¹²⁵. Understanding the link between miRNA and cisplatin-induced kidney injury would be of great importance and the scientific community has already started focusing on that direction. Some studies have already identified some miRNAs related to cisplatin-induced nephrotoxicity. These miRNAs were mainly involved in the regulation of apoptosis and cell cycle¹²⁶⁻¹²⁸. In our model, 6 downregulated (mir-5132, mir-1199, mir-196b, mir-6321, mir-10a, mir-3064) and 8 upregulated (mir-3120, mir-155, mir-214, mir-142, mir-147, mir-6328, mir-21, mir-678) miRNAs were found (Table 20) and among them, mir-155 had already been associated with cisplatin-induced nephrotoxicity¹²⁹. In order to have an idea of the miRNA-mRNA networks involved in our model, miRNAs target genes were predicted and combined with the differentially expressed genes found in the mRNAs analysis. The intersection of these two groups of genes were used for functional annotation analysis (Figure 29). The BP-GO analysis revealed the involvement of the top 5 downregulated miRNAs in the regulation of cell migration and proliferation, apoptosis, transcription and regulation of gene expression. BP-GO terms found for the top 5 upregulated miRNAs were mainly involved in the regulation of cell migration and proliferation, response to drugs, kidney development and toll-like 9 signaling pathway, an immune-system related pathway (Table 21).

Overall, taking into account all the functional, morphological and genetic changes described so far, we can assume that the cisplatin-induced nephrotoxicity model was successfully established and could be used for the application and evaluation of new therapies.

5.2. Therapeutic effect of ABCB5+ cells and conditioned media in cisplatin-induced nephrotoxicity model in SD rats

The cisplatin-induced nephrotoxicity model, which we previously established and described, was used to test the therapeutic potential of stem cells and conditioned media. Indeed, in the last decades, stem cells have been largely used as a possible treatment for several pathologies in different medical fields and encouraging results have been achieved¹³⁰. In nephrology, different cell types and sources have been used but, up to now, no consensus about what is best to be used has been reached⁴⁰. In our study, we decided to use a subpopulation of human dermal stem cells characterized by the expression of the ABCB5 peptide on their membrane⁴⁹. These cells represent a particular non-hematopoietic lineage cell subset that shows immune-regulatory functions similar to stem cells. ABCB5+ cells were purified from skin of healthy individuals of different sex, age and nationality by Ticeba-RHEACELL and were delivered as a ready-to-use solution. In our cisplatin-induced nephrotoxicity animals, ABCB5+ cells were administered not only iv, but also ip. Indeed, one of the major concerns regarding the iv administration route is that the injected cells might be trapped within the lung and could provoke embolism, which can lead to death¹³¹⁻¹³³. To overcome this problem, beside the common iv administration, we decided to additionally test the ip cell administration and to compare the outcomes obtained by the two administration routes.

We analyzed the same plasma and urine parameters we checked for the model characterization but, surprisingly, no differences were observed between the cell treated and untreated animals. All parameters remained relatively constant, indicating that no amelioration was achieved by using the cells (Table 7, Table 8). Similarly, no improvement was observed when the BW and the food intake were evaluated (Table 10). Additionally, histology of kidney section did not show any visible amelioration after cell administration (Figure 23). Moreover, the transcutaneous measurement of renal function showed an ABZWCY-HP β CD half-life even higher than the one of the cisplatin-treated animals, indicating that the ABCB5+ treatment even worsened the animals' renal function (Table 9).

To investigate the genetic effects induced by ABCB5+ cell administration on kidney, we performed gene expression profiling of renal tissue and GSEA analysis. Overall, some

differences between animals treated with the two different administration routes were observed when compared to the cisplatin-treated animals. The analysis revealed that downregulation of pathways involved in signal transduction were found in both groups but mostly in the ipABCB5+ one, evidencing that the treatments took action at the genetic level and had some effects on cell growth, metabolism, proliferation and immune system response.

Metabolic pathways regarding carbohydrate, lipid and nucleotide metabolism were upregulated in both groups (Table 16). Upregulation of DNA replication and repair in ipABCB5+ group, and upregulation of ribosome and proteasome activity in both groups were also observed, indicating that new cells were developing (Table 17).

We did not observed any difference in the RAS expression but we recorded an upregulation of the renin secretion pathway in both groups (Table 19). Accordingly, signaling pathways involved in renin synthesis, such as cAMP, cGMP and calcium signaling pathways, were also found downregulated (Table 18).

In both groups, but mainly in the animals treated with ipABCB5+ cells, immune system pathways were found downregulated, signifying that inflammation was attenuated (Table 19). Conversely, in animals treated with ipABCB5+, upregulation of pathways regarding ECM remodeling and cell adhesion were found downregulated, indicating that the tissue was not regenerating (Table 18). In support of this thesis, glycan degradation and downregulation of their biosynthesis was also found in ipABCB5+ group (Table 16).

Overall, the analysis indicated that the ipABCB5+ cell treatment displayed a higher reduction of inflammation than the ivABCB5+ cell one. The ip treatment also showed new cell formation, which was not associated to tissue remodeling.

miRNA analysis was also performed. Six significant differentially expressed miRNAs were found in ipABCB5+ treated animals (downregulated: miR-7a-1, miR-632; upregulated: miR-3562, miR-3596b, miR-let-7d, miR-3594) and only one in ivABCB5+ (upregulated: miR-6318). None of these miRNAs was found in the cisplatin model (Table 22). However, the intersection of predicted miRNA target genes with differentially expressed genes did not give a sufficient number of genes to perform BP-GO analysis (Table 23).

The results just discussed revealed that even though we have not been able to see any amelioration in the plasma and urine parameters, in the renal function and in the histology, animals treated with ABCB5+ cells underwent genetic changes.

In the last decades, the scientific community has mostly focused its attention to the stem cell secretome, assuming that the therapeutic potential of stem cells is not due to the cells themselves but it is more ascribed to what they release in the medium where they grow⁴⁶. Therefore, a paracrine therapeutic effect of stem cells has been proposed^{44,45}. In the light of this and seen the weak results achieved with the administration of ABCB5+ cells, we decided to use conditioned medium of ABCB5+ cells as an alternative therapy for the treatment of cisplatin-induced kidney injury. Conditioned medium from ABCB5+ cell culture was collected and referred as CM.

A previous study has demonstrated that local injection of ABCB5+ cells around a wound accelerates the healing process by promoting the macrophage polarization from a M1 pro-inflammatory to a M2 anti-inflammatory phenotype via paracrine release of IL-1RA (Ticeba, personal communication). The study asserted that ABCB5+ cells have immune-modulatory effects on macrophages by inducing their polarization into the M2 anti-inflammatory phenotype. Based on this data, ABCB5+ cells were co-cultured with macrophages and both cells were stimulated with LPS and IFN γ , known factors for macrophages polarization triggering¹³⁴. The medium conditioned by the co-culture was collected and called coCM+. To test a possible effect of LPS and IFN γ on ABCB5+ cells, we also cultured and stimulated ABCB5+ cells without macrophages and we collected the derived conditioned medium, which was referred as CM+.

Thereby, the therapeutic potential of the three aforementioned conditioned media, CM, CM+ and coCM+, was tested in our cisplatin-induced nephrotoxicity model, yielding promising results.

Especially on day 7, we observed a noteworthy reduction of plasma creatinine and urea in animals treated with CM and CM+. More precisely, creatinine decreased by more than 4 and 2 times while urea by 3 and almost 2 times in animals treated with CM and CM+ respectively when compared to the cisplatin treated group (Figure 18). On day 14, albuminuria was

ameliorated in animals treated with all the conditioned media (Figure 20), while glycosuria was highly decreased only in CM treated animals (Figure 21). Regarding the hepatic enzymes, GLDH levels decreased on day 7 by almost 4 and 3 times in animals treated with CM and CM+ respectively (Figure 19). Oddly, the increase of plasma triglycerides observed on day 7 on in our model, seems to be exacerbated in animals who received CM. Between day 2 and 7, which represents the critical time span when cisplatin treated animals loose gaining BW, animals who received CM+ maintained a quite stable BW, while the ones who received CM even gained weight. At the same time, the food intake in CM and CM+ treated animals was higher than in the control and coCM+ treated groups. Moreover, loss of weight gain was recorded between day 2 and 7 in animals who received coCM+ (Table 10). Renal function transcutaneously measured on day 7 and 14 showed that animals treated with CM and CM+ had faster ABZWCY-HP β CD excretion when compared with the cisplatin-treated animals (Table 9). Additionally, in CM treated animals, the histological results revealed a less severe damage in terms of affected area and protein casts accumulation. Indeed, this group presented proximal tubule damage mainly in the juxtamedullary region rather than in the whole corticomedullary region (Figure 23).

To investigate the genetic effects induced on kidney by conditioned media administration, we performed gene expression profiling of renal tissue and GSEA analysis. The analysis revealed pronounced differences among the treatments.

Indeed, we observed 20 downregulated pathways involved in signal transduction in coCM+ treated animals and only 6 of them, such as, TNF α , MAPK and NF κ B pathways, in the CM group when compared to the cisplatin-treated animals (Table 18). Interestingly, the CM+ group seemed not to be significantly affected at the signaling level, where we only observed the upregulation of Rap1 pathway, which is involved in cell adhesion. Accordingly, pathways regarding ECM and cell adhesion were mainly found downregulated in coCM+ but not in CM+ treated animals (Table 18). Following the same trend, immune system pathways resulted significantly downregulated in CM and coCM+ treated animals but not in the CM+ group (Table 19).

Therefore, the first conclusion we can draw from these results is that in CM and coCM+ treated animals we observe a downregulation of signal transduction that mainly reflects a decrease in

the inflammatory process, while CM+ treated animals showed no significant changes compared to the cisplatin treated animals.

Concerning tissue metabolism, pathways regarding carbohydrate, lipid and amino acid metabolism were upregulated in all groups, but mainly in CM and coCM+ (Table 16). Also the RAS pathway, which was found downregulated in our model, was upregulated in CM and coCM+ treated animals, indicating tubular activity (Table 16).

In coCM+ treated animals, the pronounced activation of the metabolism, the upregulation of the proteasome and ribosome formation and the downregulation of the TNF α pathways, seems to describe a possible scenario where cell death is decreased and new cells maybe forming. On the other hand, cell cycle and DNA replication pathways were not found significantly changed in this group when compared to the cisplatin-treated animals. Interestingly, cell cycle was downregulated in the CM+ group, and so all the pathways involved in translation, transcription and replication.

Based on gene expression analysis, it seems that the better results in terms of new cell formation was achieved by using the coCM+ treatment, while a reduction of inflammation was observed in both CM and coCM+ treated animals.

miRNA analysis was also performed. Six differentially expressed miRNAs were found in CM+ (downregulated: miR-147, miR-155, miR-7a-1; upregulated: miR-5132, miR-196b, miR-3594), 2 in CM (upregulated: miR-5132, miR-186) and 1 in coCM+ (downregulated: miR-142) and ivABCb5+ (upregulated: miR-6318). Five over 14 differentially expressed miRNAs found in the cisplatin-induced nephrotoxicity model were found oppositely regulated in animals treated with CM (miR-5132), coCM+ (miR-142) and CM+ (miR-5132, miR-196b, miR-147, miR-155) (Table 22). However, from the intersection of predicted miRNA target genes with differentially expressed genes only CM treated animals showed a sufficient number of genes to perform BP-GO analysis (Table 23). The analysis revealed the involvement of the downregulated miRNAs mostly in metabolic processes, cell growth and response to wounding (Table 24).

We then questioned whether a possible different cytokine content in the three conditioned media could be the reason of the different gene expression results we observed. For this purpose, we checked for 12 cytokines (IL2, IL4, IL5, IL6, IL10, IL12, IL13, IL17A, IFN γ ,

TNF α , G-CSF, TGF β 1) that are known to be involved in inflammatory processes. As expected, we found some cytokines in coCM+ and M+. Indeed, it has already been known, that macrophages can synthesize and release a large variety of cytokines, which can be involved in several processes like immunity and homeostasis^{135, 136}. We observed that in presence of ABCB5+ cells, stimulated macrophages produced less pro-inflammatory cytokine TNF α , indicating a possible presence of a M2 macrophage population (Figure 30). TGF β 1 and TNF α , predictably detected in M+, were found less abundant in coCM+, while IL-6 and G-CSF levels were found more than 10 times higher in coCM+ compared to all the other media. Excluding M+ and focusing on the three conditioned media administrated to the animals, we observe that coCM+ is the only medium in which TGF β 1, TNF α , IL-6 and G-CSF were found. We then questioned about the effects of these cytokines and whether they, once injected in the bloodstream of cisplatin-treated animals, could trigger any positive or negative response. As reported in literature, IL-6 is a pleiotropic cytokine that, depending on the situations, can have both anti-inflammatory and pro-inflammatory properties¹³⁷⁻¹³⁹. Together with TNF α , IL-6 has been associated with muscle wasting and weight loss, which were indeed observed in the animals treated with coCM+^{140, 141}. G-CSF is an immune modulator and a mobilizer of hematopoietic and mesenchymal stem cells from the bone marrow to the blood. Although the mechanism of action is still poorly understood, it is believed that, once in the bloodstream, the recruited stem cells could play a possible role in tissue recovery. Additionally, G-CSF has also been found to either modulate or exacerbate inflammatory processes depending on the context^{142, 143}. TGF β 1 has been considered as an anti-inflammatory cytokine, even though more recent findings showed its involvement in the pro-inflammatory Th17 cell differentiation^{144, 145}. Under various circumstances, it can be either an anti-inflammatory or pro-inflammatory cytokine. Therefore, due to their pleiotropic potential, it is difficult to guess whether these cytokines can trigger a pro- or anti-inflammatory effect once injected into the cisplatin-treated animals. However, based on our transcriptomic data, we observed a higher anti-inflammatory effect in the coCM+ treated animals when compared to the other groups, indicating a possible involvement of these cytokines.

In summary, this study describes the different outcomes obtained by treating cisplatin-induced nephrotoxicity with both ABCB5+ cells and derived conditioned media.

Regarding ABCB5+ cells treatment, we could demonstrate that the ip administration route could be a valid alternative to the classical and risky iv one. Although treatment with ABCB5+ cells did not show any functional amelioration. Neither of the two administration routes, ip injection of cells was able to promote important and more pronounced genetic changes in the renal tissue. Differently, conditioned media, and in particular CM, were able to induce some changes both at the functional and genetic level. coCM+ showed pronounced changes in the renal gene expression, but it failed in promoting amelioration in the plasma and urine parameters. Indeed, according to our results, CM displays the most pronounced therapeutic potential in treating cisplatin-induced nephrotoxicity, representing a promising approach. Certainly, further studies are necessary to investigate the modes of action involved and to optimize the therapeutic regimen to use for a possible translation to the clinical field.

6. Summary

Kidney diseases are a global public health problem that lacks of effective therapies to prevent progressive loss of renal function after initial damage. Every year, we witness a continuous increase in the incidence of ESRD, for which the only available treatments are dialysis or renal transplantation. Being these two therapeutic options not only invasive for the patients, but also highly expensive for the public health system, new treatments are urgently required. In this scenario, stem cell therapy represents a promising approach for the treatment of renal injuries. Several studies have been conducted in this direction, but still no consensus has been achieved in terms of cell source, dose, timing and administration route to be used. In addition, the modes of action with which stem cells perform their therapeutic effects remain unclear and need further explanations.

In this study, we established a well-defined animal model of cisplatin-induced kidney injury that was then used to assess the therapeutic potential of ABCB5+ cells and derived conditioned media.

For the development of the animal model, we induced renal damage in immunocompetent SD rats by using a single ip injection of cisplatin, a well-known nephrotoxic drug, at the dose of 7 mg/kg BW. The onset and progression of the disease has been characterized on the basis of plasma, urine and metabolic parameters, renal function transcutaneously measured, histological evaluation and both mRNA and miRNA expression profiling. The analyses performed indicated the successful establishment of a stable cisplatin-induced nephrotoxic model that was then used to assess the therapeutic potential of ABCB5+ cells and derived conditioned media. The following treatments have been tested: 1) ABCB5+ cells both iv and ip administrated; 2) ABCB5+ cells derived conditioned media iv administrated (CM, CM+, coCM+).

The results showed that when animals were treated with ABCB5+ cells, we have not been able to see any amelioration in the plasma and urine parameters, renal function and histology and we did not observe any differences between the two applied administration routes. However, these animals did undergo genomic changes, which were even different in the two groups. Indeed, based on the gene expression analysis performed in renal tissue, it seems that the ipABCB5+ cell treatment triggered new cell formation and promoted a higher reduction of inflammation compared to the ivABCB5+ cell one.

In contrast, when three different conditioned media were administered to the animals, we were able to see changes at the functional level. Indeed, markers of renal function, such as plasma creatinine and urea and urine albumin, were ameliorated especially after CM and CM+ treatments, while animals which received coCM+ did not show any deviation from the control animals. A similar trend was observed when the transcutaneous assessment of renal function was performed. Additionally, CM and CM+ treated animals did not lose appetite and therefore they did not show the typical loss of weight observed in the other experimental groups.

However, at the genomic level, coCM+ treated group exhibited better results in terms of reduction of inflammation and new cell formation, showing some similarity with the ipABC5+ cell treated group. Also in the CM treated group a reduction of inflammation was reported, while CM+ treated animals did not show any relevant changes when compared to the cisplatin-induced nephrotoxicity model. Additionally, BP-GO analysis of downregulated miRNAs found in CM treated animals, showed their involvement mostly in metabolic processes, cell growth and response to wounding.

In conclusion, all together the results presented here demonstrate that CM displays the most pronounced therapeutic potential both at functional and genomic level in treating cisplatin-induced nephrotoxicity. For a possible translation to the clinical field, further studies to optimize the therapeutic regimen and to elucidate the involved modes of action are needed.

7. References

1. Levey, AS, Inker, LA: GFR as the "Gold Standard": Estimated, Measured, and True. *Am J Kidney Dis*, 67: 9-12, 2016.
2. Couser, WG, Remuzzi, G, Mendis, S, Tonelli, M: The contribution of chronic kidney disease to the global burden of major noncommunicable diseases. *Kidney Int*, 80: 1258-1270, 2011.
3. Choudhury, D, Ahmed, Z: Drug-associated renal dysfunction and injury. *Nat Clin Pract Nephrol*, 2: 80-91, 2006.
4. Ferguson, MA, Vaidya, VS, Bonventre, JV: Biomarkers of nephrotoxic acute kidney injury. *Toxicology*, 245: 182-193, 2008.
5. Skinner, R: Nephrotoxicity--what do we know and what don't we know? *J Pediatr Hematol Oncol*, 33: 128-134, 2011.
6. Pazhayattil, GS, Shirali, AC: Drug-induced impairment of renal function. *Int J Nephrol Renovasc Dis*, 7: 457-468, 2014.
7. Awdishu, L, Mehta, RL: The 6R's of drug induced nephrotoxicity. *BMC Nephrol*, 18: 124, 2017.
8. Taber, SS, Pasko, DA: The epidemiology of drug-induced disorders: the kidney. *Expert Opin Drug Saf*, 7: 679-690, 2008.
9. Mehta, RL, Pascual, MT, Soroko, S, Savage, BR, Himmelfarb, J, Ikizler, TA, Paganini, EP, Chertow, GM: Spectrum of acute renal failure in the intensive care unit: the PICARD experience. *Kidney Int*, 66: 1613-1621, 2004.
10. Uchino, S, Kellum, JA, Bellomo, R, Doig, GS, Morimatsu, H, Morgera, S, Schetz, M, Tan, I, Bouman, C, Macedo, E, Gibney, N, Tolwani, A, Ronco, C: Acute renal failure in critically ill patients: a multinational, multicenter study. *Jama*, 294: 813-818, 2005.
11. Izzedine, H, Perazella, MA: Anticancer Drug-Induced Acute Kidney Injury. *Kidney Int Rep*, 2: 504-514, 2017.
12. Desoize, B, Madoulet, C: Particular aspects of platinum compounds used at present in cancer treatment. *Crit Rev Oncol Hematol*, 42: 317-325, 2002.
13. Rosenberg, B, Vancamp, L, Krigas, T: Inhibition of cell division in escherichia coli by electrolysis products from a platinum electrode. *Nature*, 205: 698-699, 1965.

14. Rosenberg, B, VanCamp, L, Trosko, JE, Mansour, VH: Platinum compounds: a new class of potent antitumour agents. *Nature*, 222: 385-386, 1969.
15. Prestayko, AW, D'Aoust, JC, Issell, BF, Crooke, ST: Cisplatin (cis-diamminedichloroplatinum II). *Cancer Treat Rev*, 6: 17-39, 1979.
16. Florea, AM, Busselberg, D: Cisplatin as an anti-tumor drug: cellular mechanisms of activity, drug resistance and induced side effects. *Cancers (Basel)*, 3: 1351-1371, 2011.
17. Einhorn, LH, Donohue, J: Cis-diamminedichloroplatinum, vinblastine, and bleomycin combination chemotherapy in disseminated testicular cancer. *Ann Intern Med*, 87: 293-298, 1977.
18. Manohar, S, Leung, N: Cisplatin nephrotoxicity: a review of the literature. *J Nephrol*, 31: 15-25, 2018.
19. Eljack, ND, Ma, HY, Drucker, J, Shen, C, Hambley, TW, New, EJ, Friedrich, T, Clarke, RJ: Mechanisms of cell uptake and toxicity of the anticancer drug cisplatin. *Metallomics*, 6: 2126-2133, 2014.
20. Saad, SY, Najjar, TA, Alashari, M: Role of non-selective adenosine receptor blockade and phosphodiesterase inhibition in cisplatin-induced nephrogonadal toxicity in rats. *Clin Exp Pharmacol Physiol*, 31: 862-867, 2004.
21. Ozben, T: Oxidative stress and apoptosis: impact on cancer therapy. *J Pharm Sci*, 96: 2181-2196, 2007.
22. Hampton, MB, Orrenius, S: Dual regulation of caspase activity by hydrogen peroxide: implications for apoptosis. *FEBS Lett*, 414: 552-556, 1997.
23. Shrivastava, A, Kuzontkoski, PM, Groopman, JE, Prasad, A: Cannabidiol induces programmed cell death in breast cancer cells by coordinating the cross-talk between apoptosis and autophagy. *Mol Cancer Ther*, 10: 1161-1172, 2011.
24. Tsang, RY, Al-Fayea, T, Au, HJ: Cisplatin overdose: toxicities and management. *Drug Saf*, 32: 1109-1122, 2009.
25. Rabik, CA, Dolan, ME: Molecular mechanisms of resistance and toxicity associated with platinating agents. *Cancer Treat Rev*, 33: 9-23, 2007.
26. Madias, NE, Harrington, JT: Platinum nephrotoxicity. *Am J Med*, 65: 307-314, 1978.
27. Goldstein, RS, Mayor, GH: Minireview. The nephrotoxicity of cisplatin. *Life Sci*, 32: 685-690, 1983.
28. Miller, RP, Tadagavadi, RK, Ramesh, G, Reeves, WB: Mechanisms of Cisplatin nephrotoxicity. *Toxins (Basel)*, 2: 2490-2518, 2010.
29. Peres, LA, da Cunha, AD, Jr.: Acute nephrotoxicity of cisplatin: molecular mechanisms. *J Bras Nefrol*, 35: 332-340, 2013.

30. Yao, X, Panichpisal, K, Kurtzman, N, Nugent, K: Cisplatin nephrotoxicity: a review. *Am J Med Sci*, 334: 115-124, 2007.
31. Stan K. Bardal, JEW, Douglas S. Martin,: Chapter 2 - Pharmacokinetics. *Applied Pharmacology*,: 17-34, 2011.
32. Ciarimboli, G, Ludwig, T, Lang, D, Pavenstadt, H, Koepsell, H, Piechota, HJ, Haier, J, Jaehde, U, Zisowsky, J, Schlatter, E: Cisplatin nephrotoxicity is critically mediated via the human organic cation transporter 2. *Am J Pathol*, 167: 1477-1484, 2005.
33. Filipski, KK, Loos, WJ, Verweij, J, Sparreboom, A: Interaction of Cisplatin with the human organic cation transporter 2. *Clin Cancer Res*, 14: 3875-3880, 2008.
34. dos Santos, NA, Carvalho Rodrigues, MA, Martins, NM, dos Santos, AC: Cisplatin-induced nephrotoxicity and targets of nephroprotection: an update. *Arch Toxicol*, 86: 1233-1250, 2012.
35. Kuhlmann, MK, Burkhardt, G, Kohler, H: Insights into potential cellular mechanisms of cisplatin nephrotoxicity and their clinical application. *Nephrol Dial Transplant*, 12: 2478-2480, 1997.
36. Pabla, N, Dong, Z: Cisplatin nephrotoxicity: mechanisms and renoprotective strategies. *Kidney Int*, 73: 994-1007, 2008.
37. de Castria, TB, da Silva, EM, Gois, AF, Riera, R: Cisplatin versus carboplatin in combination with third-generation drugs for advanced non-small cell lung cancer. *Cochrane Database Syst Rev*: Cd009256, 2013.
38. McKeage, MJ: Comparative adverse effect profiles of platinum drugs. *Drug Saf*, 13: 228-244, 1995.
39. Perse, M, Veceric-Haler, Z: Cisplatin-Induced Rodent Model of Kidney Injury: Characteristics and Challenges. *Biomed Res Int*, 2018: 1462802, 2018.
40. Torres Crigna, A, Daniele, C, Gamez, C, Medina Balbuena, S, Pastene, DO, Nardozi, D, Brenna, C, Yard, B, Gretz, N, Bieback, K: Stem/Stromal Cells for Treatment of Kidney Injuries With Focus on Preclinical Models. *Front Med (Lausanne)*, 5: 179, 2018.
41. Ankrum, JA, Ong, JF, Karp, JM: Mesenchymal stem cells: immune evasive, not immune privileged. *Nat Biotechnol*, 32: 252-260, 2014.
42. Grinnemo, KH, Mansson, A, Dellgren, G, Klingberg, D, Wardell, E, Drvota, V, Tammik, C, Holgersson, J, Ringden, O, Sylven, C, Le Blanc, K: Xenoreactivity and engraftment of human mesenchymal stem cells transplanted into infarcted rat myocardium. *J Thorac Cardiovasc Surg*, 127: 1293-1300, 2004.
43. Lohan, P, Treacy, O, Morcos, M, Donohoe, E, O'Donoghue, Y, Ryan, AE, Elliman, SJ, Ritter, T, Griffin, MD: Interspecies Incompatibilities Limit the Immunomodulatory

- Effect of Human Mesenchymal Stromal Cells in the Rat. *Stem Cells*, 36: 1210-1215, 2018.
44. Danieli, P, Malpasso, G, Ciuffreda, MC, Gneccchi, M: Testing the Paracrine Properties of Human Mesenchymal Stem Cells Using Conditioned Medium. *Methods Mol Biol*, 1416: 445-456, 2016.
 45. Gneccchi, M, Danieli, P, Malpasso, G, Ciuffreda, MC: Paracrine Mechanisms of Mesenchymal Stem Cells in Tissue Repair. *Methods Mol Biol*, 1416: 123-146, 2016.
 46. Makridakis, M, Roubelakis, MG, Vlahou, A: Stem cells: insights into the secretome. *Biochim Biophys Acta*, 1834: 2380-2384, 2013.
 47. Kim, JH, Park, DJ, Yun, JC, Jung, MH, Yeo, HD, Kim, HJ, Kim, DW, Yang, JI, Lee, GW, Jeong, SH, Roh, GS, Chang, SH: Human adipose tissue-derived mesenchymal stem cells protect kidneys from cisplatin nephrotoxicity in rats. *Am J Physiol Renal Physiol*, 302: F1141-1150, 2012.
 48. Gheisari, Y, Ahmadbeigi, N, Naderi, M, Nassiri, SM, Nadri, S, Soleimani, M: Stem cell-conditioned medium does not protect against kidney failure. *Cell Biol Int*, 35: 209-213, 2011.
 49. Schatton, T, Yang, J, Kleffel, S, Uehara, M, Barthel, SR, Schlapbach, C, Zhan, Q, Dudeney, S, Mueller, H, Lee, N, de Vries, JC, Meier, B, Vander Beken, S, Kluth, MA, Ganss, C, Sharpe, AH, Waaga-Gasser, AM, Sayegh, MH, Abdi, R, Scharffetter-Kochanek, K, Murphy, GF, Kupper, TS, Frank, NY, Frank, MH: ABCB5 Identifies Immunoregulatory Dermal Cells. *Cell Rep*, 12: 1564-1574, 2015.
 50. Huang, J, Gretz, N: Light-Emitting Agents for Noninvasive Assessment of Kidney Function. *ChemistryOpen*, 6: 456-471, 2017.
 51. Geraci, S, Herrera-Perez, Z, Huang, J, Weinfurter, S, Neudecker, S, Shulhevich, Y, Friedemann, J, Pill, J, Gretz, N: Transcutaneous assessment of glomerular filtration rate. *Stud Health Technol Inform*, 200: 105-110, 2014.
 52. Schock-Kusch, D, Xie, Q, Shulhevich, Y, Hesser, J, Stsepankou, D, Sadick, M, Koenig, S, Hoecklin, F, Pill, J, Gretz, N: Transcutaneous assessment of renal function in conscious rats with a device for measuring FITC-sinistrin disappearance curves. *Kidney Int*, 79: 1254-1258, 2011.
 53. Schreiber, A, Shulhevich, Y, Geraci, S, Hesser, J, Stsepankou, D, Neudecker, S, Koenig, S, Heinrich, R, Hoecklin, F, Pill, J, Friedemann, J, Schweda, F, Gretz, N, Schock-Kusch, D: Transcutaneous measurement of renal function in conscious mice. *Am J Physiol Renal Physiol*, 303: F783-788, 2012.
 54. Huang, J, Weinfurter, S, Daniele, C, Perciaccante, R, Federica, R, Della Ciana, L, Pill, J, Gretz, N: Zwitterionic near infrared fluorescent agents for noninvasive real-time transcutaneous assessment of kidney function. *Chem Sci*, 8: 2652-2660, 2017.

55. Sticht, C, De La Torre, C, Parveen, A, Gretz, N: miRWalk: An online resource for prediction of microRNA binding sites. *PLoS One*, 13: e0206239, 2018.
56. Huang da W, Sherman, BT, Lempicki, RA: Bioinformatics enrichment tools: paths toward the comprehensive functional analysis of large gene lists. *Nucleic Acids Res*, 37: 1-13, 2009.
57. Huang da W, Sherman, BT, Lempicki, RA: Systematic and integrative analysis of large gene lists using DAVID bioinformatics resources. *Nat Protoc*, 4: 44-57, 2009.
58. Perazella, MA: Onco-nephrology: renal toxicities of chemotherapeutic agents. *Clin J Am Soc Nephrol*, 7: 1713-1721, 2012.
59. Cornelison, TL, Reed, E: Nephrotoxicity and hydration management for cisplatin, carboplatin, and ormaplatin. *Gynecol Oncol*, 50: 147-158, 1993.
60. Vinken, P, Starckx, S, Barale-Thomas, E, Looszova, A, Sonee, M, Goeminne, N, Versmissen, L, Buyens, K, Lampo, A: Tissue Kim-1 and urinary clusterin as early indicators of cisplatin-induced acute kidney injury in rats. *Toxicol Pathol*, 40: 1049-1062, 2012.
61. Uehara, T, Watanabe, H, Itoh, F, Inoue, S, Koshida, H, Nakamura, M, Yamate, J, Maruyama, T: Nephrotoxicity of a novel antineoplastic platinum complex, nedaplatin: a comparative study with cisplatin in rats. *Arch Toxicol*, 79: 451-460, 2005.
62. Choie, DD, Longnecker, DS, del Campo, AA: Acute and chronic cisplatin nephropathy in rats. *Lab Invest*, 44: 397-402, 1981.
63. Hall, MD, Telma, KA, Chang, KE, Lee, TD, Madigan, JP, Lloyd, JR, Goldlust, IS, Hoeschele, JD, Gottesman, MM: Say no to DMSO: dimethylsulfoxide inactivates cisplatin, carboplatin, and other platinum complexes. *Cancer Res*, 74: 3913-3922, 2014.
64. Karbownik, A, Szałek, E, Urjasz, H, Głębocka, A, Mierzwa, E, Grześkowiak, E: The physical and chemical stability of cisplatin (Teva) in concentrate and diluted in sodium chloride 0.9%. *Contemp Oncol (Pozn)*, 16: 435-439, 2012.
65. Coria-Avila, GA, Gavrila, AM, Menard, S, Ismail, N, Pfaus, JG: Cecum location in rats and the implications for intraperitoneal injections. *Lab Anim (NY)*, 36: 25-30, 2007.
66. Chen, Y, Brott, D, Luo, W, Gangl, E, Kamendi, H, Barthlow, H, Lengel, D, Fikes, J, Kinter, L, Valentin, JP, Bialecki, R: Assessment of cisplatin-induced kidney injury using an integrated rodent platform. *Toxicol Appl Pharmacol*, 268: 352-361, 2013.
67. Rule, AD: Understanding estimated glomerular filtration rate: implications for identifying chronic kidney disease. *Curr Opin Nephrol Hypertens*, 16: 242-249, 2007.
68. Tonomura, Y, Morikawa, Y, Takagi, S, Torii, M, Matsubara, M: Underestimation of urinary biomarker-to-creatinine ratio resulting from age-related gain in muscle mass in rats. *Toxicology*, 303: 169-176, 2013.

69. Baxmann, AC, Ahmed, MS, Marques, NC, Menon, VB, Pereira, AB, Kirsztajn, GM, Heilberg, IP: Influence of muscle mass and physical activity on serum and urinary creatinine and serum cystatin C. *Clin J Am Soc Nephrol*, 3: 348-354, 2008.
70. Tesch, GH: Review: Serum and urine biomarkers of kidney disease: A pathophysiological perspective. *Nephrology (Carlton)*, 15: 609-616, 2010.
71. Abdel-Gayoum, AA, El-Jenjan, KB, Ghwarsha, KA: Hyperlipidaemia in cisplatin-induced nephrotic rats. *Hum Exp Toxicol*, 18: 454-459, 1999.
72. Johnson, AC, Stahl, A, Zager, RA: Triglyceride accumulation in injured renal tubular cells: alterations in both synthetic and catabolic pathways. *Kidney Int*, 67: 2196-2209, 2005.
73. Portilla, D, Li, S, Nagothu, KK, Megyesi, J, Kaissling, B, Schnackenberg, L, Safirstein, RL, Beger, RD: Metabolomic study of cisplatin-induced nephrotoxicity. *Kidney Int*, 69: 2194-2204, 2006.
74. Oronsky, B, Caroen, S, Oronsky, A, Dobalian, VE, Oronsky, N, Lybeck, M, Reid, TR, Carter, CA: Electrolyte disorders with platinum-based chemotherapy: mechanisms, manifestations and management. *Cancer Chemother Pharmacol*, 80: 895-907, 2017.
75. Jilanchi, S, Talebi, A, Nematbakhsh, M: Cisplatin Alters Sodium Excretion and Renal Clearance in Rats: Gender and Drug Dose Related. *Adv Biomed Res*, 7: 54, 2018.
76. Goren, MP: Cisplatin nephrotoxicity affects magnesium and calcium metabolism. *Med Pediatr Oncol*, 41: 186-189, 2003.
77. Solomon, R: The relationship between disorders of K⁺ and Mg⁺ homeostasis. *Semin Nephrol*, 7: 253-262, 1987.
78. Dickson, LE, Wagner, MC, Sandoval, RM, Molitoris, BA: The proximal tubule and albuminuria: really! *J Am Soc Nephrol*, 25: 443-453, 2014.
79. Hung, CC, Lin, HY, Lee, JJ, Lim, LM, Chiu, YW, Chiang, HP, Hwang, SJ, Chen, HC: Glycosuria and Renal Outcomes in Patients with Nondiabetic Advanced Chronic Kidney Disease. *Sci Rep*, 6: 39372, 2016.
80. Wong, NL, Walker, VR, Wong, EF, Sutton, RA: Mechanism of polyuria after cisplatin therapy. *Nephron*, 65: 623-627, 1993.
81. Hattori, T, Yakabi, K, Takeda, H: Cisplatin-induced anorexia and ghrelin. *Vitam Horm*, 92: 301-317, 2013.
82. Pollera, CF, Ameglio, F, Nardi, M, Vitelli, G, Marolla, P: Cisplatin-induced hepatic toxicity. *J Clin Oncol*, 5: 318-319, 1987.
83. Cersosimo, RJ: Hepatotoxicity associated with cisplatin chemotherapy. *Ann Pharmacother*, 27: 438-441, 1993.

84. Palipoch, S, Punsawad, C: Biochemical and histological study of rat liver and kidney injury induced by Cisplatin. *J Toxicol Pathol*, 26: 293-299, 2013.
85. Ludwig, T, Riethmuller, C, Gekle, M, Schwerdt, G, Oberleithner, H: Nephrotoxicity of platinum complexes is related to basolateral organic cation transport. *Kidney Int*, 66: 196-202, 2004.
86. Yonezawa, A, Masuda, S, Nishihara, K, Yano, I, Katsura, T, Inui, K: Association between tubular toxicity of cisplatin and expression of organic cation transporter rOCT2 (Slc22a2) in the rat. *Biochem Pharmacol*, 70: 1823-1831, 2005.
87. Osman, AM, El-Sayed, EM, El-Demerdash, E, Al-Hyder, A, El-Didi, M, Attia, AS, Hamada, FM: Prevention of cisplatin-induced nephrotoxicity by methimazole. *Pharmacol Res*, 41: 115-121, 2000.
88. Brillet, G, Deray, G, Dubois, M, Beaufiles, H, Maksud, P, Bourbouze, R, Jouanneau, C, Jacobs, C: Chronic cisplatin nephropathy in rats. *Nephrol Dial Transplant*, 8: 206-212, 1993.
89. Sanchez-Gonzalez, PD, Lopez-Hernandez, FJ, Lopez-Novoa, JM, Morales, AI: An integrative view of the pathophysiological events leading to cisplatin nephrotoxicity. *Crit Rev Toxicol*, 41: 803-821, 2011.
90. Cummings, BS, Schnellmann, RG: Cisplatin-induced renal cell apoptosis: caspase 3-dependent and -independent pathways. *J Pharmacol Exp Ther*, 302: 8-17, 2002.
91. Jiang, M, Yi, X, Hsu, S, Wang, CY, Dong, Z: Role of p53 in cisplatin-induced tubular cell apoptosis: dependence on p53 transcriptional activity. *Am J Physiol Renal Physiol*, 287: F1140-1147, 2004.
92. Ju, SM, Kang, JG, Bae, JS, Pae, HO, Lyu, YS, Jeon, BH: The Flavonoid Apigenin Ameliorates Cisplatin-Induced Nephrotoxicity through Reduction of p53 Activation and Promotion of PI3K/Akt Pathway in Human Renal Proximal Tubular Epithelial Cells. *Evid Based Complement Alternat Med*, 2015: 186436, 2015.
93. Seth, R, Yang, C, Kaushal, V, Shah, SV, Kaushal, GP: p53-dependent caspase-2 activation in mitochondrial release of apoptosis-inducing factor and its role in renal tubular epithelial cell injury. *J Biol Chem*, 280: 31230-31239, 2005.
94. Wei, Q, Dong, G, Yang, T, Megyesi, J, Price, PM, Dong, Z: Activation and involvement of p53 in cisplatin-induced nephrotoxicity. *Am J Physiol Renal Physiol*, 293: F1282-1291, 2007.
95. Ramesh, G, Reeves, WB: TNF-alpha mediates chemokine and cytokine expression and renal injury in cisplatin nephrotoxicity. *J Clin Invest*, 110: 835-842, 2002.
96. Ramesh, G, Reeves, WB: TNFR2-mediated apoptosis and necrosis in cisplatin-induced acute renal failure. *Am J Physiol Renal Physiol*, 285: F610-618, 2003.

97. Razzaque, MS, Koji, T, Kumatori, A, Taguchi, T: Cisplatin-induced apoptosis in human proximal tubular epithelial cells is associated with the activation of the Fas/Fas ligand system. *Histochem Cell Biol*, 111: 359-365, 1999.
98. Annibaldi, A, Meier, P: Checkpoints in TNF-Induced Cell Death: Implications in Inflammation and Cancer. *Trends Mol Med*, 24: 49-65, 2018.
99. Deegan, PM, Nolan, C, Ryan, MP, Basinger, MA, Jones, MM, Hande, KR: The role of the renin-angiotensin system in cisplatin nephrotoxicity. *Ren Fail*, 17: 665-674, 1995.
100. Ferrao, FM, Lara, LS, Lowe, J: Renin-angiotensin system in the kidney: What is new? *World J Nephrol*, 3: 64-76, 2014.
101. Li, XC, Zhuo, JL: Recent Updates on the Proximal Tubule Renin-Angiotensin System in Angiotensin II-Dependent Hypertension. *Curr Hypertens Rep*, 18: 63, 2016.
102. Sparks, MA, Crowley, SD, Gurley, SB, Mirososou, M, Coffman, TM: Classical Renin-Angiotensin system in kidney physiology. *Compr Physiol*, 4: 1201-1228, 2014.
103. He, G, Siddik, ZH, Huang, Z, Wang, R, Koomen, J, Kobayashi, R, Khokhar, AR, Kuang, J: Induction of p21 by p53 following DNA damage inhibits both Cdk4 and Cdk2 activities. *Oncogene*, 24: 2929-2943, 2005.
104. Megyesi, J, Udvarhelyi, N, Safirstein, RL, Price, PM: The p53-independent activation of transcription of p21 WAF1/CIP1/SDI1 after acute renal failure. *Am J Physiol*, 271: F1211-1216, 1996.
105. Megyesi, J, Safirstein, RL, Price, PM: Induction of p21WAF1/CIP1/SDI1 in kidney tubule cells affects the course of cisplatin-induced acute renal failure. *J Clin Invest*, 101: 777-782, 1998.
106. Price, PM, Yu, F, Kaldis, P, Aleem, E, Nowak, G, Safirstein, RL, Megyesi, J: Dependence of cisplatin-induced cell death in vitro and in vivo on cyclin-dependent kinase 2. *J Am Soc Nephrol*, 17: 2434-2442, 2006.
107. Ramesh, G, Reeves, WB: p38 MAP kinase inhibition ameliorates cisplatin nephrotoxicity in mice. *Am J Physiol Renal Physiol*, 289: F166-174, 2005.
108. Song, H, Sondak, VK, Barber, DL, Reid, TJ, Lin, J: Modulation of Janus kinase 2 by cisplatin in cancer cells. *Int J Oncol*, 24: 1017-1026, 2004.
109. Tsogbadrakh, B, Ryu, H, Ju, KD, Lee, J, Yun, S, Yu, KS, Kim, HJ, Ahn, C, Oh, KH: AICAR, an AMPK activator, protects against cisplatin-induced acute kidney injury through the JAK/STAT/SOCS pathway. *Biochem Biophys Res Commun*, 2019.
110. Zhao, K, Wen, LB: DMF attenuates cisplatin-induced kidney injury via activating Nrf2 signaling pathway and inhibiting NF- κ B signaling pathway. *Eur Rev Med Pharmacol Sci*, 22: 8924-8931, 2018.

111. Arany, I, Megyesi, JK, Kaneto, H, Price, PM, Safirstein, RL: Cisplatin-induced cell death is EGFR/src/ERK signaling dependent in mouse proximal tubule cells. *Am J Physiol Renal Physiol*, 287: F543-549, 2004.
112. Afratis, N, Gialeli, C, Nikitovic, D, Tsegenidis, T, Karousou, E, Theocharis, AD, Pavao, MS, Tzanakakis, GN, Karamanos, NK: Glycosaminoglycans: key players in cancer cell biology and treatment. *Febs j*, 279: 1177-1197, 2012.
113. Ghiselli, G: Drug-Mediated Regulation of Glycosaminoglycan Biosynthesis. *Med Res Rev*, 37: 1051-1094, 2017.
114. Melrose, J: Glycosaminoglycans in Wound Healing. *Bone and Tissue Regeneration Insights*, 7: BTRIS38670, 2016.
115. Coelho, S, Cabral, G, Lopes, JA, Jacinto, A: Renal regeneration after acute kidney injury. *Nephrology (Carlton)*, 23: 805-814, 2018.
116. Berger, K, Moeller, MJ: Mechanisms of epithelial repair and regeneration after acute kidney injury. *Semin Nephrol*, 34: 394-403, 2014.
117. Chang-Panesso, M, Humphreys, BD: Cellular plasticity in kidney injury and repair. *Nat Rev Nephrol*, 13: 39-46, 2017.
118. Kusaba, T, Lalli, M, Kramann, R, Kobayashi, A, Humphreys, BD: Differentiated kidney epithelial cells repair injured proximal tubule. *Proc Natl Acad Sci U S A*, 111: 1527-1532, 2014.
119. Kulkarni, OP, Hartter, I, Mulay, SR, Hagemann, J, Darisipudi, MN, Kumar Vr, S, Romoli, S, Thomasova, D, Ryu, M, Kobold, S, Anders, HJ: Toll-like receptor 4-induced IL-22 accelerates kidney regeneration. *J Am Soc Nephrol*, 25: 978-989, 2014.
120. Lee, S, Huen, S, Nishio, H, Nishio, S, Lee, HK, Choi, BS, Ruhrberg, C, Cantley, LG: Distinct macrophage phenotypes contribute to kidney injury and repair. *J Am Soc Nephrol*, 22: 317-326, 2011.
121. Tadagavadi, RK, Reeves, WB: Renal dendritic cells ameliorate nephrotoxic acute kidney injury. *J Am Soc Nephrol*, 21: 53-63, 2010.
122. Zhang, MZ, Wang, X, Wang, Y, Niu, A, Wang, S, Zou, C, Harris, RC: IL-4/IL-13-mediated polarization of renal macrophages/dendritic cells to an M2a phenotype is essential for recovery from acute kidney injury. *Kidney Int*, 91: 375-386, 2017.
123. Lewis, BP, Burge, CB, Bartel, DP: Conserved seed pairing, often flanked by adenosines, indicates that thousands of human genes are microRNA targets. *Cell*, 120: 15-20, 2005.
124. Zhang, B, Wang, Q, Pan, X: MicroRNAs and their regulatory roles in animals and plants. *J Cell Physiol*, 210: 279-289, 2007.

125. Krek, A, Grun, D, Poy, MN, Wolf, R, Rosenberg, L, Epstein, EJ, MacMenamin, P, da Piedade, I, Gunsalus, KC, Stoffel, M, Rajewsky, N: Combinatorial microRNA target predictions. *Nat Genet*, 37: 495-500, 2005.
126. Herrera-Pérez, Z, Gretz, N, Dweep, H: A Comprehensive Review on the Genetic Regulation of Cisplatin-induced Nephrotoxicity. *Curr Genomics*, 17: 279-293, 2016.
127. Wu, J, Li, DD, Li, JY, Yin, YC, Li, PC, Qiu, L, Chen, LM: Identification of microRNA-mRNA networks involved in cisplatin-induced renal tubular epithelial cells injury. *Eur J Pharmacol*, 851: 1-12, 2019.
128. Fan, PC, Chen, CC, Chen, YC, Chang, YS, Chu, PH: MicroRNAs in acute kidney injury. *Hum Genomics*, 10: 29, 2016.
129. Pellegrini, KL, Han, T, Bijol, V, Saikumar, J, Craciun, FL, Chen, WW, Fuscoe, JC, Vaidya, VS: MicroRNA-155 deficient mice experience heightened kidney toxicity when dosed with cisplatin. *Toxicol Sci*, 141: 484-492, 2014.
130. Uccelli, A, Moretta, L, Pistoia, V: Mesenchymal stem cells in health and disease. *Nat Rev Immunol*, 8: 726-736, 2008.
131. Fischer, UM, Harting, MT, Jimenez, F, Monzon-Posadas, WO, Xue, H, Savitz, SI, Laine, GA, Cox, CS, Jr.: Pulmonary passage is a major obstacle for intravenous stem cell delivery: the pulmonary first-pass effect. *Stem Cells Dev*, 18: 683-692, 2009.
132. Kurtz, A: Mesenchymal stem cell delivery routes and fate. *Int J Stem Cells*, 1: 1-7, 2008.
133. Schrepfer, S, Deuse, T, Reichenspurner, H, Fischbein, MP, Robbins, RC, Pelletier, MP: Stem cell transplantation: the lung barrier. *Transplant Proc*, 39: 573-576, 2007.
134. Murray, PJ: Macrophage Polarization. *Annu Rev Physiol*, 79: 541-566, 2017.
135. Cavaillon, JM: Cytokines and macrophages. *Biomed Pharmacother*, 48: 445-453, 1994.
136. Arango Duque, G, Descoteaux, A: Macrophage cytokines: involvement in immunity and infectious diseases. *Front Immunol*, 5: 491, 2014.
137. Hunter, CA, Jones, SA: IL-6 as a keystone cytokine in health and disease. *Nat Immunol*, 16: 448-457, 2015.
138. Su, H, Lei, CT, Zhang, C: Interleukin-6 Signaling Pathway and Its Role in Kidney Disease: An Update. *Front Immunol*, 8: 405, 2017.
139. Tanaka, T, Narazaki, M, Kishimoto, T: IL-6 in inflammation, immunity, and disease. *Cold Spring Harb Perspect Biol*, 6: a016295, 2014.
140. Goodman, MN: Interleukin-6 induces skeletal muscle protein breakdown in rats. *Proc Soc Exp Biol Med*, 205: 182-185, 1994.

141. Strassmann, G, Fong, M, Kenney, JS, Jacob, CO: Evidence for the involvement of interleukin 6 in experimental cancer cachexia. *J Clin Invest*, 89: 1681-1684, 1992.
142. Roberts, AW: G-CSF: a key regulator of neutrophil production, but that's not all! *Growth Factors*, 23: 33-41, 2005.
143. Xu, Y, Zeng, S, Zhang, Q, Zhang, Z, Hu, X: Stem Cell Mobilizers: Novel Therapeutics for Acute Kidney Injury. *Curr Protein Pept Sci*, 18: 1195-1199, 2017.
144. Han, G, Li, F, Singh, TP, Wolf, P, Wang, XJ: The pro-inflammatory role of TGFbeta1: a paradox? *Int J Biol Sci*, 8: 228-235, 2012.
145. Pourgholaminejad, A, Aghdami, N, Baharvand, H, Moazzeni, SM: Is TGFbeta as an anti-inflammatory cytokine required for differentiation of inflammatory TH17 cells? *J Immunotoxicol*, 13: 775-783, 2016.

8. Curriculum vitae

Personal information

Name: Cristina

Surname: Daniele

Date of birth: 06.04.1990

Place of birth: Chiaravalle Centrale (CZ), Italy

Nationality: Italian

Civil status: Unmarried

Address: Rheinhäuserstraße 27, 68165 Mannheim

Mobile: +49 174 9584279

Email address: crisrina.daniele@medma.uni-heidelberg.de crisrina.dan556@gmail.com

Skype: Cristina Dan (crisrina.daniele.98)

LinkedIn: Cristina Daniele

Academic qualifications

May 2016-May 2019 Mannheim, Germany	Doctoal studies, Medical Research Center, University of Heidelberg Thesis: Therapeutic potential of human ABCB5+ cells and different conditioned media in a cisplatin-induced nephrotoxicity model
September 2012-July 2015, Florence, Italy	Master of Science in Biomedicine, School of Mathematical, Physical and Natural Sciences, University of Florence Thesis: "Preliminary analysis of the functional role of CREBBP and EP300 in the preeclamptic placenta" Final mark: magna (110/110) cum laude
September 2014-March 2015, Amsterdam, The Netherlands	Exchange trainee Uva, University of Amsterdam
February 2014-July 2014, Amsterdam, The Netherlands	Exchange student VU, Vrije Universiteit Amsterdam
September 2009-December 2012 Florence, Italy	Bachelor of Science in Biology, School of Mathematical, Physical and Natural Sciences, University of Florence Thesis: "Type-specific PCR for some beta-HPVs detection in clinical samples" Final mark: 106/110
September 2004-July 2009 Chiaravalle Centrale, Italy	High School "Leonardo Da Vinci", Scientific leaving certificate Final mark: 98/100

Publications

Huang J, Weinfurter S, **Daniele C**, Perciaccante R, Federica R, Della Ciana L, Pill J, Gretz N. Zwitterionic near infrared fluorescent agents for noninvasive real-time transcutaneous assessment of kidney function.

Chemical Science 2017; 8(4):2652-2660.

Daniele C, Torres Crigna A, Gamez C, Medina Balbuena S, Pastene DO, Nardozi D, Brenna C, Yard B, Gretz N, Bieback K.

Stem/Stromal Cells for Treatment of Kidney Injuries with Focus on Preclinical Models.

Frontiers Medicine 2018; 5:179.

Huang J, Brenna C, Maula Khan A, **Daniele C**, Rudolf R, Heuveline V, Gretz N.

A cationic near infrared fluorescent agent and ethyl-cinnamate tissue clearing protocol for vascular staining and imaging.

Scientific Reports 2019; 9:521.

Daniele C, Nardozi D, Torelli A, Maula Khan A, Gretz N.

Transcutaneous measurement of glomerular filtration rate in rodents.

Springer, under revision

9. Acknowledgment

I would like to express my sincere gratitude to Prof. Norbert Gretz for his supervision, support and guidance throughout the whole period of research and writing of this thesis.

I also thank him for letting me take part in the Doctoral Program ‘Cooperative Research Training Group Tissue Analytics for Stem Cell based Diagnostics and Therapy (TASCDT)’.

It has been a highly formative experience for me and I will treasure the teachings I have learned during these years.

I sincerely thank him and Dr. Kluth for giving me the opportunity to work on this project in collaboration with Ticeba/REHACELL.

I thank Dr. Carsten Sticht for helping me in gene expression analysis, Dr. Bettina Kränzlin and Dr. Arif ul Maula Khan for histological evaluation and Dr. Karen Bieback for her advice and steady support in answering questions and helping me in problem solving.

I deeply thank Viktoria Skude for her supervision and training in animal facility and for the immense patience she especially had with me at the beginning.

Thanks to all my ZMF and TASCDT colleagues for sharing knowledge and especially to Stefania Palumbo and Fabiola Arpino for the daily brainstorming and support.

A special thank goes to ‘the Italian crew’; it has been a pleasure to share this way with you.

Abbreviations

ABCB5	ATP-binding cassette member B5
ABCB5+	Cells expressing ABCB5
AKI	Acute Kidney Injury
BW	Body Weight
CM	Medium conditioned by ABCB5+ cells
CM+	Medium conditioned by ABCB5+ cells stimulated with IFN- γ and LPS
coCM+	Medium conditioned by a co-culture of ABCB5+ cells and human monocyte cell line THP-1 stimulated with IFN- γ and LPS
DIRCs	Dermal Immunoregulatory Cells
ECM	Extracellular Matrix
ESRD	End-Stage Renal Disease
GAG	Glycosaminoglycan
G-CSF	Granulocyte colony-stimulating factor
GFR	Glomerular Filtration Rate
GSEA	Gene Set Enrichment Analysis
H&E	Hematoxylin and Eosin
IFN γ	Interferon gamma
IL	Interleukin
Ip	Intraperitoneal
Iv	Intravenous
KEGG	Kyoto Encyclopedia of Genes and Genomes database
M+	Medium conditioned from human monocyte cell line THP-1 stimulated with IFN- γ and LPS
RAS	Renin-Angiotensin System
SD	Sprague Dawley
TGF β 1	Transforming Growth Factor beta 1
TNF α	Tumor Necrosis Factor alpha